Supporting Information

for

[Mes-B-TMP]$^+$ Borinium Cation Initiated Cyanosilylation and Catalysed Hydrosilylation of Ketones and Aldehydes

Po-Han Chen, Ching-Pei Hsu, Hsi-Ching Tseng, Yi-Hung Liu and Ching-Wen Chiu

Department of Chemistry, National Taiwan University, No. 1, Section 4, Roosevelt Road, Taipei, Taiwan 10617

1. Synthesis:

General information.

All the reactions are carried out by using Schlenk system or glovebox under nitrogen atmosphere. Dichloromethane, ether, and toluene were purified by the molecular sieves packed solvent purification system. Et_3SiH were dried by molecular sieves and distilled under nitrogen. Chlorobenzene, CD_2Cl_2, and $CDCl_3$ were dried by P_2O_5 and distilled under nitrogen. Pentane and hexane were dried by Na/K alloy and distilled under nitrogen. TMSCN and silver tetrakis(perfluoro-*tert*-butoxy) aluminate ($Ag[Al(OC(CF_3)_3]_4$) were purchased and used without further purification. NMR spectra were collected by using Bruker Advance III-400 (^1H: 400.2 MHz, ^{11}B: 128.4 MHz, ^{13}C: 100.6 MHz, ^{19}F: 376.5 MHz, ^{27}Al: 104.2 MHz, ^{29}Si: 99.4 MHz, ^{31}P: 162.0 MHz).

Synthesis of 1a

A solution of $MesBCl_2$ (4.00 g, 0.02 mol) in toluene (20 mL) was transferred into the suspension of TMPLi (2.93 g, 0.02 mol) in hexane (50 mL), and the mixture was heated to 110 ℃ for 4 days. Afterward, the orange-beige opaque solution was filtered through celite to remove solid and the collected liquid phase was dried under vacuum to give an orange oil. Colorless crystalline products were then obtained after sublimation (1.20 g, 20% yield). ^1H NMR (400.2 MHz, $CDCl_3$): δ = 6.73 (s, 2 H), 2.32

(s, 6 H), 2.23 (s, 3 H), 1.86 (t, 2 H, $^{3}J_{HH}$ = 7.80 Hz), 1.75 (m, 2 H), 1.72 (s, 6 H), 1.66 (t, 2 H, $^{3}J_{HH}$ = 7.80 Hz) and 1.15 (s, 6 H) ppm. ^{11}B NMR (128.4 MHz, $CDCl_3$): δ = 39.3 (s) ppm. ^{13}C NMR (100.6 MHz, $CDCl_3$): δ = 142.8(br), 136.8, 136.6, 127.6, 57.9, 57.6, 32.3, 31.5, 22.9, 21.0 and 14.7 ppm. Anal. Calcd for $C_{18}H_{29}BNCl$ (%): Calcd: C 70.72, H 9.56, N 4.58; Exp: C 71.76, H 9.50, N 4.29.

Synthesis of 1b:

A solution of $MesBCl_2$ (530.0 mg, 2.63 mmol) in hexane (20 mL) was transferred into the suspension of LiHMDS (441.0 mg, 2.63 mmol) in hexane (50 mL) at − 78 °C. The mixture was slowly warmed to room temperature and stirred for 2 h to give an off-white opaque solution. The reaction mixture was filtered through celite to remove LiCl and dried under vacuum to give white solids, which were re-crystallized from a concentrated pentane solution at − 30 °C (818 mg, 95% yield). ^{1}H NMR (400.2 MHz, C_6D_6): δ = 6.65 (s, 2 H), 2.30 (s, 6 H), 2.12 (s, 3 H), 0.49 (br, 9 H) and − 0.04 (br, 9 H) ppm. ^{11}B NMR (128.4 MHz, C_6D_6): δ = 44.8 (s) ppm. ^{13}C NMR (100.6 MHz, C_6D_6): δ = 140.7 (br), 137.6, 137.3, 128.2, 127.7, 22.4, 21.2, 4.7 (br) and 4.1 (br) ppm. ^{29}Si NMR (99.4 MHz, C_6D_6): δ = 8.7 (s) ppm. Anal. Calcd for $C_{15}H_{29}BNSi_2Cl$ (%): Calcd: C 55.29, H 8.97, N 4.30; Exp: C 55.87, H 9.01, N 4.44.

Synthesis of [2][Al(OC(CF$_3$)$_3$)$_4$]:

1a (10.0 mg, 0.033 mmol) was mixed with Ag[Al(OC(CF$_3$)$_3$)$_4$] (35.2 mg, 0.033 mmol) in 0.5 mL of $CDCl_3$ to give a pink solution with brownish solid precipitates. After filtered off the solid, the solution was transferred to a J Young's NMR tube for characterization. Afterward, solvent was removed under vacuum to give a pink oil (35.6 mg, 88% yield). ^{1}H NMR (400.2 MHz, $CDCl_3$): δ = 7.14 (s, 2 H), 2.63 (s, 6 H), 2.44 (s, 3 H), 1.89 (m, 2 H), 1.74 (t, 4 H, $^3J_{HH}$ = 5.78 Hz) and 1.61 (s, 12 H) ppm. ^{11}B NMR (128.4 MHz, $CDCl_3$): δ = 55.5 (br) ppm. ^{13}C NMR (100.6 MHz, $CDCl_3$): δ = 156.3, 153.3, 130.1, 121.1 (q, $^1J_{CF}$ = 292.8 Hz), 114.1 (br), 60.4, 37.4, 30.9, 23.1, 22.7 and 16.2 ppm. ^{19}F NMR (376.5 MHz, $CDCl_3$): δ = − 75.4 (s) ppm. ^{27}Al NMR (104.2 MHz, $CDCl_3$): δ = 34.1 (s) ppm. Anal. Calcd for $C_{34}H_{29}BAlNO_4F_{36}$ (%): Calcd: C 33.0, H 2.36, N 1.13; Exp: C 32.71, H 2.48, N 1.14.

Synthesis of [3][Al(OC(CF$_3$)$_3$)$_4$]:

1b (20.0 mg, 0.061 mmol) and Ag[Al(OC(CF$_3$)$_3$)$_4$] (65.9 mg, 0.061 mmol) were mixed in 0.5 mL of DCM to give a pink solution with brownish solids in the bottom. The solution was filtered and dried under vacuum to yield a pink oil, which was re-dissolved in chlorobenzene. Light brown crystals of [**3**][Al(OC(CF$_3$)$_3$)$_4$] were obtained after diffusion of hexane in to the chlorobenzene solution of [**3**][Al(OC(CF$_3$)$_3$)$_4$] at

room temperature. Crystalline solids were collected and dried under vacuum (35.5 mg, 46% yield). ^{1}H NMR (400.2 MHz, CD_2Cl_2): δ = 7.35 (s, 2 H), 2.54 (s, 3 H), 2.51 (s, 6 H), 0.79 (s, 3 H), 0.64 (s, 6 H) and 0.38 (s, 9 H) ppm. ^{11}B NMR (128.4 MHz, CD_2Cl_2): δ = 49.5 (s) ppm. ^{13}C NMR (100.6 MHz, CD_2Cl_2): δ = 169.5, 163.1, 132.1, 129.8, 121.1 (q, $^{1}J_{CF}$ = 292.8 Hz), 79.0 (br), 24.4, 22.8, 4.05, 1.67 and 0.42 ppm. ^{19}F NMR (376 MHz, $CDCl_3$): δ = − 75.4 (s) ppm. ^{27}Al NMR (104.2 MHz, $CDCl_3$): δ = 34.1 (s) ppm. ^{29}Si NMR (99.4 MHz, CD_2Cl_2): δ = 22.6 (s), 21.5 (s) and 9.7 (s) ppm. Anal. Calcd for $C_{31}H_{29}BAlNO_4Si_2F_{36}$ (%): Calcd: C 29.61, H 2.32, N 1.11; Exp: C 29.35, H 2.52, N 1.39.

Synthesis of 4:

1b (20.0 mg, 0.061 mmol) and $Na[B(C_6F_5)_4]$ (43.1 mg, 0.061 mmol) were mixed in 1 mL DCM. Afterward, the mixture was dried under vacuum and extracted with hexane. The collected hexane solution was then dried to give a colorless oil (18 mg, 90% yield). ^{1}H NMR (400.2 MHz, CD_2Cl_2): δ = 6.76 (s, 2 H), 2.28 (s, 3 H), 2.23 (s, 6 H), 0.88 (s, 3 H), 0.51 (br, 9 H) and 0.18 (br, 6 H) ppm. ^{11}B NMR (128.4 MHz, CD_2Cl_2): δ = 56.5 (br) and − 16.6 (s) ppm. ^{13}C NMR (100.6 MHz, C_6D_6): δ = 144.8 (br), 136.6, 136.3, 128.2, 22.1, 21.1, 13.5 (br), 8.1 (br), 7.2, 4.8 and 4.4 (br) ppm. ^{29}Si NMR (99.4 MHz, C_6D_6): δ = 16.9 (s) and 8.2 (s) ppm.

Synthesis of [7][Al(OC(CF$_3$)$_3$)$_4$]

MesB(CN)TMP. A C_6D_6 solution consisting of **1a** (10.0 mg, 0.033 mmol) and TMSCN (6.14 μL, 0.049 mmol) was heated to reflux for 12 h. The reaction progress was monitored with NMR. After the complete consumption of **1a**, all volatiles were removed under vacuum to give **MesB(CN)TMP** as white solid, which was then recrystallized from pentane at − 30 °C (5.4 mg, 56% yield). ^{1}H NMR (400.2 MHz, $CDCl_3$): δ = 6.75 (s, 2 H), 2.30 (s, 6 H), 2.24 (s, 3 H), 1.87 (t, 2 H, $^3J_{HH}$ = 7.19 Hz), 1.80 (s, 6 H), 1.77 (m, 2 H), 1.65 (t, 2 H, $^3J_{HH}$ = 7.4 Hz) and 1.14 (s, 6 H) ppm. ^{11}B NMR (128.4 MHz, $CDCl_3$): δ = 31.4 (s) ppm. ^{13}C NMR (100.6 MHz, $CDCl_3$): δ = 139.4 (br), 137.3, 137.1, 128.8 (br), 127.7, 58.8, 58.3, 36.1 (d, $^1J_{CF}$ = 5.74 Hz), 33.3, 32.1, 22.7, 21.1 and 14.4 ppm. Anal. Calcd for $C_{19}H_{29}BN_2$ (%): Calcd: C 77.03, H 9.87, N 9.46; Exp: C 77.08, H 9.72, N 9.38.

[7][Al(OC(CF$_3$)$_3$)$_4$]. A freshly prepared [**2**][Al(OC(CF$_3$)$_3$)$_4$] generated from **1a** (3.3 mg, 0.01 mmol) and Ag[Al(OC(CF$_3$)$_3$)$_4$] (11.6 mg, 0.01 mmol) was mixed with **MesB(CN)TMP** (3.2 mg, 0.01 mmol) in $CDCl_3$. After confirming the formation of [**7**][Al(OC(CF$_3$)$_3$)$_4$] with ^{1}H NMR, all volatiles were removed to give white solid, which were washed with 1 mL hexane. Crystalline products were obtained by diffusion pentane into a $CHCl_3$ solution of [**7**][Al(OC(CF$_3$)$_3$)$_4$] at − 30 °C (11.8 mg, 77% yield). ^{1}H NMR (400.2 MHz, $CDCl_3$): δ = 6.87 (s, 2 H), 6.84 (s, 2 H), 2.31 (s, 3 H), 2.30 (s, 3

H), 2.19 (s, 6 H), 2.16 (s, 6 H), 1.86 – 1.77 (m, 8 H), 1.72 – 1.66 (m, 4 H), 1.37 (s, 6 H), 1.29 (s, 6 H), 1.24 (s, 6 H) and 1.20 (s, 6 H) ppm. ^{11}B NMR (128.4 MHz, $CDCl_3$): δ = 29.6 (bs) ppm. ^{13}C NMR (100.6 MHz, $CDCl_3$): δ = 141.0, 140.2, 137.6, 137.1, 134.2 (br), 132.7 (br), 128.8, 128.4, 121.1 (q, $^1J_{CF}$ = 292.8 Hz), 61.7, 59.9, 59.7, 58.9, 35.6, 35.16, 35.1, 34.7, 32.2, 32.0, 31.8, 22.6, 21.0 and 13.8 ppm. ^{19}F NMR (376 MHz, $CDCl_3$): δ = – 75.4 (s) ppm. ^{27}Al NMR (104.2 MHz, $CDCl_3$): δ = 34.6 (s) ppm. Anal. Calcd for $C_{53}H_{58}AlB_2N_3F_{36}O_4$ (%): Calcd: C 41.51, H 3.81, N 2.74; Exp: C 41.73, H 3.69, N 2.85.

Generation of [7]$^+$ from reaction of [2][Al(OC(CF$_3$)$_3$)$_4$] and TMSCN. In a J. Young's NMR tube, TMSCN (4.1 μL; 0.03 mmol) was mixed with [**2**][$Al(OC(CF_3)_3)_4$] (40.5 mg; 0.03 mmol) in $CDCl_3$. The ^{1}H NMR spectra is consistent with that of [**7**][$Al(OC(CF_3)_3)_4$].

2. Acidity determination with Gutmann-Beckett method

When [**2**][$Al(OC(CF_3)_3)_4$] reacts with an equimolar amount of Et_3PO, the corresponding Lewis adduct, Et_3PO-[**2**][$Al(OC(CF_3)_3)_4$], formed immediately. The coordination of base at [**2**]$^+$ leads to splitting of the methyl proton signal of TMP to two singlets with the ^{11}B resonance shifted to 31.5 ppm. The ^{31}P NMR signal detected at 91.3 ppm can be covered to an AN of 86.6. The Lewis acidity of [**2**][$Al(OC(CF_3)_3)_4$] is

lower than that of Cp*-substituted $[Cp^*\text{-B-Mes}]^+$ (AN = 104.5). Compared with $B(C_6F_5)_3$ (AN = 52.2) a commonly used boron Lewis acid catalyst, it is unambiguous that [**2**][$Al(OC(CF_3)_3)_4$] possesses much higher Lewis acidity than $B(C_6F_5)_3$. **NMR data Et_3PO-[2][$Al(OC(CF_3)_3)_4$]:** ^1H NMR (400.2 MHz, $CDCl_3$): δ = 6.19 (s, 2 H), 2.35 (s, 6 H), 2.31 (s, 3 H), 1.89 (m, 9 H) 1.81 (m, 4 H), 1.67 (m, 2 H), 1.54 (s, 6 H), 1.21 (m, 6 H) and 1.15 (s, 6 H) ppm. ^{11}B NMR (128.4 MHz, $CDCl_3$): δ = 31.5 (s) ppm. ^{31}P NMR (162.0 MHz, $CDCl_3$): δ = 91.3 (s) ppm.

Table S1. Gutmann-Beckett acidity determination result

Lewis acid	**^{31}P NMR δ (ppm)**	**^{31}P NMR Δδ (ppm)[a]**	**Acceptor number[b]**
$B(C_6F_5)_3$	75.7	23.6	52.2
[**2**][$Al(OC(CF_3)_3)_4$]	91.3	39.2	86.6
$[Cp^*\text{-}B^+\text{-Mes}][B(C_6F_5)_4]$	97.6	47.3	104.5

[a]Et_3PO : ^{31}P δ = 52.1 ppm in $CDCl_3$; [b]AN = 2.21 × Δδ.

3. Reactivity studies

The interconversion between [3][Al(OC(CF$_3$)$_3$)$_4$] and 4

As the conversion of [**3**][Al(OC(CF$_3$)$_3$)$_4$] to **4** is accomplished through the addition of one equivalent of [^{n}Bu$_4$N]Cl in CD_2Cl_2, mixing an equimolar amount of **4** and Ag[Al(OC(CF$_3$)$_3$)$_4$] resulted in the formation of [**3**][Al(OC(CF$_3$)$_3$)$_4$].

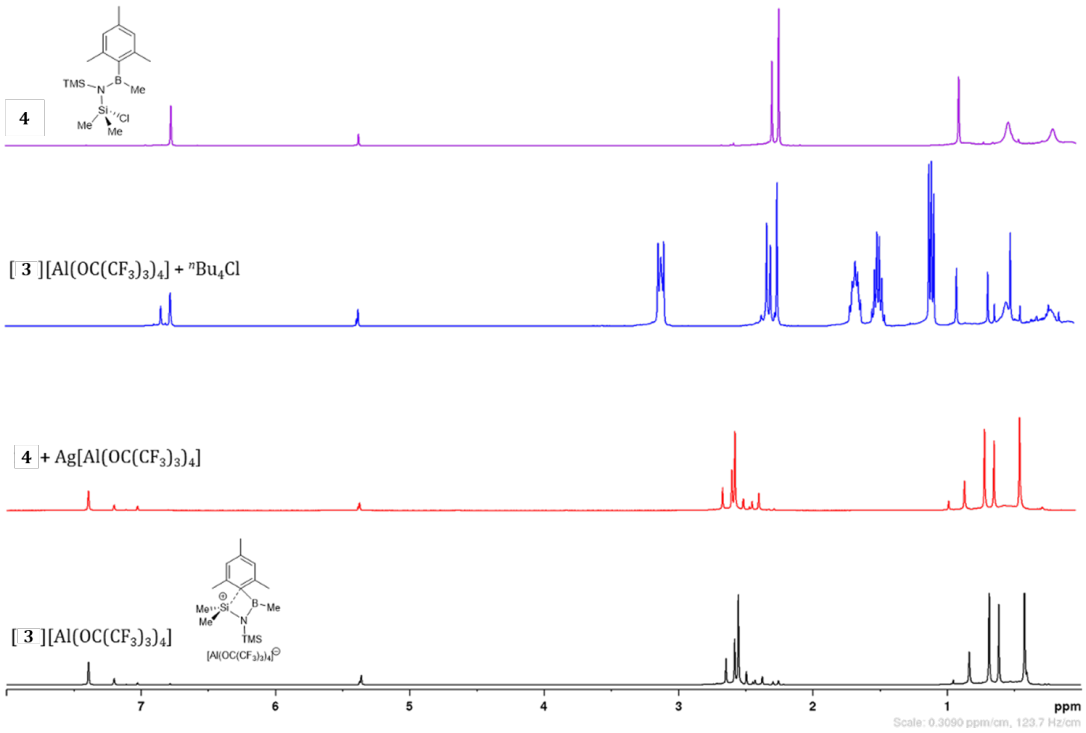

Figure S1. ^{1}H NMR spectra of the interconversion between [**3**][Al(OC(CF$_3$)$_3$)$_4$] and **4** via chloride addition and abstraction in CD_2Cl_2.

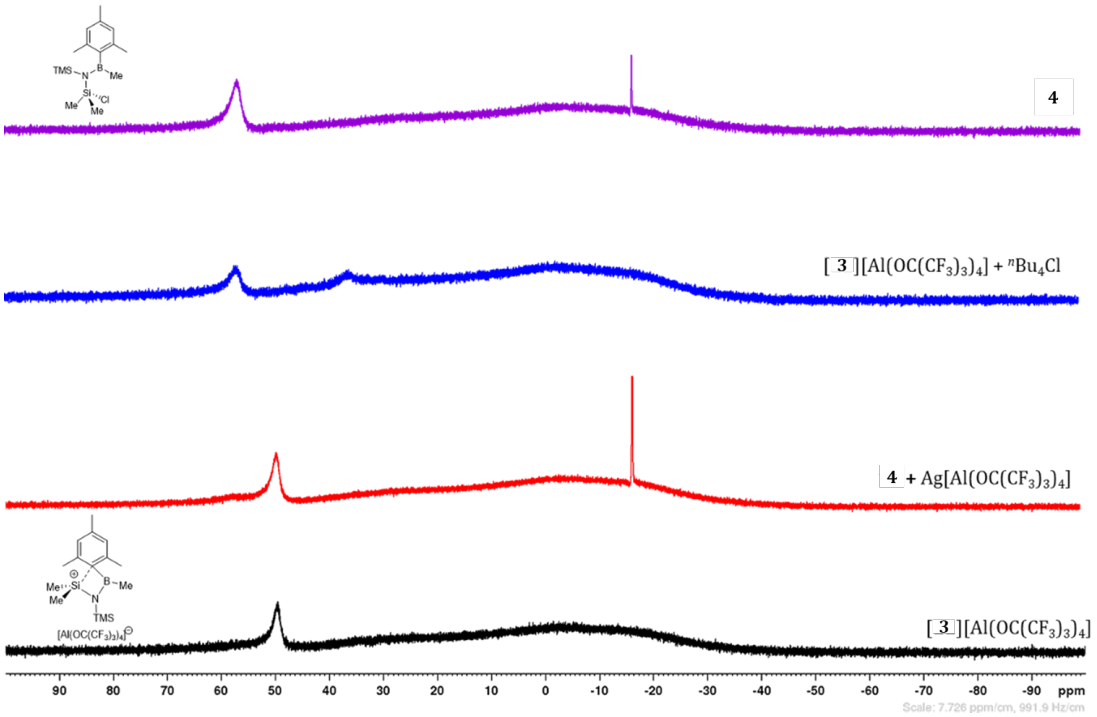

Figure S2. ^{11}B NMR spectra of the interconversion between [**3**][Al(OC(CF$_3$)$_3$)$_4$] and **4** via chloride addition and abstraction in CD_2Cl_2.

Reaction of [2][Al(OC(CF$_3$)$_3$)$_4$] and TMSCN

TMSCN (4.1 μL; 0.03 mmol) is added to [**2**][Al(OC(CF$_3$)$_3$)$_4$] (40.5 mg; 0.03 mmol) in $CDCl_3$ in a J. Young's NMR tube. The obtained ^{1}H NMR spectrum is consistent with that of [**7**][Al(OC(CF$_3$)$_3$)$_4$] (**Figure S3**). On the next day, crystalline solids of [TMS-CN-TMS][Al(OC(CF$_3$)$_3$)$_4$] formed at the bottom of the NMR tube were collected, dried under vacuum, and re-dissolved in CD_2Cl_2. ^{1}H NMR (400.2 MHz, DCM-*d*$_2$): δ = 0.74 (s, 9 H) and 0.73 (s, 9 H) ppm. ^{19}F NMR (376.5 MHz, DCM-*d*$_2$): δ = − 76.6 (s) ppm.

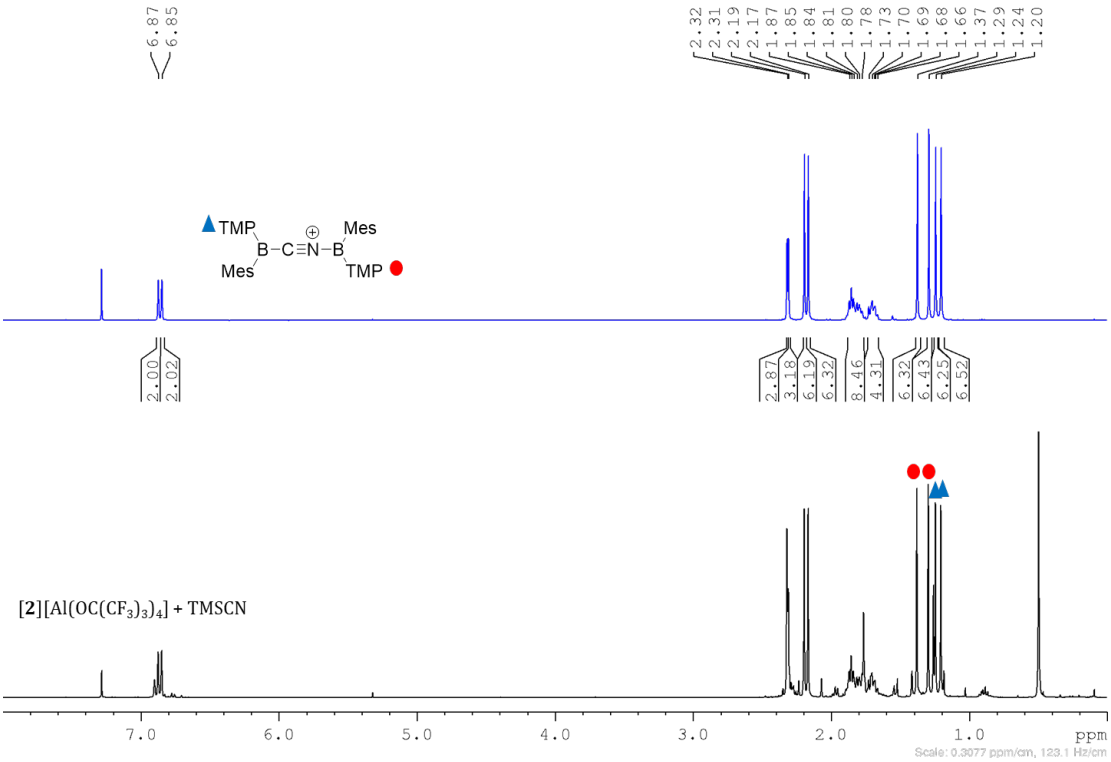

Figure S3. ^{1}H NMR spectra of [**7**][Al(OC(CF$_3$)$_3$)$_4$] (top) and [**2**][Al(OC(CF$_3$)$_3$)$_4$] + TMSCN (bottom).

Reaction of [2][Al(OC(CF$_3$)$_3$)$_4$] and acetophenone

Acetophenone (3.8 µL; 0.03 mmol) is added to [**2**][Al(OC(CF$_3$)$_3$)$_4$] (40.5 mg; 0.03 mmol) in $CDCl_3$ in a J. Young's NMR tube. The resulting reaction mixture was then quenched by adding diethyl ether, and purified by column chromatography. 1-Phenyl-1-meistylethylene was obtained as colorless oil in 82 % yield. ^{1}H NMR (400.2 MHz, $CDCl_3$): δ = 7.26 -7.21 (m, 5H), 6.89 (s, 2H), 5.93 (d, 1H, $^{2}J_{HH}$ = 1.4 Hz), 5.07 (d, 1H, $^{2}J_{HH}$ = 1.4 Hz), 2.29 (s, 3H) and 2.08 (s, 6H) ppm.

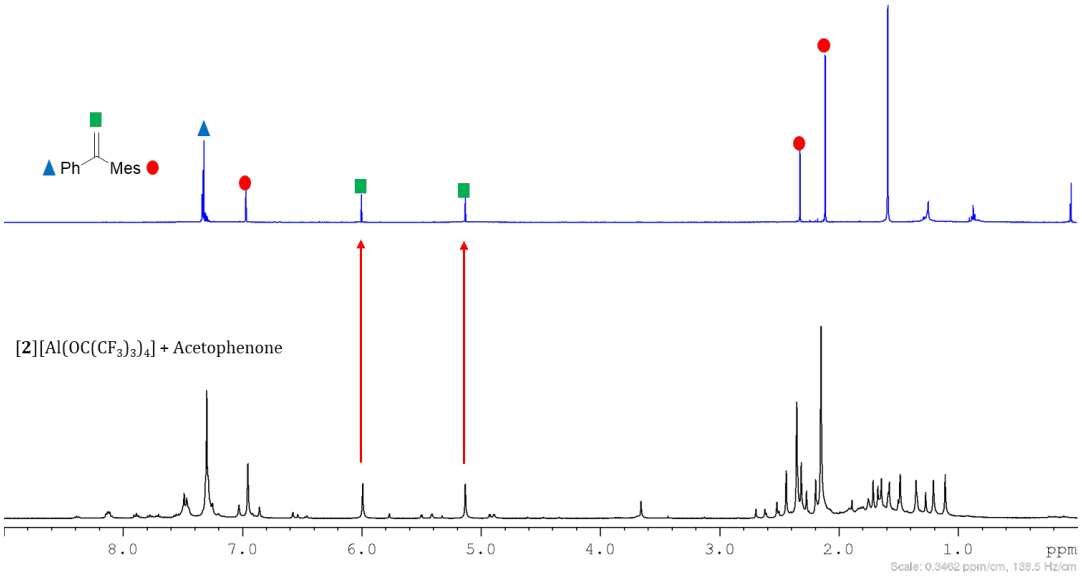

Figure S4. ^{1}H NMR spectra of 1-phenyl-1-mesityl ethylene (top) and the crude reaction mixture [**2**][Al(OC(CF$_3$)$_3$)$_4$] + acetophenone (bottom).

Reaction of [2][Al(OC(CF$_3$)$_3$)$_4$] and Et$_3$SiH

Et$_3$SiH (5.2 µL; 0.03 mmol) is added to [**2**][Al(OC(CF$_3$)$_3$)$_4$] (40.5 mg; 0.03 mmol) in CDCl$_3$ in a J. Young's NMR tube. As shown in Figure S5, no decomposition of [**2**]$^+$ was identified, and Et$_3$SiH is converted to a new species which is assigned to (Et$_3$Si)$_2$.

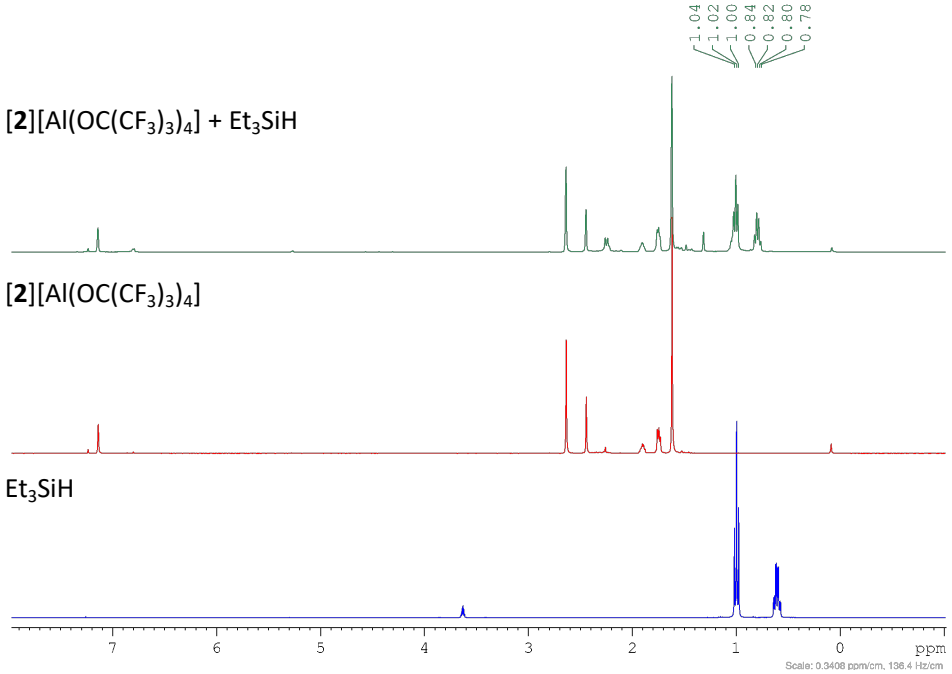

Figure S5. ^{1}H NMR spectra of the crude reaction mixture [**2**][Al(OC(CF$_3$)$_3$)$_4$] and Et$_3$SiH (top), [**2**]$^+$ (middle), and Et$_3$SiH (bottom).

4. Catalysis studies.

Catalytic cyanosilylation of ketones and aldehydes.

In the J. Young NMR tube, the substrate (0.28 mmol) and TMSCN (52.5 μL, 0.42 mmol) are mixed into the $CDCl_3$ solution (0.4 mL). Catalyst [**2**][BAr^F] (13.3 mg, 0.014 mmol) was added to the mixed solution. The reaction was then monitored using ^1H NMR spectroscopy. Afterward, 0.04 mmol of naphthalene (50 μL, 0.8 M in $CDCl_3$) was added to the J. Young NMR tube to determine the product yield.

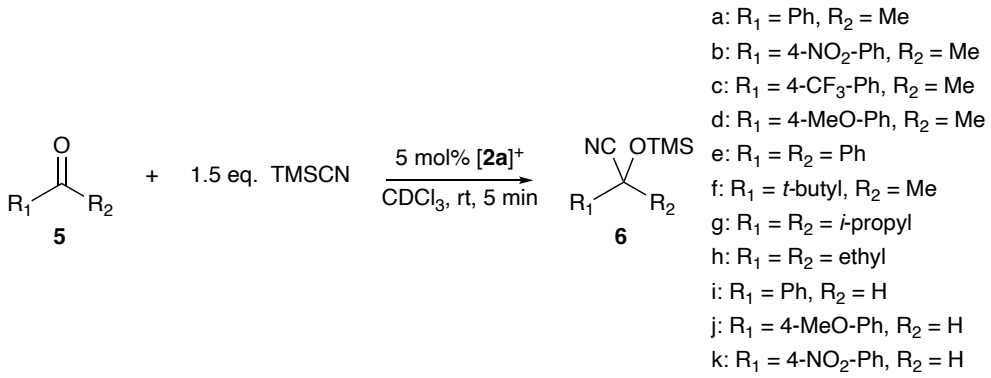

6a: 99% NMR yield. ^1H NMR (400.2 MHz, $CDCl_3$): δ = 7.56 – 7.60 (m, 2 H), 7.35 – 7.44 (m, 3 H), 1.89 (s, 3 H) and 0.22 (s, 9 H) ppm.

6b: 99% NMR yield. ^1H NMR (400.2 MHz, $CDCl_3$): δ = 8.26 (d, 2 H, $^3J_{HH}$ = 8.91 Hz), 7.75 (d, 2 H, $^3J_{HH}$ = 8.89 Hz), 1.88 (s, 3 H) and 0.25 (s, 9 H) ppm.

6c: 99% NMR yield. ^1H NMR (400.2 MHz, $CDCl_3$): δ = 7.67 – 7.72 (m, 4 H), 1.89 (s, 3 H) and 0.25 (s, 9 H) ppm.

6d: 99% NMR yield. ^1H NMR (400.2 MHz, $CDCl_3$): δ = 7.49 (d, 2 H, $^3J_{HH}$ = 8.4 Hz), 6.93 (d, 2 H, $^3J_{HH}$ = 9.0 Hz), 3.83 (s, 3 H), 1.88 (s, 3 H) and 0.19 (s, 9 H) ppm.

6e: 99% NMR yield. ^{1}H NMR (400.2 MHz, $CDCl_3$): δ = 7.54 – 7.58 (m, 4 H), 7.35 – 7.43 (m, 6 H) and 0.20 (s, 9 H) ppm.

6f: 99% NMR yield. ^{1}H NMR (400.2 MHz, $CDCl_3$): δ = 1.52 (s, 3H), 1.04 (s, 9 H), 5.54 (s, 1 H) and 0.25 (s, 9 H) ppm.

6g: 99% NMR yield. ^{1}H NMR (400.2 MHz, $CDCl_3$): δ = 2.02 (set, 2 H, J = 6.79 Hz), 1.07 (d, 6 H, $^{3}J_{HH}$ = 6.75 Hz), 1.00 (d, 6 H, $^{3}J_{HH}$ = 6.63 Hz) and 0.26 (s, 9 H) ppm.

6h: 99% NMR yield. ^{1}H NMR (400.2 MHz, $CDCl_3$): δ = 1.77 (q, 4H, J = 7.42 Hz), 1.04 (t, 6 H, J = 7.35 Hz) and 0.25 (s, 9 H) ppm.

6i: 99% NMR yield. ^{1}H NMR (400.2 MHz, $CDCl_3$): δ = 7.5 – 7.53 (m, 3H), 7.43 – 7.45 (m, 2 H), 5.54 (s, 1 H) and 0.28 (s, 9 H) ppm.

6j: 99% NMR yield. ^{1}H NMR (400.2 MHz, $CDCl_3$): δ = 7.42 (d, 2 H, $^{3}J_{HH}$ = 8.51 Hz), 6.96 (d, 2 H, $^{3}J_{HH}$ = 8.73 Hz), 5.48 (s, 1 H), 3.83 (s, 3 H) and 0.25 (s, 9 H) ppm.

6k: 99% NMR yield. ^{1}H NMR (400.2 MHz, $CDCl_3$): δ = 8.27 (d, 2 H, $^{3}J_{HH}$ = 8.64 Hz), 7.68 (d, 2H, $^{3}J_{HH}$ = 8.68 Hz), 5.63 (s, 1 H) and 0.29 (s, 9 H) ppm.

Catalytic hydrosilylation of ketones and aldehydes by $[2]^{+}$

In the J. Young NMR tube, the substrate (0.28 mmol) and Et_3SiH (44.7 μL, 0.28 mmol) are mixed in $CDCl_3$ solution (0.4 mL). Then, catalyst [**2**][BAr^{F}] (13.3 mg, 0.014 mmol) was added to the mixture. The reaction was then monitored using ^{1}H NMR

spectroscopy. When no further change in ^{1}H NMR was observed, 0.04 mmol of naphthalene (50 μL, 0.8 M in $CDCl_3$) was added to the J. Young's NMR tube to determine the product yield.

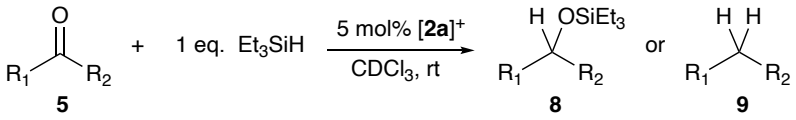

a: R_1 = Ph, R_2 = Me
b: R_1 = 4-NO_2-Ph, R_2 = Me
c: R_1 = 4-CF_3-Ph, R_2 = Me
d: R_1 = 4-MeO-Ph, R_2 = Me
e: R_1 = R_2 = Ph
f: R_1 = *t*-butyl, R_2 = Me
g: R_1 = R_2 = *i*-propyl
h: R_1 = R_2 = ethyl
i: R_1 = Ph, R_2 = H
j: R_1 = 4-MeO-Ph, R_2 = H
k: R_1 = 4-NO_2-Ph, R_2 = H

8a: 99% NMR yield. ^{1}H NMR (400 MHz, $CDCl_3$): δ = 7.34 – 7.44 (m, 5 H), 4.95 (q, 1 H, $^3J_{HH}$ = 6.22 Hz), 1.51 (d, 3 H, $^3J_{HH}$ = 6.52 Hz), 1.00 (t, 9 H, $^3J_{HH}$ = 7.92 Hz) and 0.61 – 0.69 (m, 6 H) ppm.

8b: 99% NMR yield. ^{1}H NMR (400.2 MHz, $CDCl_3$): δ = 8.20 (d, 2 H, $^3J_{HH}$ = 8.72 Hz), 7.54 (d, 2 H, $^3J_{HH}$ = 8.69 Hz), 4.99 (q, 1 H, $^3J_{HH}$ = 6.23 Hz), 1.46 (d, 3 H, $^3J_{HH}$ = 6.29 Hz), 0.95 (t, 9 H, $^3J_{HH}$ = 7.67 Hz) and 0.58 – 0.66 (m, 6 H) ppm.

8c: 99% NMR yield. ^{1}H NMR (400.2 MHz, $CDCl_3$): δ = 7.62 (d, 2 H, $^3J_{HH}$ = 8.37 Hz), 7.51 (d, 2 H, $^3J_{HH}$ = 8.48 Hz), 4.98 (q, 1 H, $^3J_{HH}$ = 6.4 Hz), 1.48 (d, 3 H, $^3J_{HH}$ = 5.94 Hz), 0.98 (t, 9 H, $^3J_{HH}$ = 8.18 Hz) and 0.61 – 0.69 (m, 6 H) ppm.

9d: 28% NMR yield. ^{1}H NMR (400.2 MHz, $CDCl_3$): δ = 7.15 (d, 2 H, $^3J_{HH}$ = 8.52 Hz), 6.87 (d, 2 H, $^3J_{HH}$ = 8.75 Hz), 3.81 (s, 3 H), 1.25 (t, 3 H, $^3J_{HH}$ = 7.48 Hz) and 0.85 (t, 2 H, $^3J_{HH}$ = 7.41 Hz) ppm.

9e: 51.3% NMR yield. ^{1}H NMR (400.2 MHz, $CDCl_3$): δ = 7.34 – 7.38 (m, 4 H), 7.24 – 7.3 (m, 6 H) and 4.06 (s, 2 H) ppm.

8f: 93.9% NMR yield. ^{1}H NMR (400.2 MHz, $CDCl_3$): δ = 3.5 (q, 1 H, $^{3}J_{HH}$ = 6.68 Hz), 1.09 (d, 3 H, $^{3}J_{HH}$ = 5.93 Hz), 1.01 (t, 9 H, $^{3}J_{HH}$ = 7.71 Hz), 0.89 (s, 9 H) and 0.63 (q, 6 H, $^{3}J_{HH}$ = 7.89 Hz) ppm.

8g: 71.9% NMR yield. ^{1}H NMR (400.2 MHz, $CDCl_3$): δ = 3.20 (t, 1 H, $^{3}J_{HH}$ = 4.99 Hz), 1.74 – 1.82 (m, 2 H), 1.02 (t, 9 H, $^{3}J_{HH}$ = 8.01 Hz), 0.92 (d, 6 H, $^{3}J_{HH}$ = 2.37 Hz), 0.90 (d, 6 H, $^{3}J_{HH}$ = 2.29 Hz) and 0.67 (q, 6 H, $^{3}J_{HH}$ = 7.79 Hz) ppm.

8h: 99% NMR yield. ^{1}H NMR (400.2 MHz, $CDCl_3$): δ = 3.56 (quin, 1 H, $^{3}J_{HH}$ = 5.78 Hz), 1.45 – 1.55 (m, 4 H), 1.01 (t, 9 H, $^{3}J_{HH}$ = 7.78 Hz), 0.91 (d, 6 H, $^{3}J_{HH}$ = 7.53 Hz) and 0.64 (q, 6 H, $^{3}J_{HH}$ = 7.98 Hz) ppm.

8i: 99% NMR yield. ^{1}H NMR (400.2 MHz, $CDCl_3$): δ = 7.39 – 7.45 (m, 5 H), 4.83 (s, 2 H), 1.07 (t, 9 H, $^{3}J_{HH}$ = 7.88 Hz) and 0.75 (q, 6 H, $^{3}J_{HH}$ = 7.81 Hz) ppm.

8j: 49.6% NMR yield. ^{1}H NMR (400.2 MHz, $CDCl_3$): δ = 7.31 (d, 2 H, $^{3}J_{HH}$ = 8.44 Hz), 6.92 (d, 2 H, $^{3}J_{HH}$ = 7.84 Hz), 4.72 (s, 2 H), 3.83 (s, 3. H), 1.03 (m, 9 H) and 0.70 (q, 6 H, $^{3}J_{HH}$ = 7.83 Hz) ppm.

8k: 99% NMR yield. ^{1}H NMR (400.2 MHz, $CDCl_3$): δ = 8.21 (d, 2 H, $^{3}J_{HH}$ = 8.86 Hz), 7.53 (d, 2 H, $^{3}J_{HH}$ = 7.86 Hz), 4.86 (s, 2 H), 1.03 (t, 9 H, J = 7.61 Hz) and 0.71 (q, 6 H, $^{3}J_{HH}$ = 7.86 Hz) ppm.

5. Crystal Data.

Crystallographic data collections were carried out with an Oxford Gemini Duo system diffractometer with graphite-monochromated Mo Kα radiation (150 K, λ = 0.71073 Å). Data were all collected at 150(2) K. Structures were solved by the direct method and refined by least-square cycles. All calculations were performed using the SHELXTL-97 package. Crystallographic data have been deposited at the Cambridge Crystallographic Data Center with deposition number of CCDC 2120763 (**1a**), CCDC 2120765 (**1b**), and CCDC 2120764 ([**3**][Al(OC(CF_3)$_3$)$_4$]).

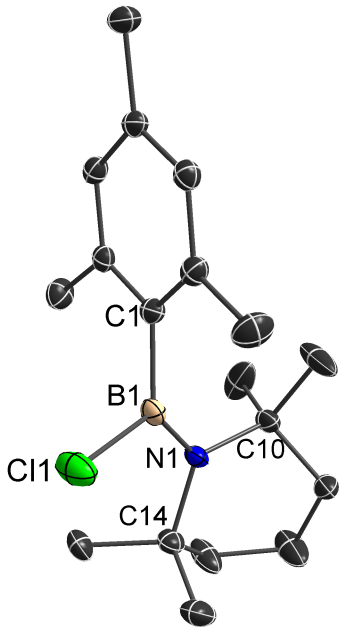

Figure S6: Molecular structure of compound **1a**. Hydrogen atoms are omitted for clarity. Thermal ellipsoids are set at 50% probability. Selected bond lengths [Å] and angles [º]: Cl(1)-B(1) 1.839(3), N(1)-B(1) 1.402(3), N(1)-C(10) 1.521(3), N(1)-C(14) 1.533(3), B(1)-C(1) 1.591(3), B(1)-N(1)-C(10), 121.74(19), B(1)-N(1)-C(14) 122.14(18), C(10)-N(1)-C(14) 116.12(17), N(1)-B(1)-C(1) 130.7(2), N(1)-B(1)-Cl(1) 121.49(18), C(1)-B(1)-Cl(1) 107.81(16).

Table S2. Crystal data and experimental details for **1a** (ic20807)

Identification code	ic20807	
Empirical formula	C18 H29 B Cl N	
Formula weight	305.68	
Crystal system	Monoclinic	
Space group	$P2_1/c$	
Unit cell dimensions	a = 11.2578(14) Å	α= 90°.
	b = 13.1467(15) Å	β= 106.814(12)°.
	c = 12.4351(15) Å	γ = 90°.
Volume	1761.8(4) $Å^3$	
Z	4	
F(000)	664	
Density (calculated)	1.152 Mg/m^3	
Wavelength	0.71073 Å	
Cell parameters reflections used	3600	
Theta range for Cell parameters	4.0340 to 29.8370°.	
Absorption coefficient	0.211 mm^{-1}	
Temperature	100(2) K	
Crystal size	0.20 x 0.20 x 0.15 mm^3	
Diffractometer	Xcalibur, Atlas, Gemini	
Absorption correction	Semi-empirical from equivalents	
Max. and min. transmission	1.00000 and 0.91888	
No. of measured reflections	9249	
No. of independent reflections	4047 [R(int) = 0.0408]	
No. of observed [I>2_igma(I)]	3090	
Completeness to theta = 25.242°	99.8 %	
Theta range for data collection	3.099 to 27.497°.	
Final R indices [I>2sigma(I)]	R1 = 0.0634, wR2 = 0.1751	
R indices (all data)	R1 = 0.0821, wR2 = 0.1934	
Goodness-of-fit on F^2	1.017	
No. of reflections	4047	
No. of parameters	190	
No. of restraints	0	
Largest diff. peak and hole	0.471 and -0.570 e.$Å^{-3}$	

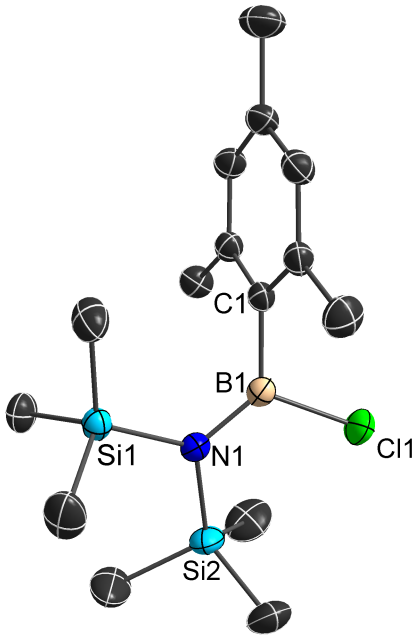

Figure S7. Molecular structure of compound **1b**. Hydrogen atoms are omitted for clarity. Thermal ellipsoids are set at 50% probability. Selected bond lengths [Å] and angles [º]: B(1)-N(1) 1.4076(18), B(1)-C(1) 1.5679(19), B(1)-Cl(1) 1.8214(14), Si(1)-N(1) 1.7865(11), Si(2)-N(1) 1.7868(11), N(1)-B(1)-C(1) 128.49(11), N(1)-B(1)-Cl(1) 119.51(10), C(1)-B(1)-Cl(1) 111.98(9), B(1)-N(1)-Si(1) 121.65(9), B(1)-N(1)-Si(2) 119.28(9), Si(1)-N(1)-Si(2) 119.05(6).

Table S3. Crystal data and structure refinement for **1b** (ic20564).

Identification code	ic20564	
Empirical formula	C15 H29 B Cl N Si2	
Formula weight	325.83	
Temperature	200(2) K	
Wavelength	0.71073 Å	
Crystal system	Monoclinic	
Space group	$P2_1/c$	
Unit cell dimensions	a = 8.7219(3) Å	α= 90°.
	b = 13.0132(4) Å	β= 91.2092(11)°.
	c = 17.0764(6) Å	γ = 90°.
Volume	1937.74(11) $Å^3$	
Z	4	
Density (calculated)	1.117 Mg/m^3	
Absorption coefficient	0.313 mm^{-1}	
F(000)	704	
Crystal size	0.283 x 0.273 x 0.175 mm^3	
Theta range for data collection	1.968 to 29.997°.	
Index ranges	-12<=h<=12, -18<=k<=18, -24<=l<=23	
Reflections collected	17559	
Independent reflections	5643 [R(int) = 0.0299]	
Completeness to theta = 25.242°	99.9 %	
Absorption correction	Semi-empirical from equivalents	
Max. and min. transmission	0.9281 and 0.8280	
Refinement method	Full-matrix least-squares on F^2	
Data / restraints / parameters	5643 / 0 / 190	
Goodness-of-fit on F^2	1.035	
Final R indices [I>2sigma(I)]	R1 = 0.0389, wR2 = 0.1105	
R indices (all data)	R1 = 0.0456, wR2 = 0.1165	
Extinction coefficient	n/a	
Largest diff. peak and hole	0.393 and -0.372 $e.Å^{-3}$	

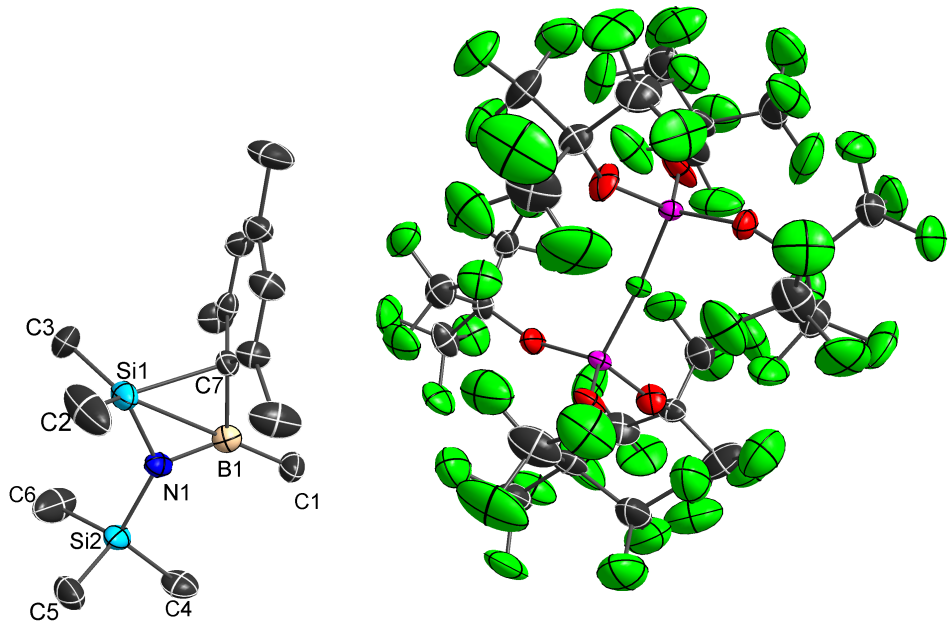

Figure S8. Molecular structure of compound [**3**][Al(OC(CF$_3$)$_3$)$_4$]. Hydrogen atoms are omitted for clarity. Thermal ellipsoids are set at 50% probability. Selected bond lengths [Å] and angles [º]: Si(1)-N(1) 1.717(6), Si(1)-C(2) 1.844(11), Si(1)-C(3) 1.855(12), Si(1)-C(7) 2.040(7), Si(1)-B(1) 2.296(9), Si(2)-N(1) 1.783(6), Si(2)-C(4) 1.840(9), Si(2)-C(5) 1.855(9), Si(2)-C(6) 1.859(10), B(1)-N(1) 1.417(10), B(1)-C(1) 1.544(11), B(1)-C(7) 1.666(10), N(1)-Si(1)-C(2) 116.3(5), N(1)-Si(1)-C(3) 116.9(5), C(2)-Si(1)-C(3) 112.5(7), N(1)-Si(1)-C(7) 82.7(3), C(2)-Si(1)-C(7) 111.9(5), C(3)-Si(1)-C(7) 113.1(4), N(1)-Si(1)-B(1) 38.0(3), C(2)-Si(1)-B(1) 122.5(6), C(3)-Si(1)-B(1) 124.9(5), C(7)-Si(1)-B(1) 44.7(3), N(1)-Si(2)-C(4) 110.5(4), N(1)-Si(2)-C(5) 107.9(4), C(4)-Si(2)-C(5) 110.6(4), N(1)-Si(2)-C(6) 106.1(4), C(4)-Si(2)-C(6) 111.4(5), C(5)-Si(2)-C(6) 110.2(6), N(1)-B(1)-C(1) 131.8(7), N(1)-B(1)-C(7) 107.7(6), C(1)-B(1)-C(7) 120.4(6), N(1)-B(1)-Si(1) 48.3(3), C(1)-B(1)-Si(1) 177.8(6), C(7)-B(1)-Si(1) 59.5(3), B(1)-N(1)-Si(1) 93.7(4), B(1)-N(1)-Si(2) 134.8(5), Si(1)-N(1)-Si(2) 131.5(4), B(1)-C(7)-Si(1) 75.8(4)

Table S4. Crystal data and structure refinement for [**3**][Al(OC(CF_3)$_3$)$_4$] (ic20708).

Identification code	ic20708	
Empirical formula	C39 H29 Al2 B F55 N O6 Si2	
Formula weight	1773.58	
Temperature	150(2) K	
Wavelength	0.71073 Å	
Crystal system	Orthorhombic	
Space group	$P2_12_12_1$	
Unit cell dimensions	a = 14.8299(5) Å	α= 90°.
	b = 17.7594(6) Å	β= 90°.
	c = 23.7368(8) Å	γ = 90°.
Volume	6251.6(4) $Å^3$	
Z	4	
Density (calculated)	1.884 Mg/m^3	
Absorption coefficient	0.294 mm^{-1}	
F(000)	3488	
Crystal size	0.356 x 0.074 x 0.064 mm^3	
Theta range for data collection	2.064 to 26.436°.	
Index ranges	-16<=h<=18, -22<=k<=20, -25<=l<=29	
Reflections collected	28151	
Independent reflections	12829 [R(int) = 0.0391]	
Completeness to theta = 25.242°	99.9 %	
Absorption correction	Semi-empirical from equivalents	
Max. and min. transmission	0.9705 and 0.7601	
Refinement method	Full-matrix least-squares on F^2	
Data / restraints / parameters	12829 / 58 / 966	
Goodness-of-fit on F^2	1.046	
Final R indices [I>2sigma(I)]	R1 = 0.0766, wR2 = 0.2002	
R indices (all data)	R1 = 0.0961, wR2 = 0.2183	
Absolute structure parameter	0.6(3)	
Extinction coefficient	n/a	
Largest diff. peak and hole	1.029 and -0.587 e.$Å^{-3}$	

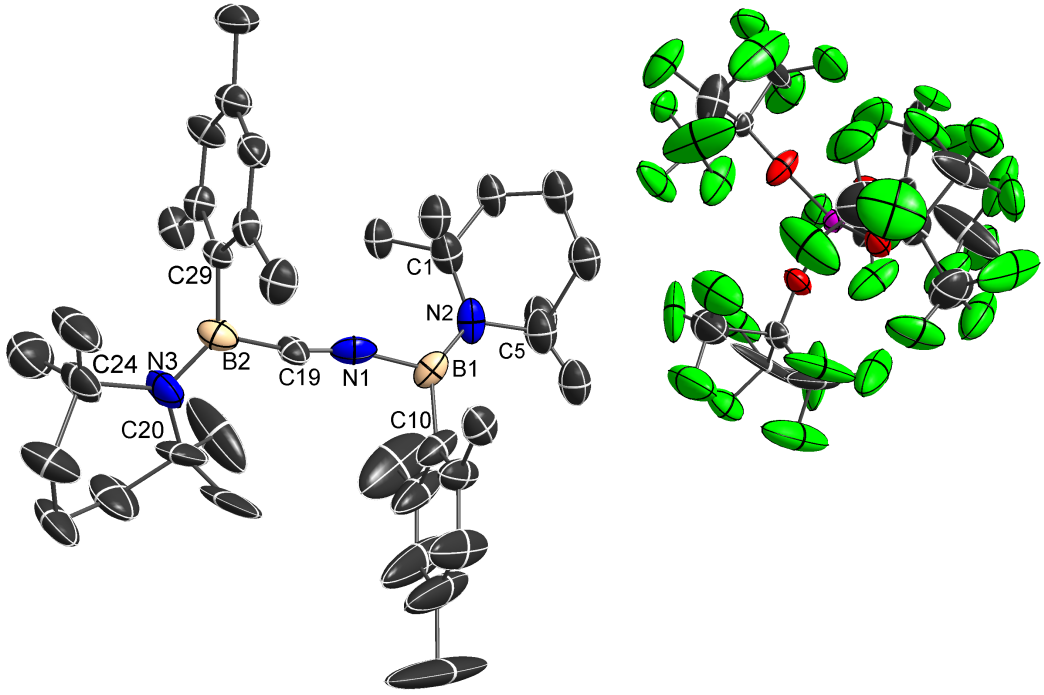

Figure S9. Molecular structure of [**7**][Al(OC(CF$_3$)$_3$)$_4$]. Hydrogen atoms are omitted for clarity. Thermal ellipsoids are set at 50% probability. As high-quality crystals of [**7**][Al(OC(CF$_3$)$_3$)$_4$] could not be obtained, no bond distances and angles is discussed.

Table S5. Crystal data and experimental details for [**7**][$Al(OC(CF_3)_3)_4$] (ic20861).

Identification code	ic20861	
Empirical formula	C53 H58 Al B2 F36 N3 O4	
Formula weight	1533.62	
Crystal system	Monoclinic	
Space group	C2/c	
Unit cell dimensions	a = 32.938(5) Å	α= 90°.
	b = 14.8849(12) Å	β= 121.58(2)°.
	c = 30.752(7) Å	γ = 90°.
Volume	12844(4) $Å^3$	
Z	8	
F(000)	6208	
Density (calculated)	1.586 Mg/m^3	
Wavelength	0.71073 Å	
Cell parameters reflections used	5519	
Theta range for Cell parameters	3.5720 to 25.1070°.	
Absorption coefficient	0.183 mm^{-1}	
Temperature	100(2) K	
Crystal size	0.15 x 0.10 x 0.05 mm^3	
Diffractometer	Xcalibur, Atlas, Gemini	
Absorption correction	Semi-empirical from equivalents	
Max. and min. transmission	1.00000 and 0.32004	
No. of measured reflections	26472	
No. of independent reflections	14660 [R(int) = 0.0751]	
No. of observed [I>2_igma(I)]	7808	
Completeness to theta = 25.242°	99.7 %	
Theta range for data collection	3.101 to 27.499°.	
Final R indices [I>2sigma(I)]	R1 = 0.2453, wR2 = 0.5071	
R indices (all data)	R1 = 0.3182, wR2 = 0.5396	
Goodness-of-fit on F^2	2.505	
No. of reflections	14660	
No. of parameters	935	
No. of restraints	486	
Largest diff. peak and hole	1.981 and -1.126 e.$Å^{-3}$	

NMR Spectra

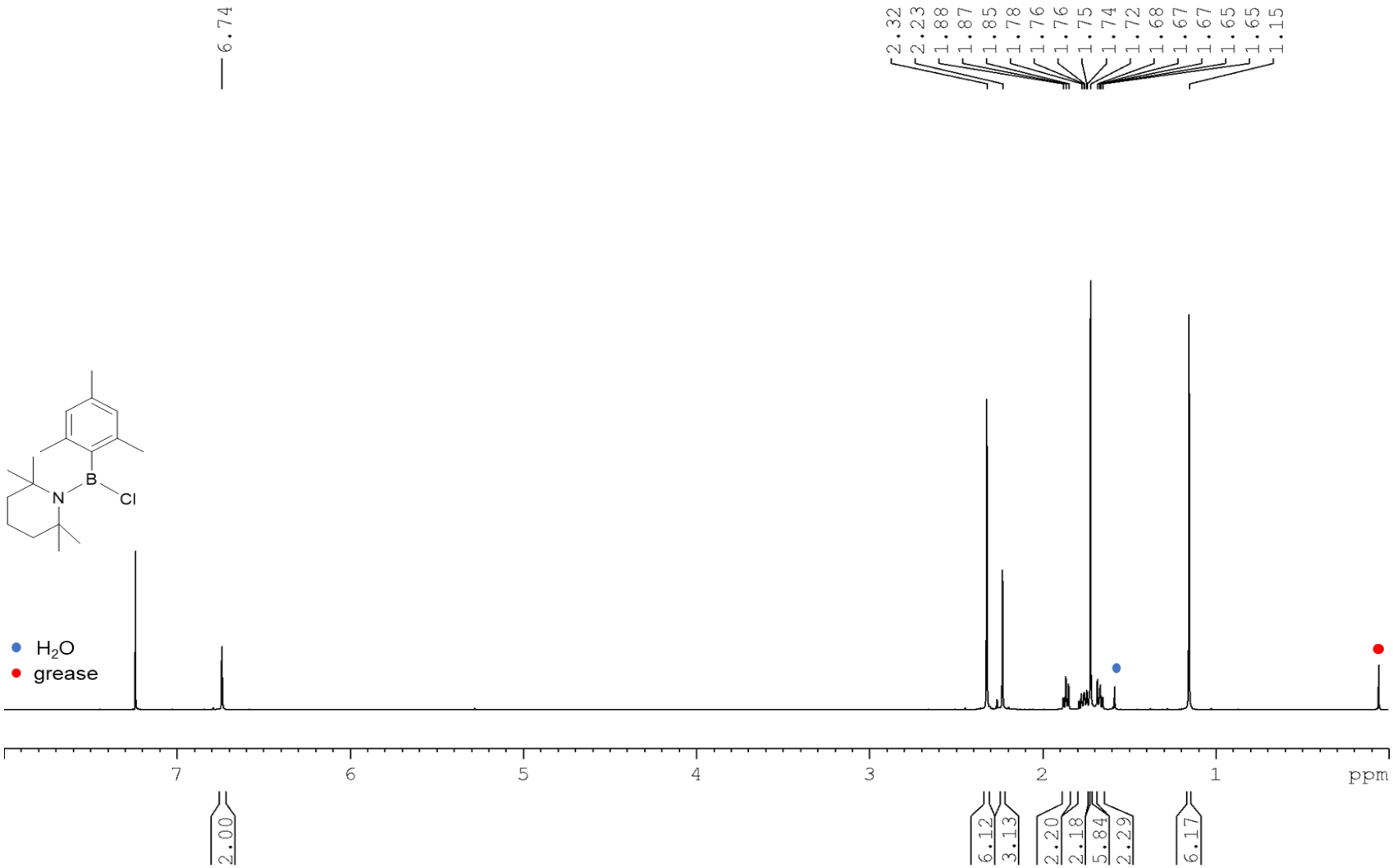

Figure S10. ^{1}H NMR spectrum of **1a** in $CDCl_3$.

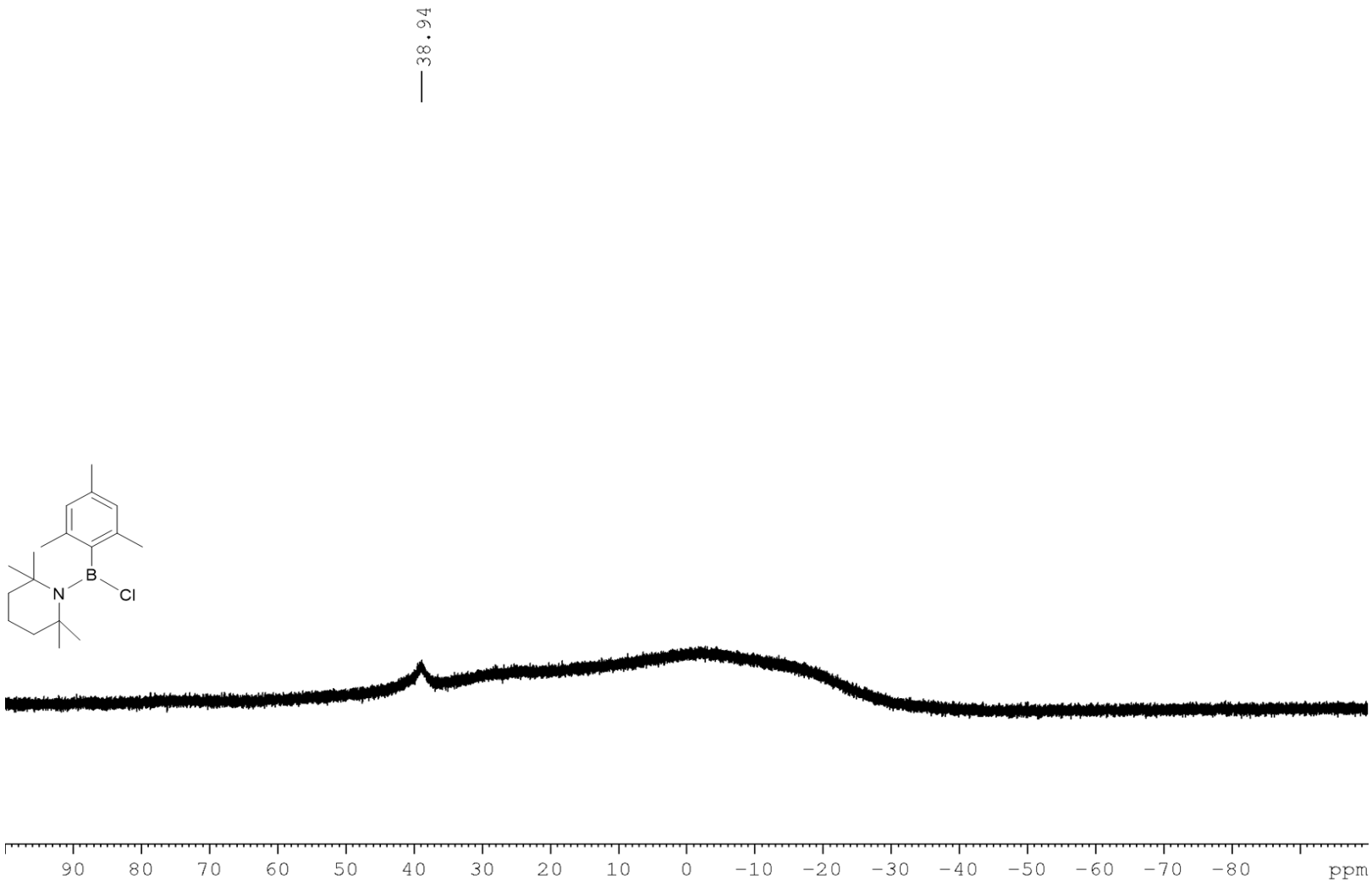

Figure S11. ^{11}B NMR spectrum of **1a** in $CDCl_3$.

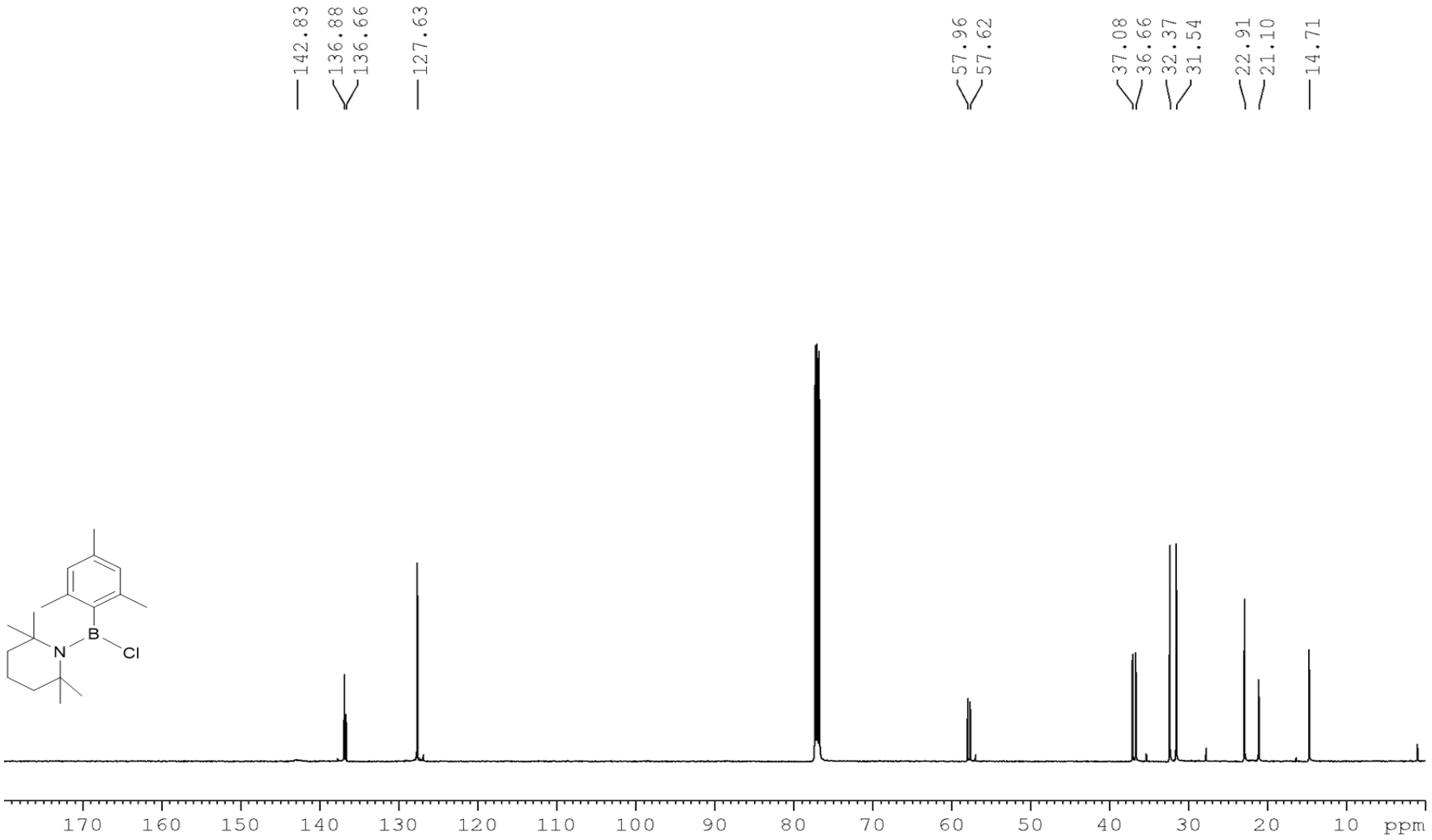

Figure S12. ^{13}C NMR spectrum of **1a** in $CDCl_3$.

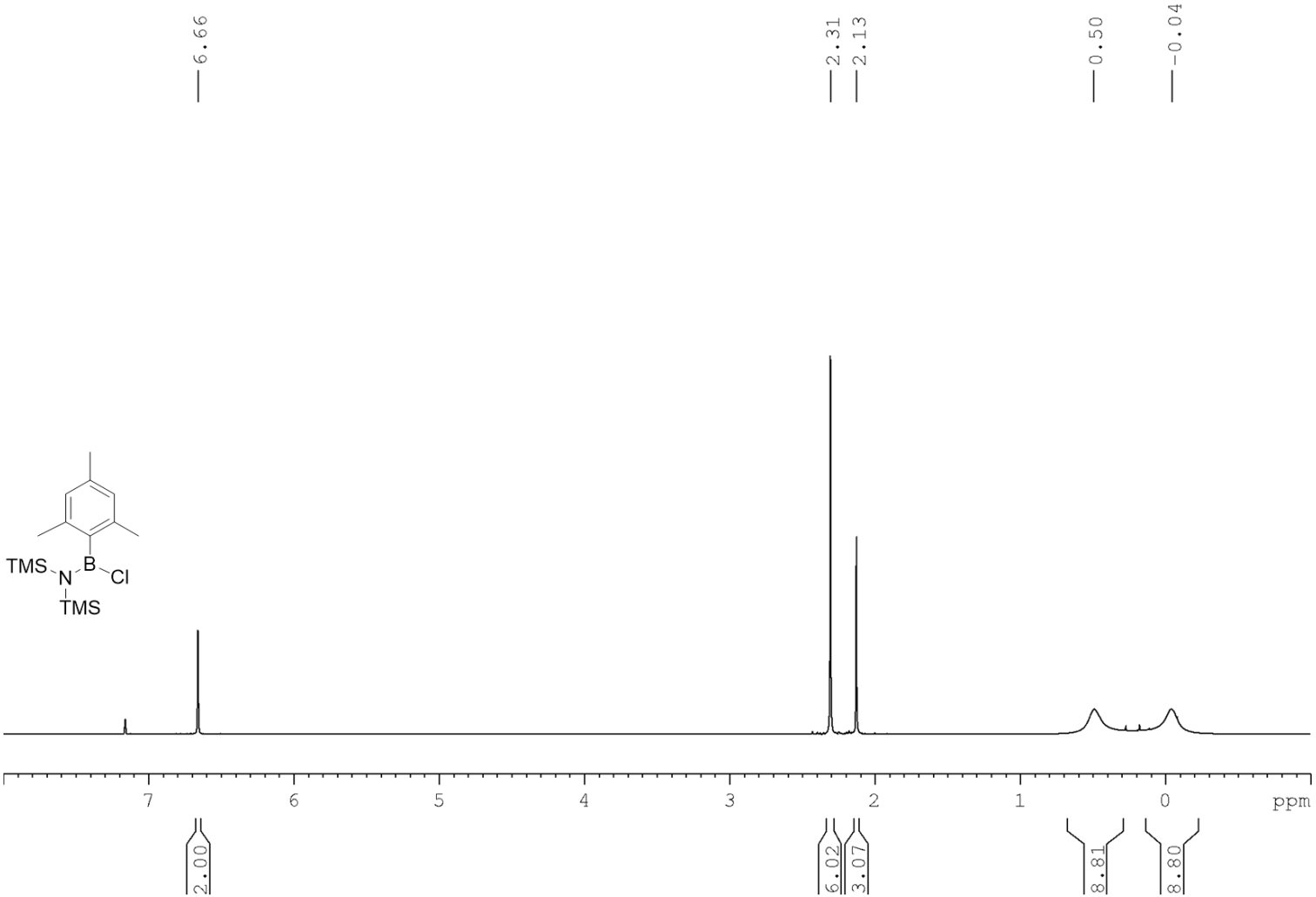

Figure S13. ^{1}H NMR spectrum of **1b** in C_6D_6.

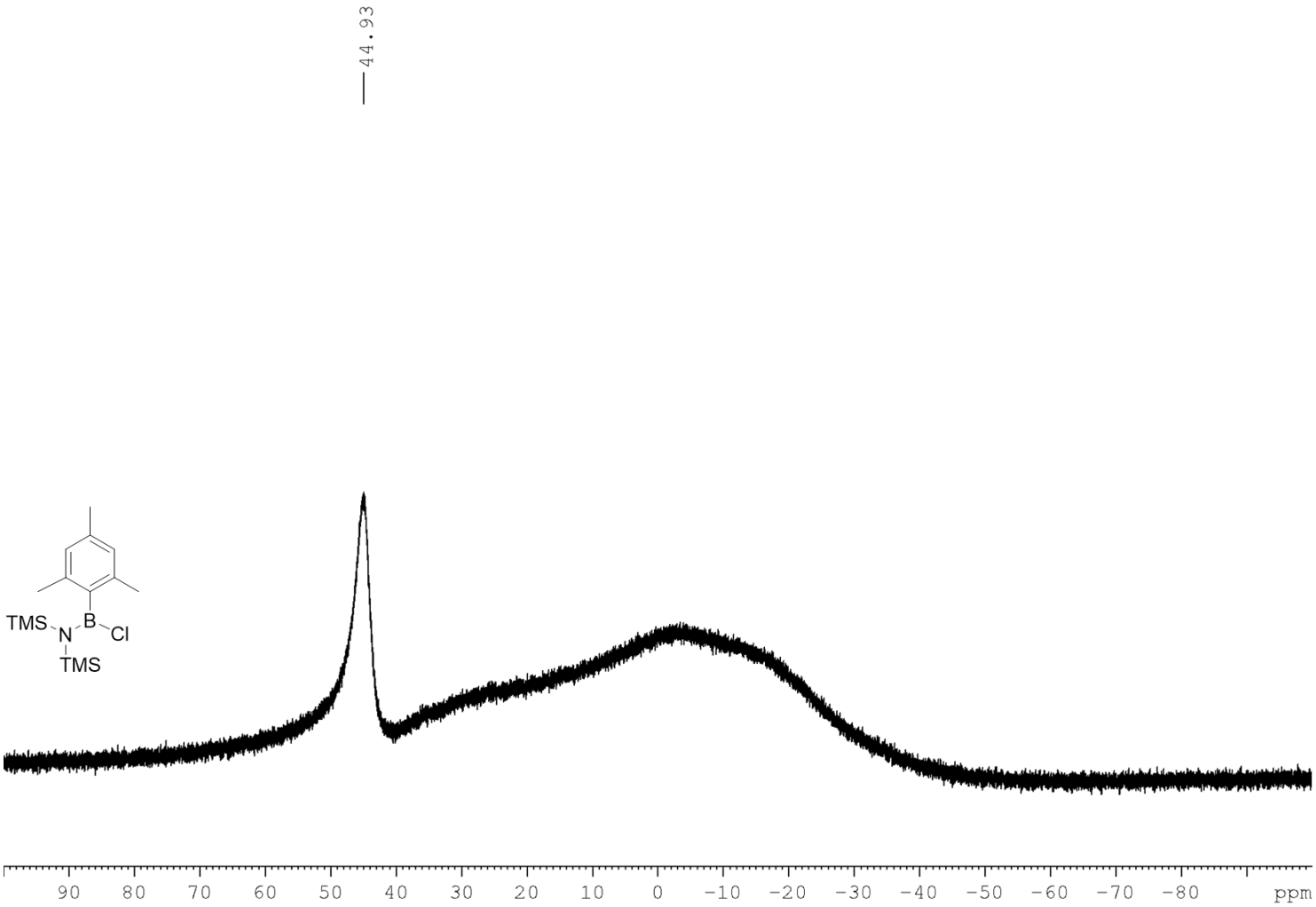

Figure S14. ^{11}B NMR spectrum of **1b** in C_6D_6.

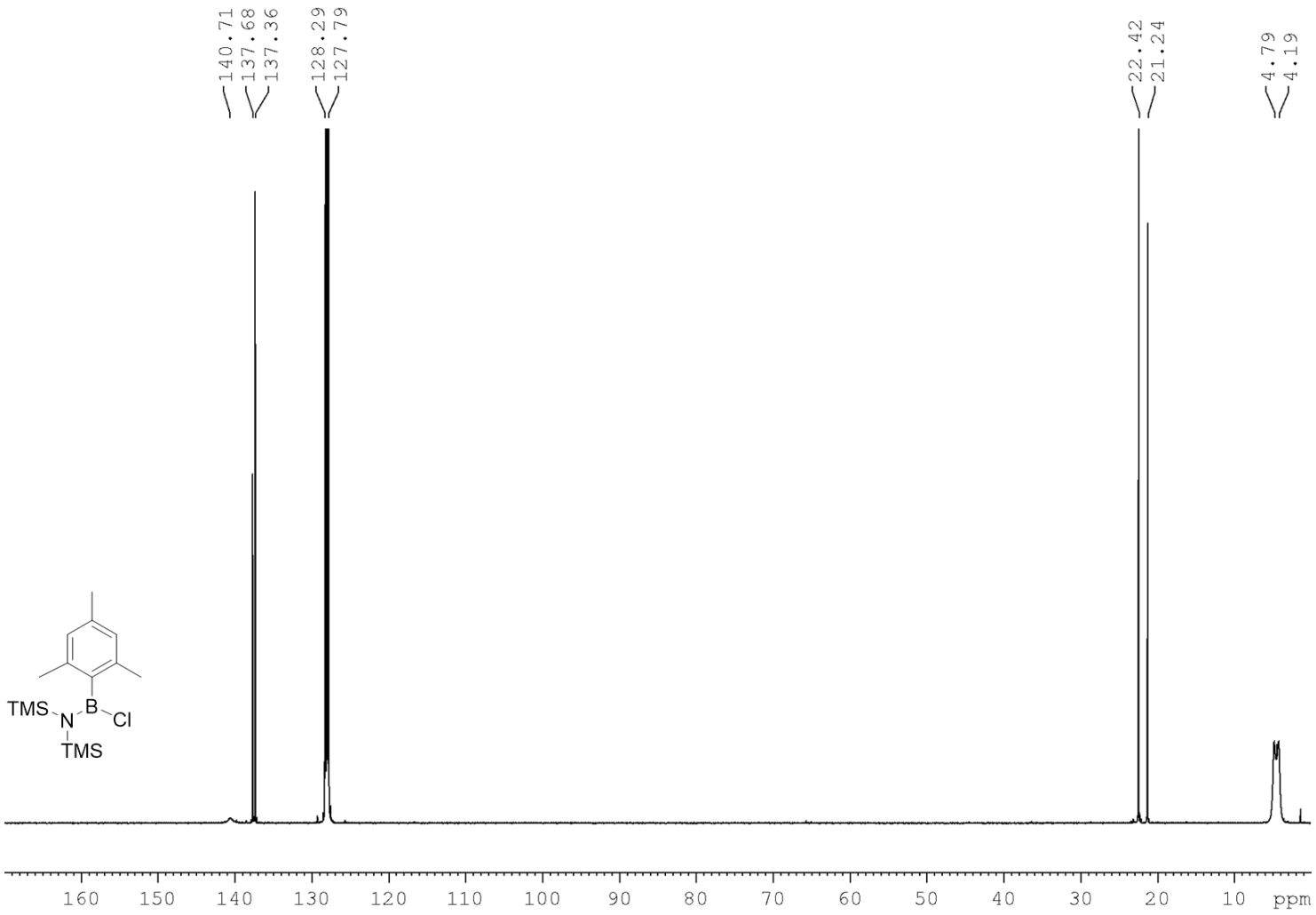

Figure S15. ^{13}C NMR spectrum of **1b** in C_6D_6.

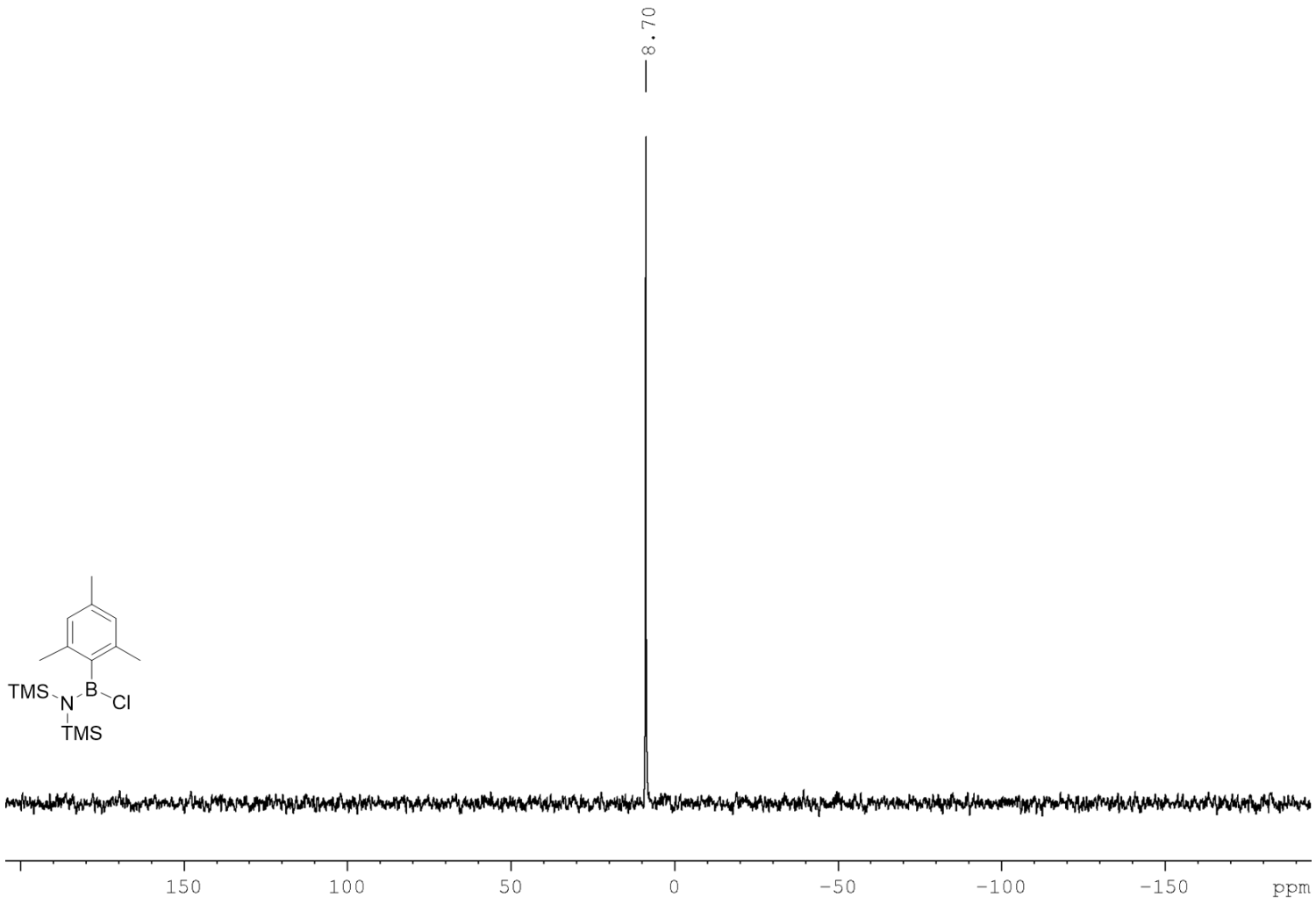

Figure S16. ^{29}Si NMR spectrum of **1b** in C_6D_6.

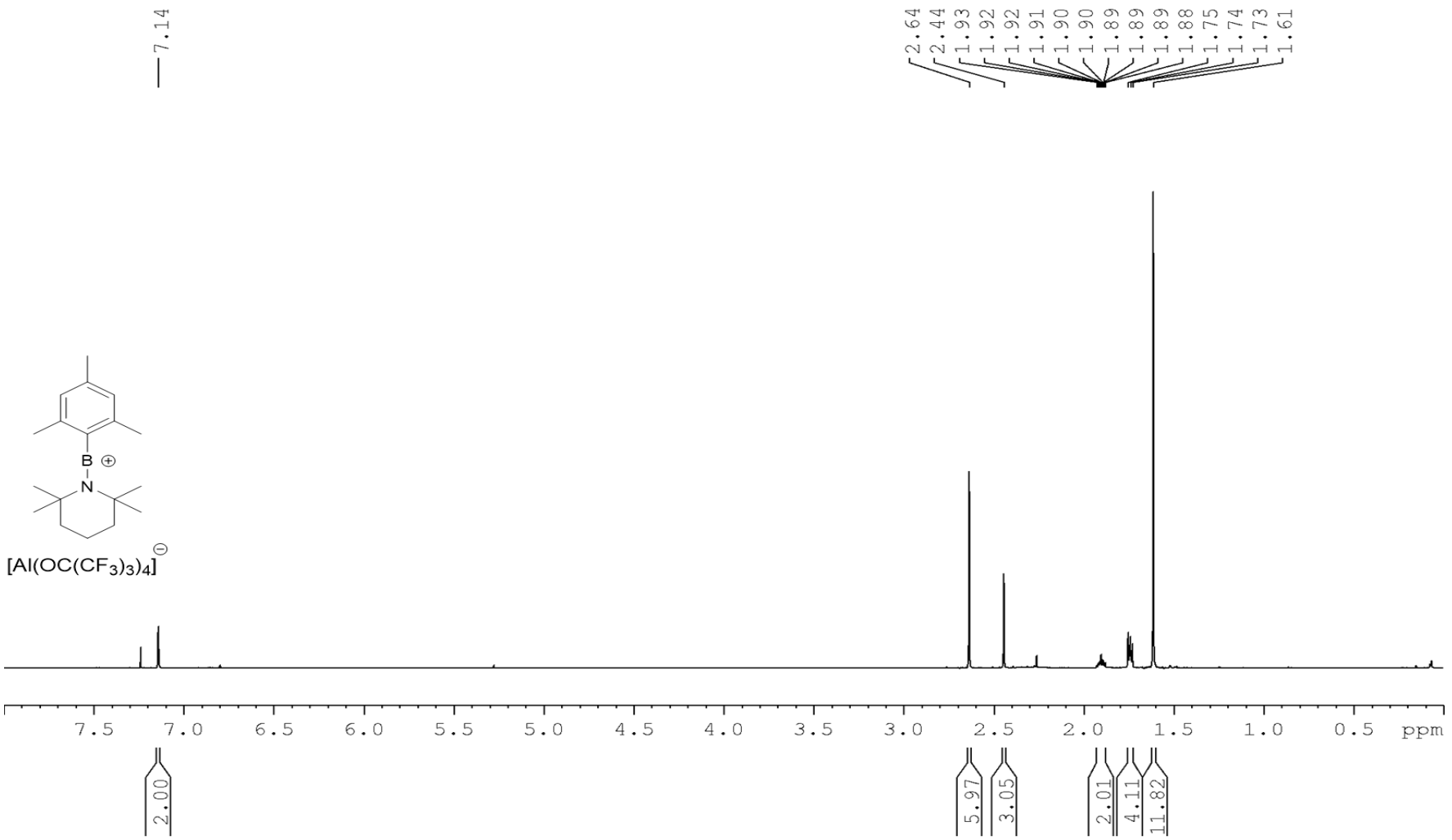

Figure S17. ^{1}H NMR spectrum of [**2**][$Al(OC(CF_3)_3)_4$] in $CDCl_3$.

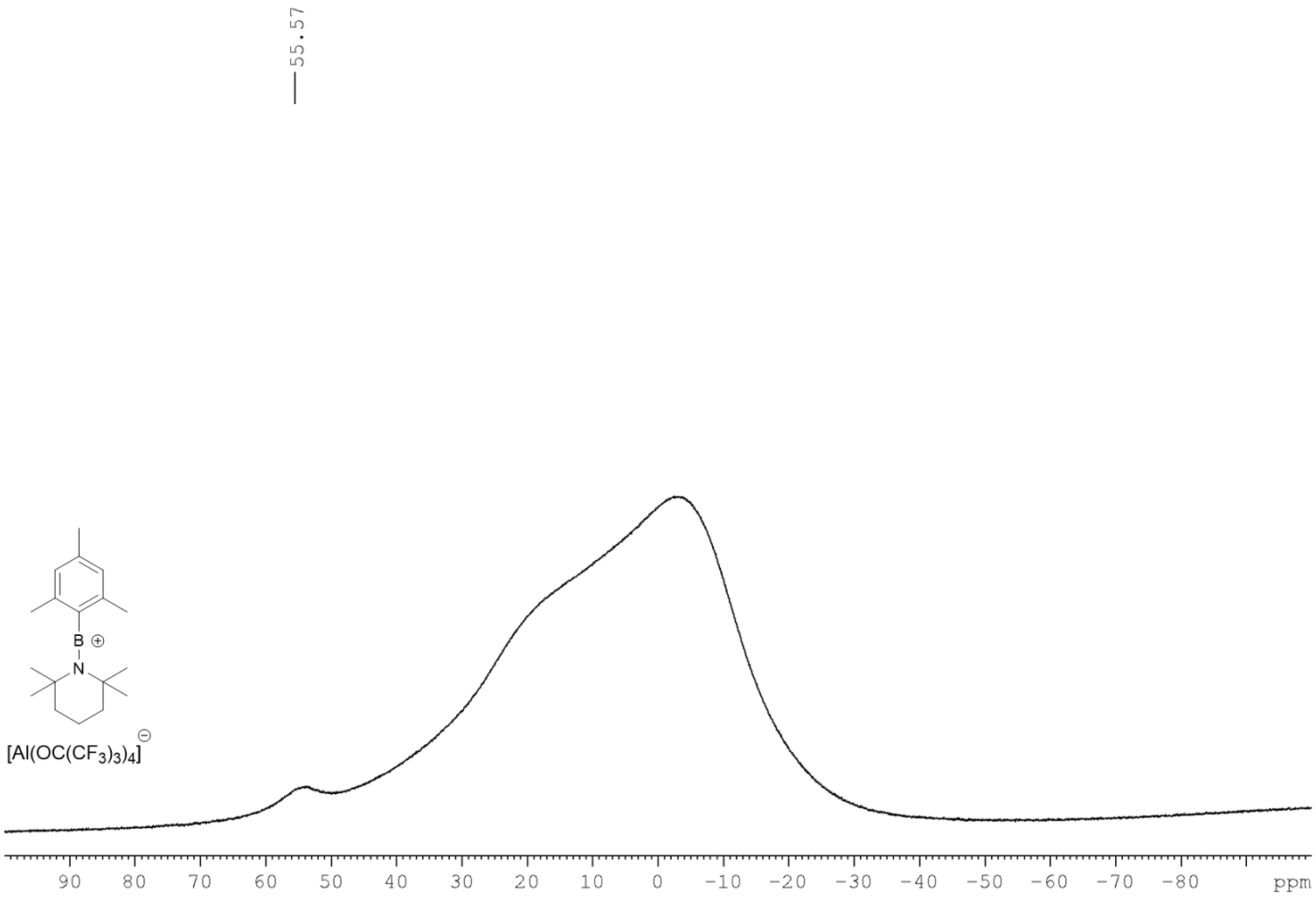

Figure S18. ^{11}B NMR spectrum of [**2**][$Al(OC(CF_3)_3)_4$] in $CDCl_3$.

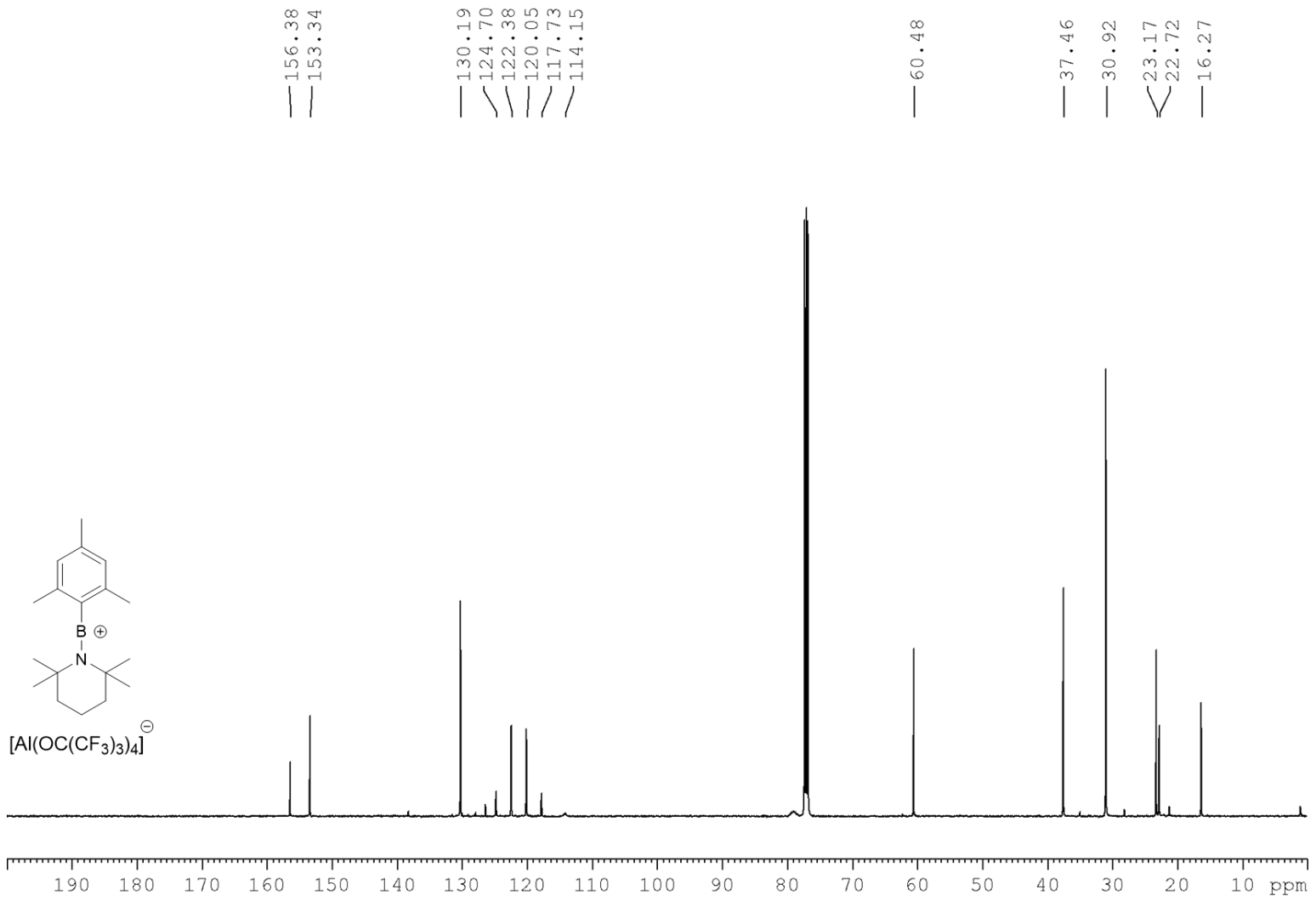

Figure S19.^{13}C NMR spectrum of [**2**][Al(OC(CF$_3$)$_3$)$_4$] in CDCl$_3$.

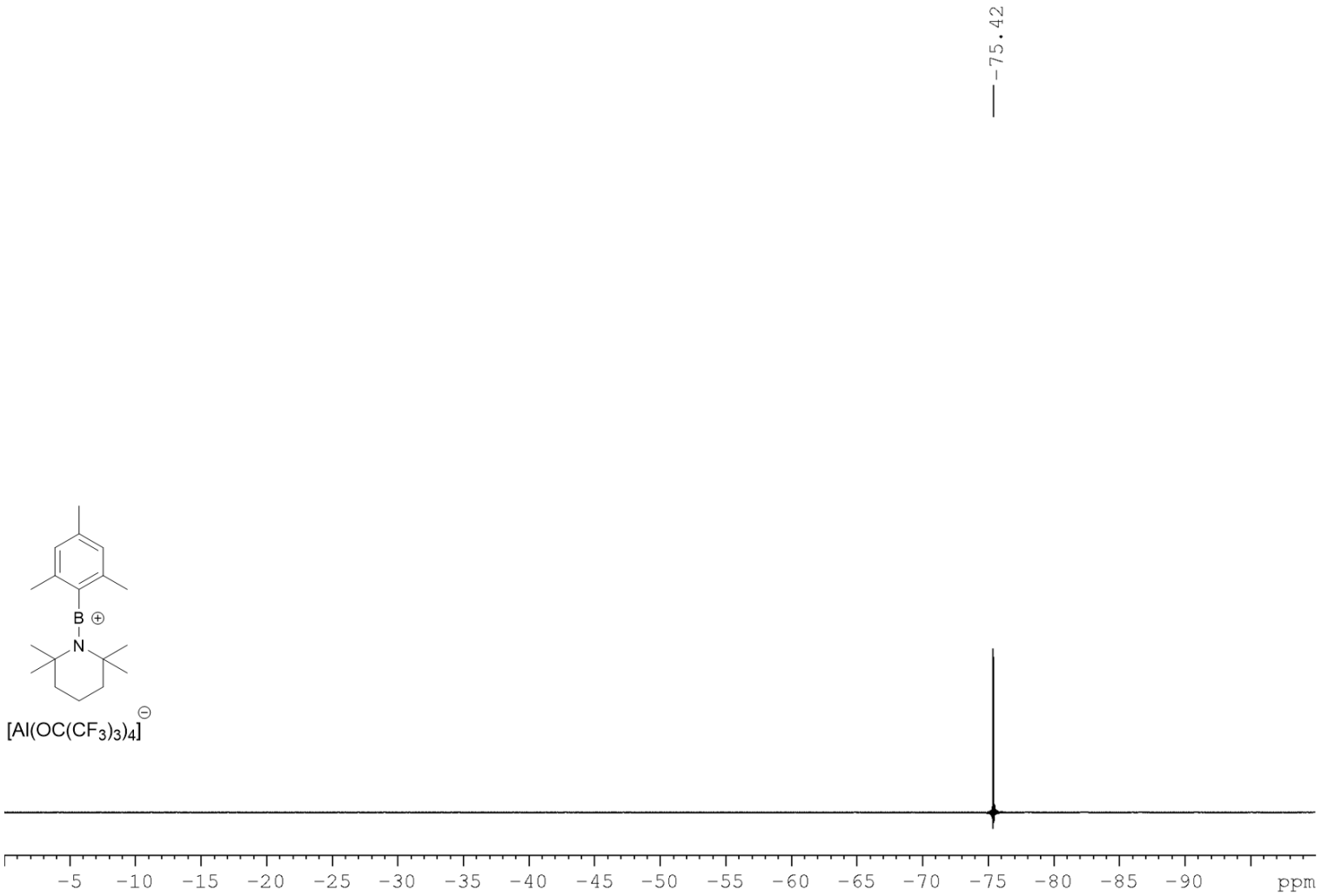

Figure S20. ^{19}F NMR spectrum of [**2**][$Al(OC(CF_3)_3)_4$] in $CDCl_3$.

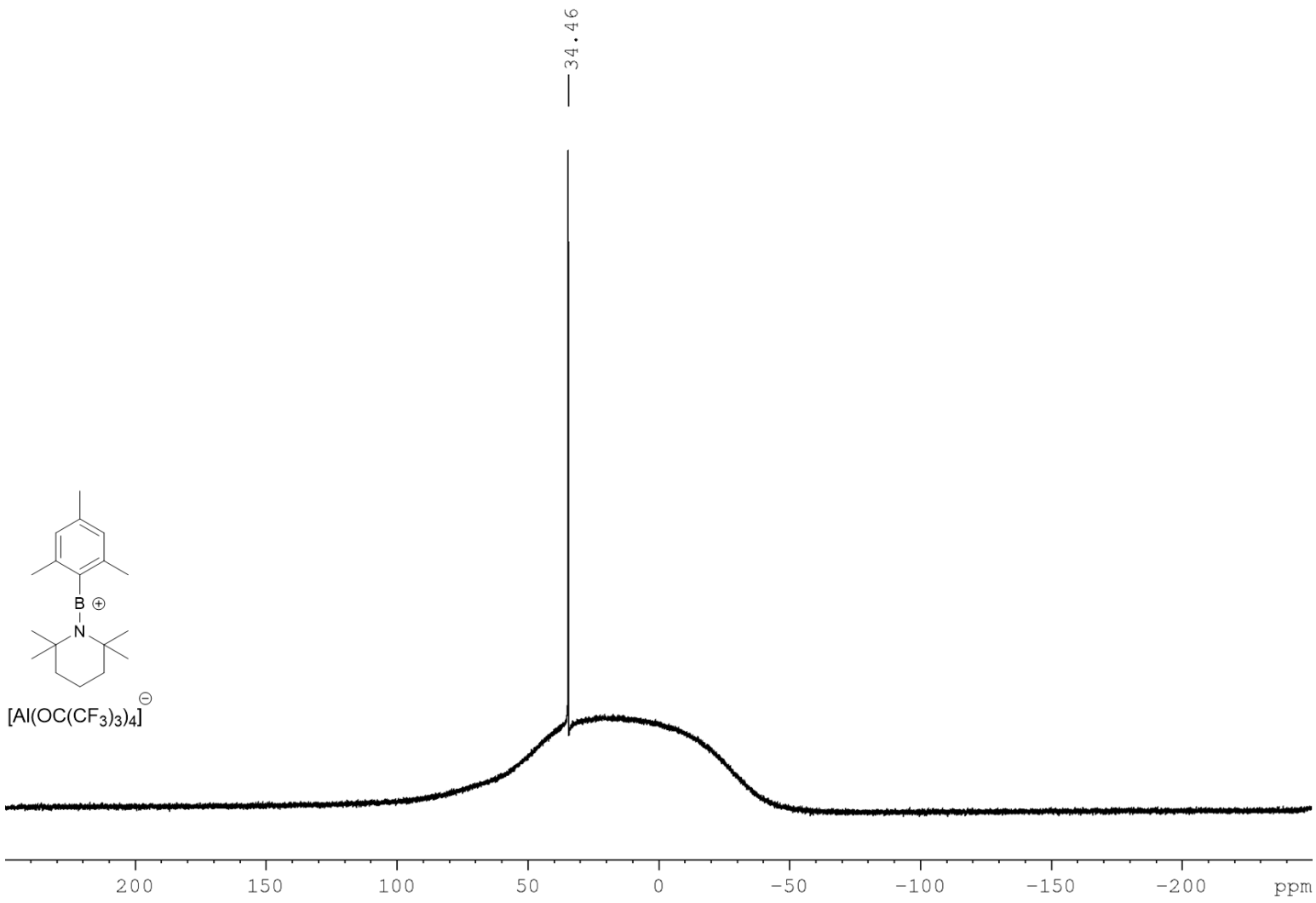

Figure S21. ^{27}Al NMR spectrum of [**2**][Al(OC(CF$_3$)$_3$)$_4$] in CDCl$_3$.

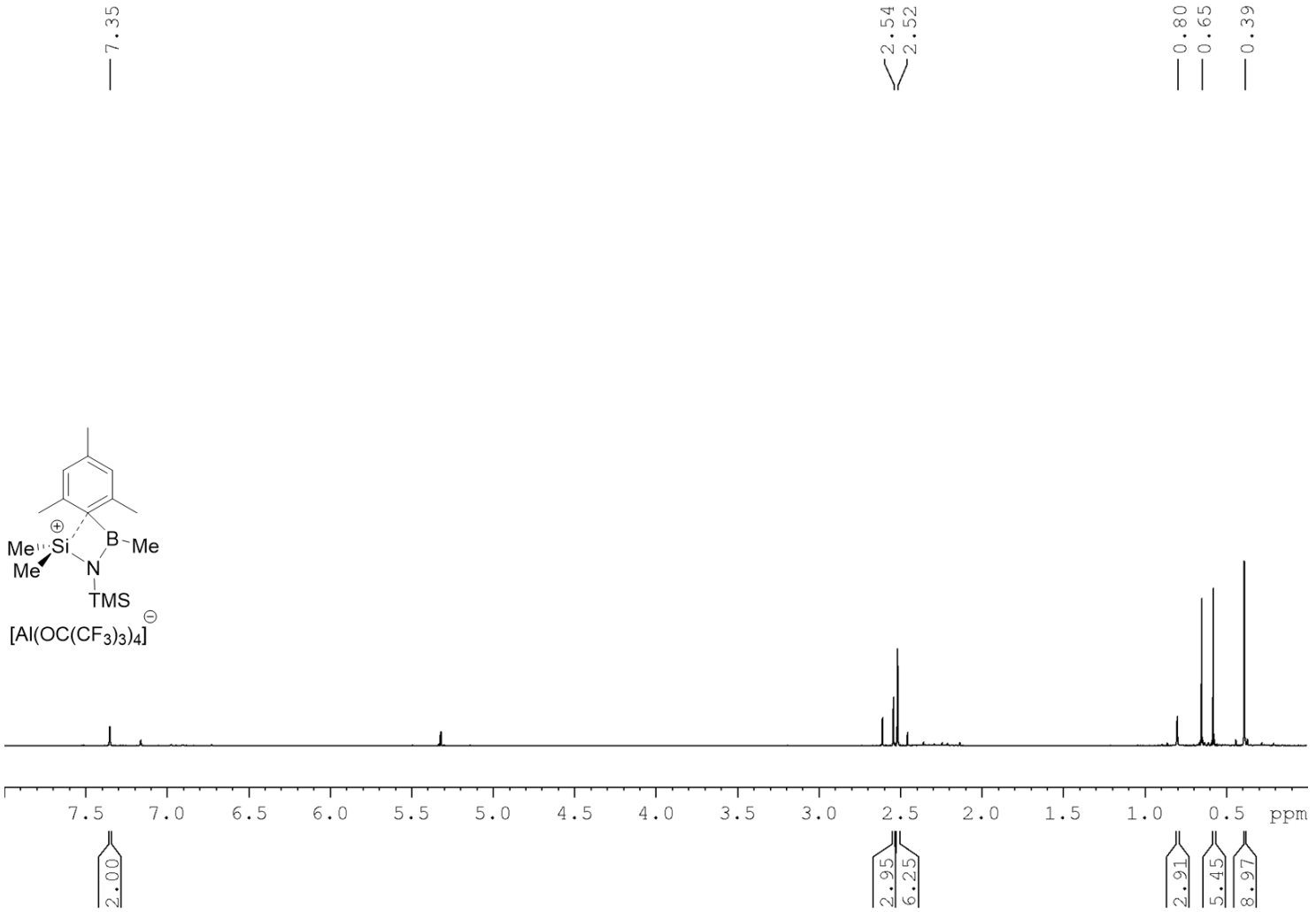

Figure S22. ^{1}H NMR spectrum of [**3**][Al(OC(CF$_3$)$_3$)$_4$] in CD_2Cl_2.

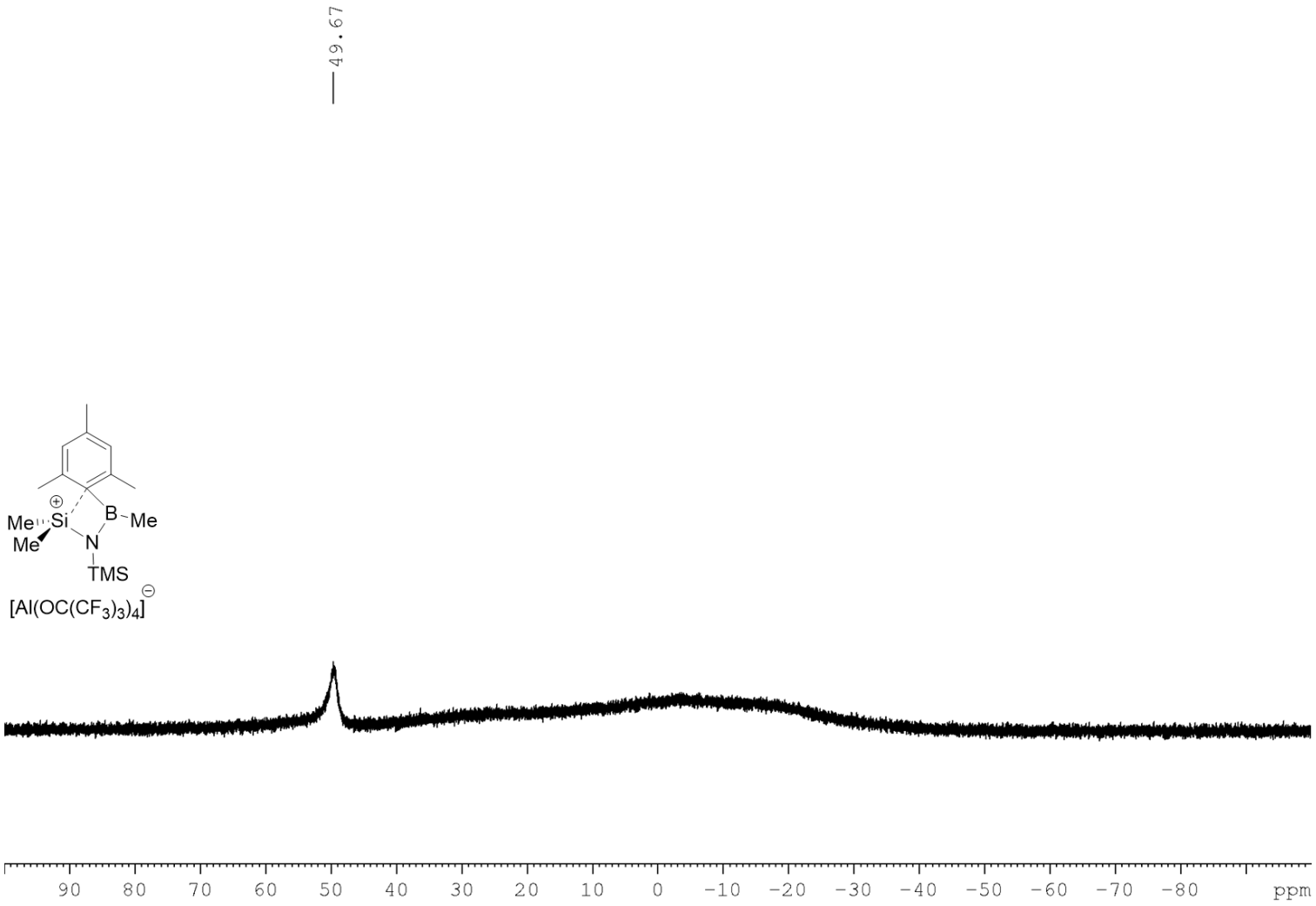

Figure S23. ^{11}B NMR spectrum of [**3**][Al(OC(CF$_3$)$_3$)$_4$] in CD_2Cl_2.

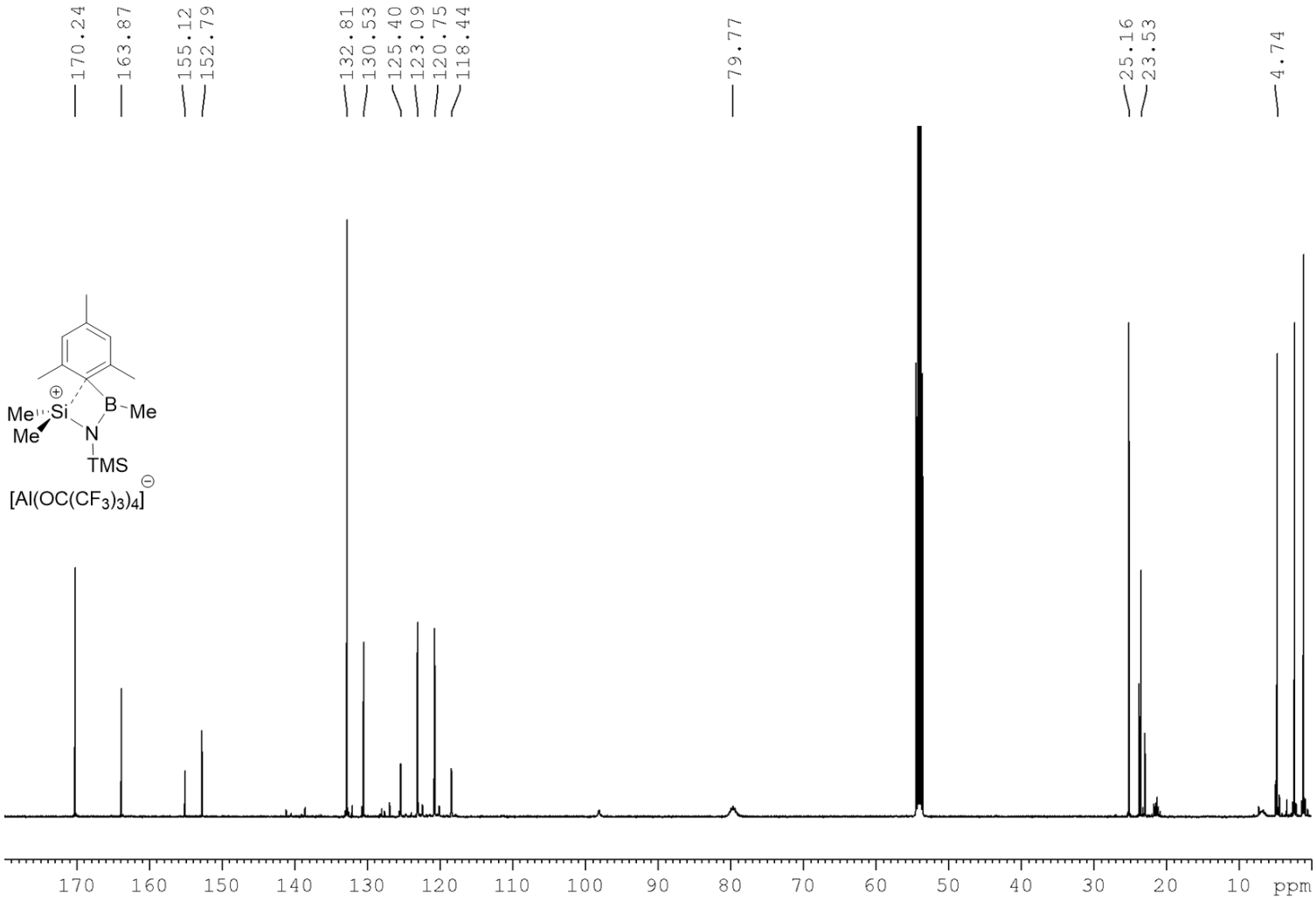

Figure S24. ^{13}C NMR spectrum of [**3**][Al(OC(CF$_3$)$_3$)$_4$] in CD_2Cl_2.

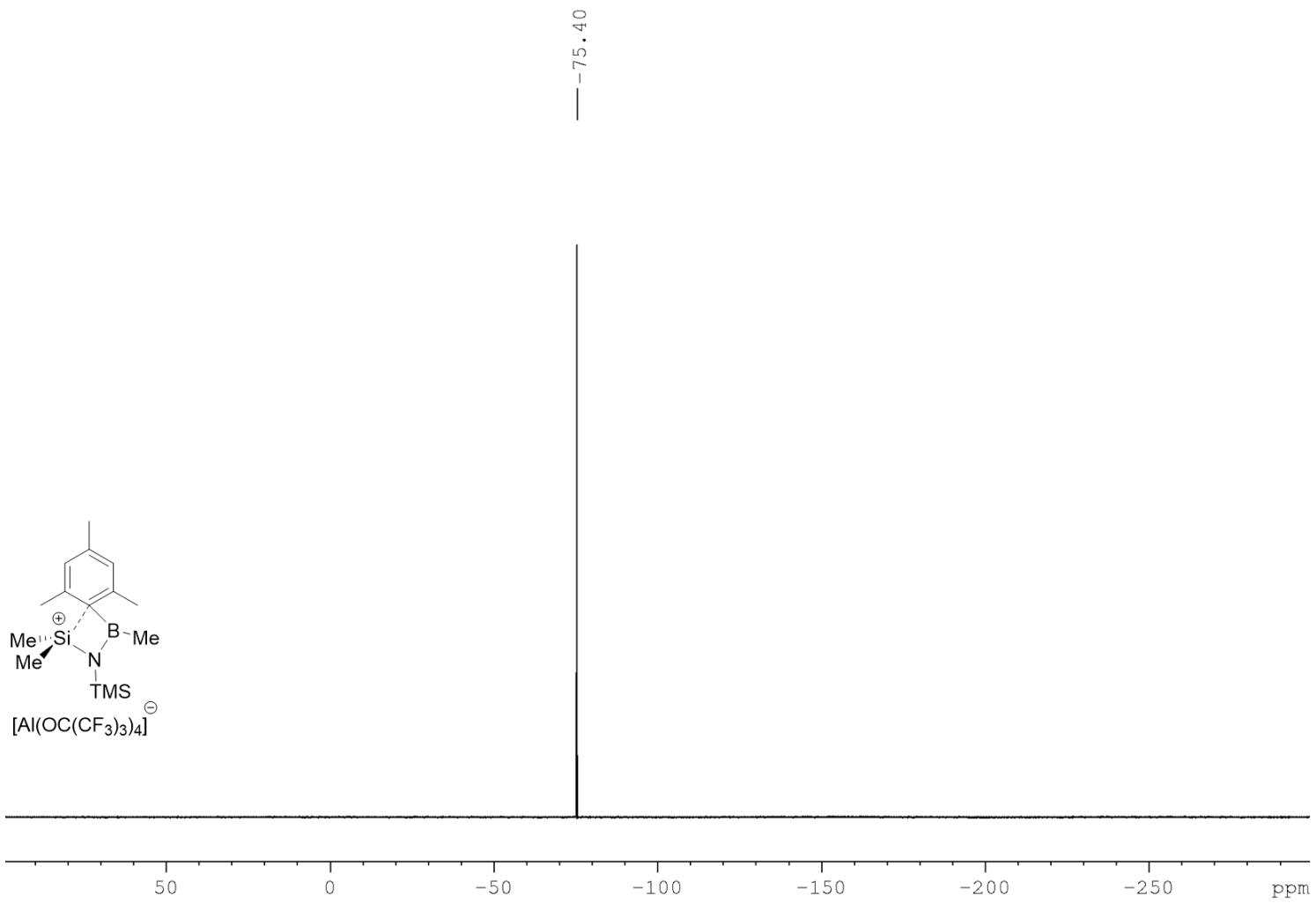

Figure S25. ^{19}F NMR spectrum of [**3**][$Al(OC(CF_3)_3)_4$] in CD_2Cl_2.

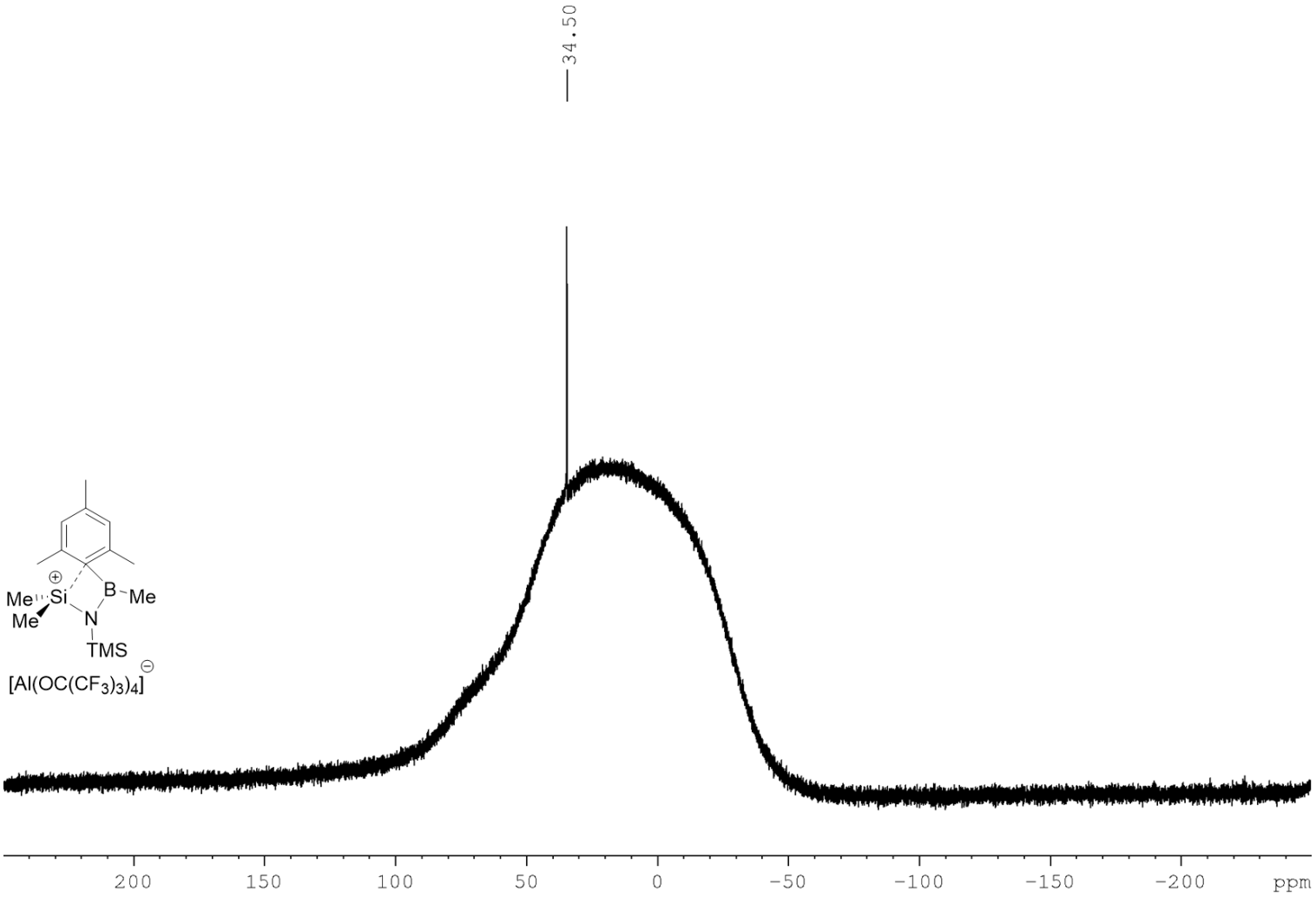

Figure S26. ^{27}Al NMR spectrum of [**3**][Al(OC(CF$_3$)$_3$)$_4$] in CD_2Cl_2.

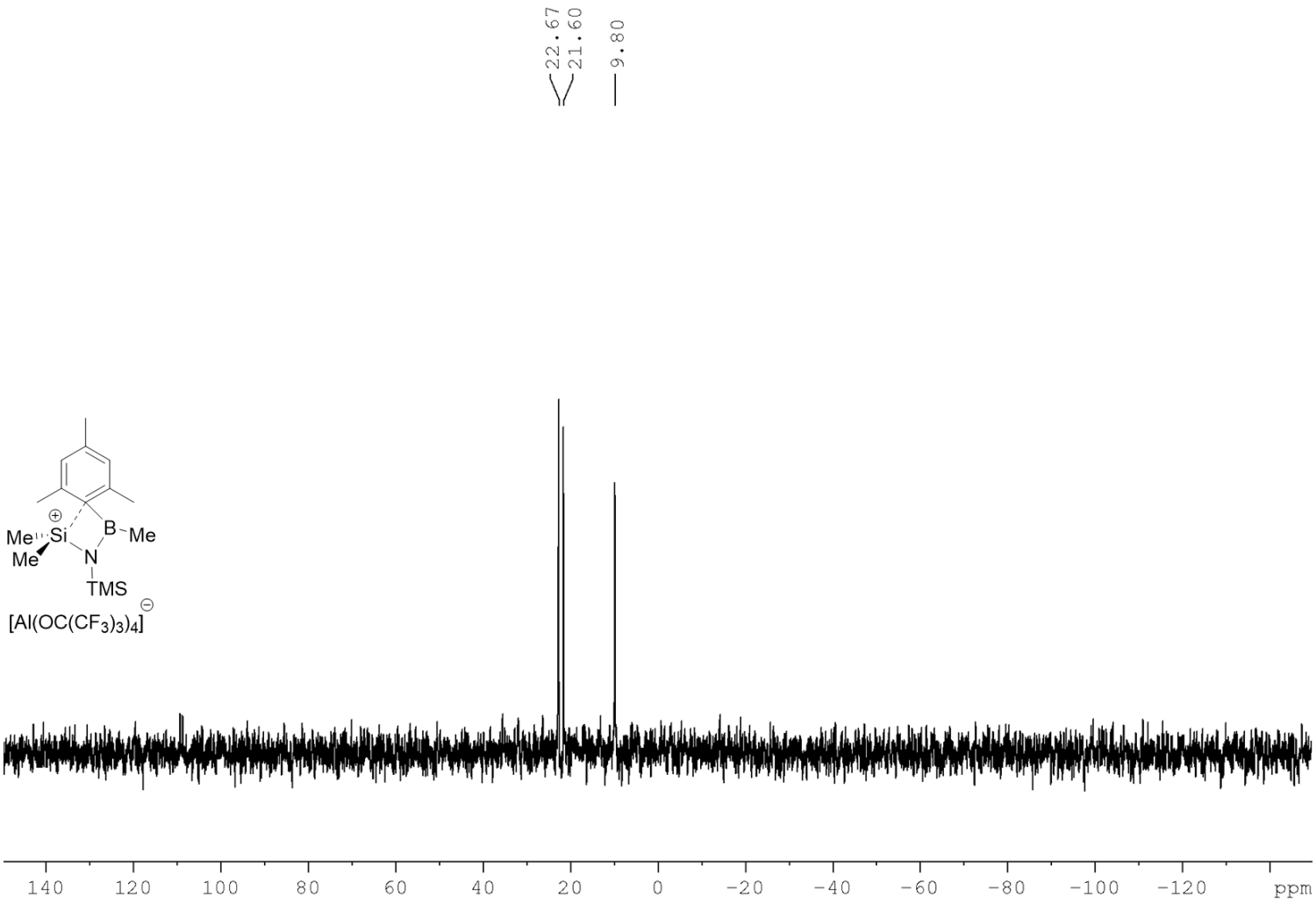

Figure S27. ^{29}Si NMR spectrum of [**3**][Al(OC(CF$_3$)$_3$)$_4$] in CD_2Cl_2.

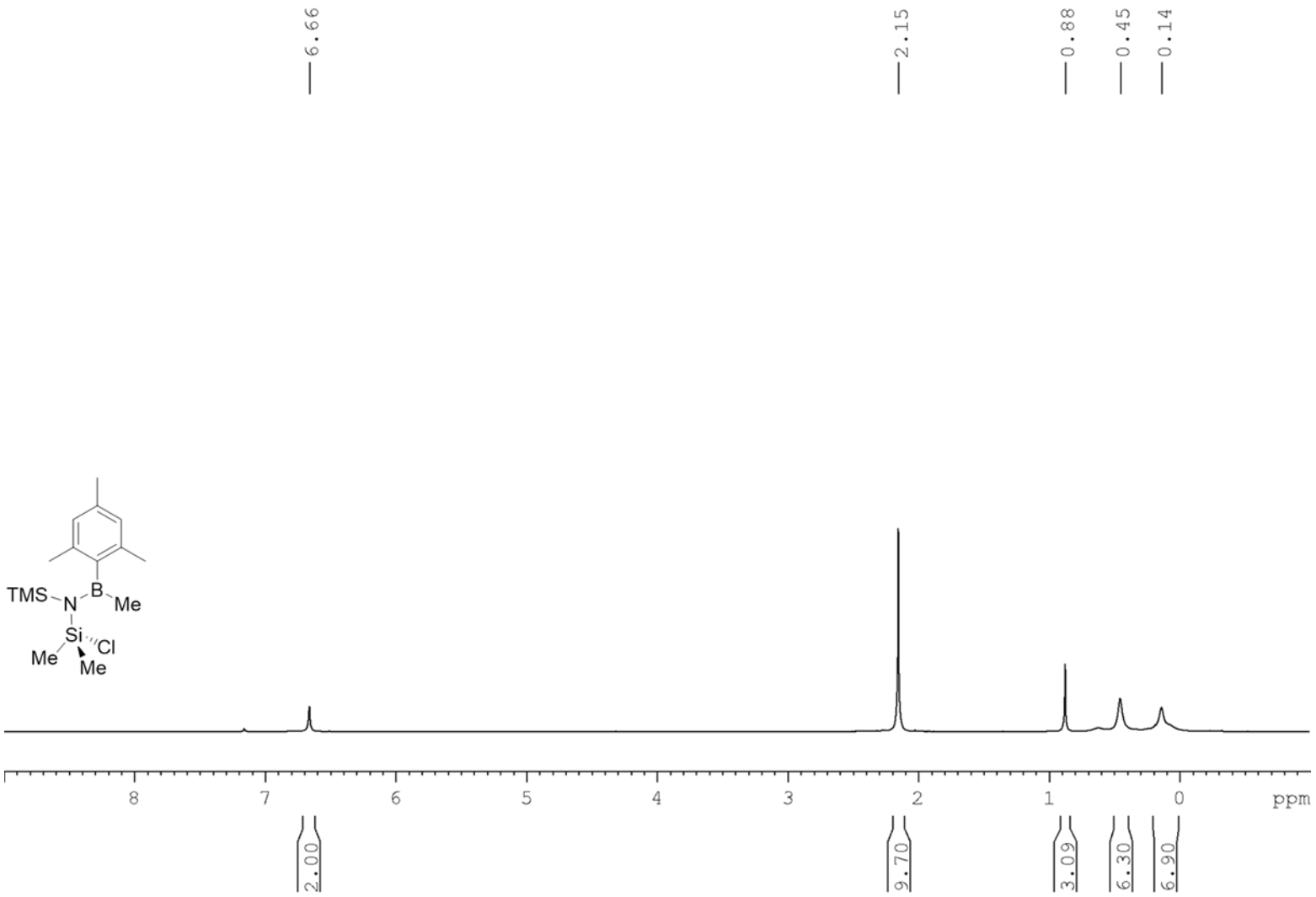

Figure S28. ^{1}H NMR spectrum of **4** in C_6D_6.

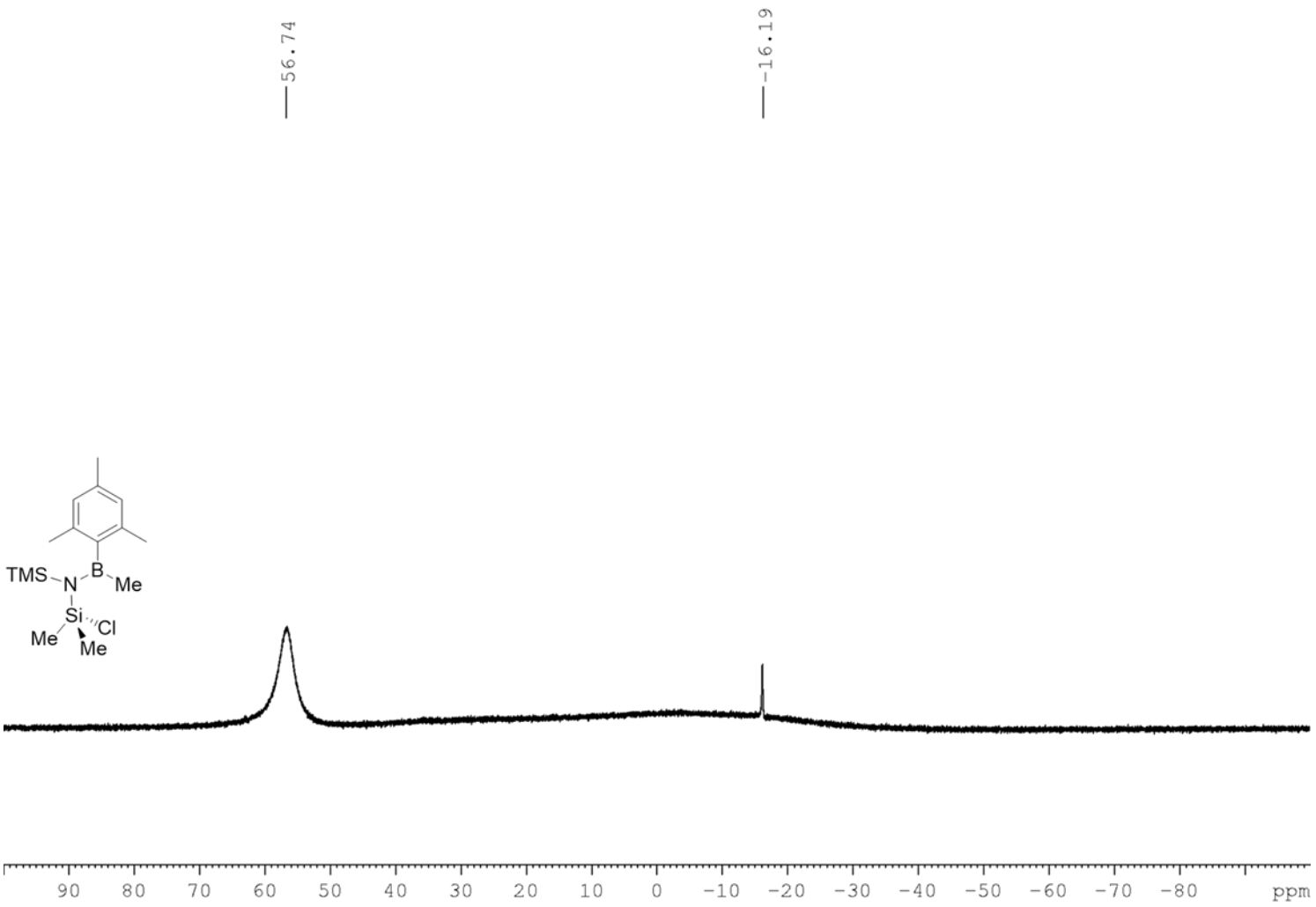

Figure S29. ^{11}B NMR spectrum of **4** in C_6D_6.

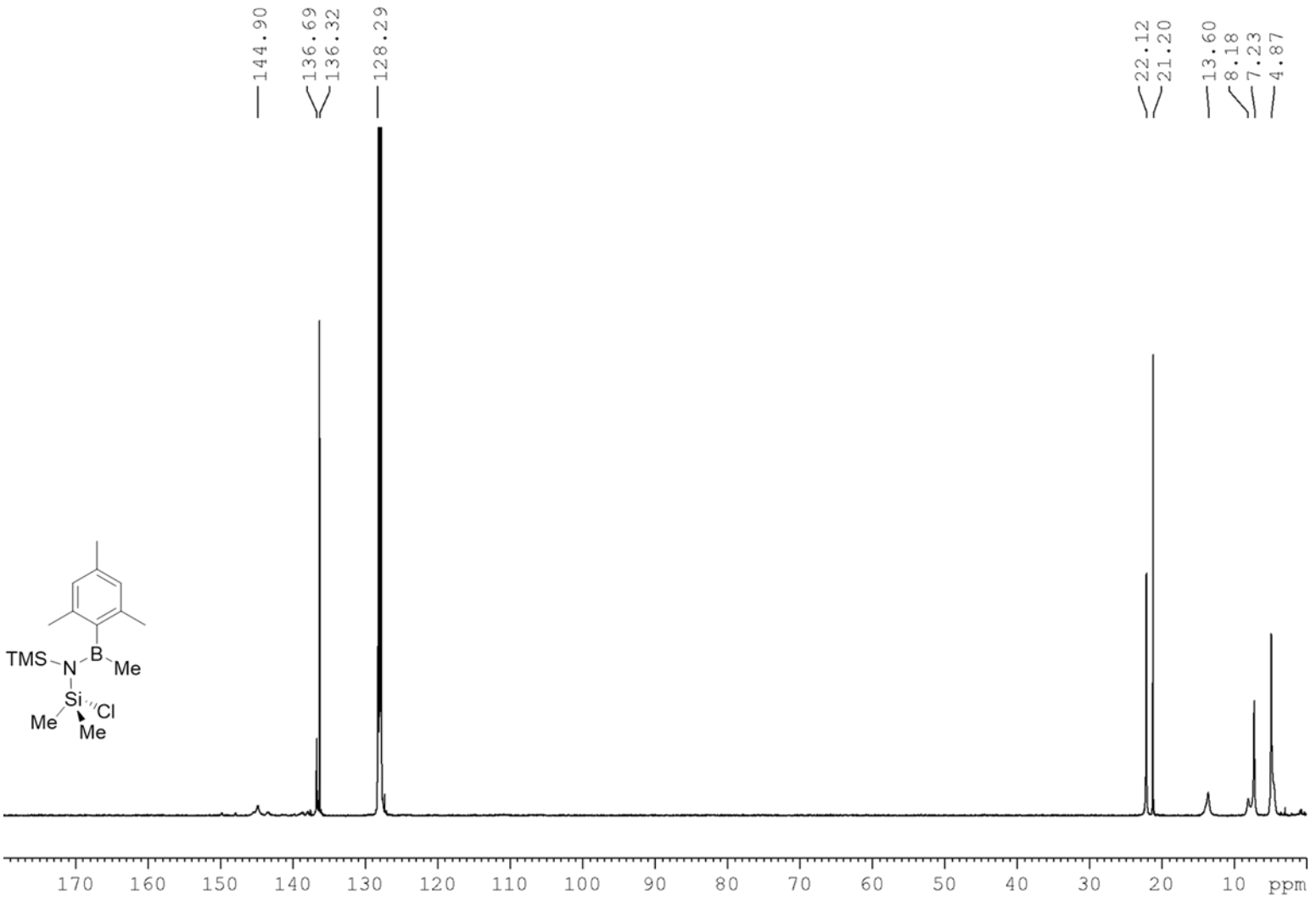

Figure S30. ^{13}C NMR spectrum of **4** in C_6D_6.

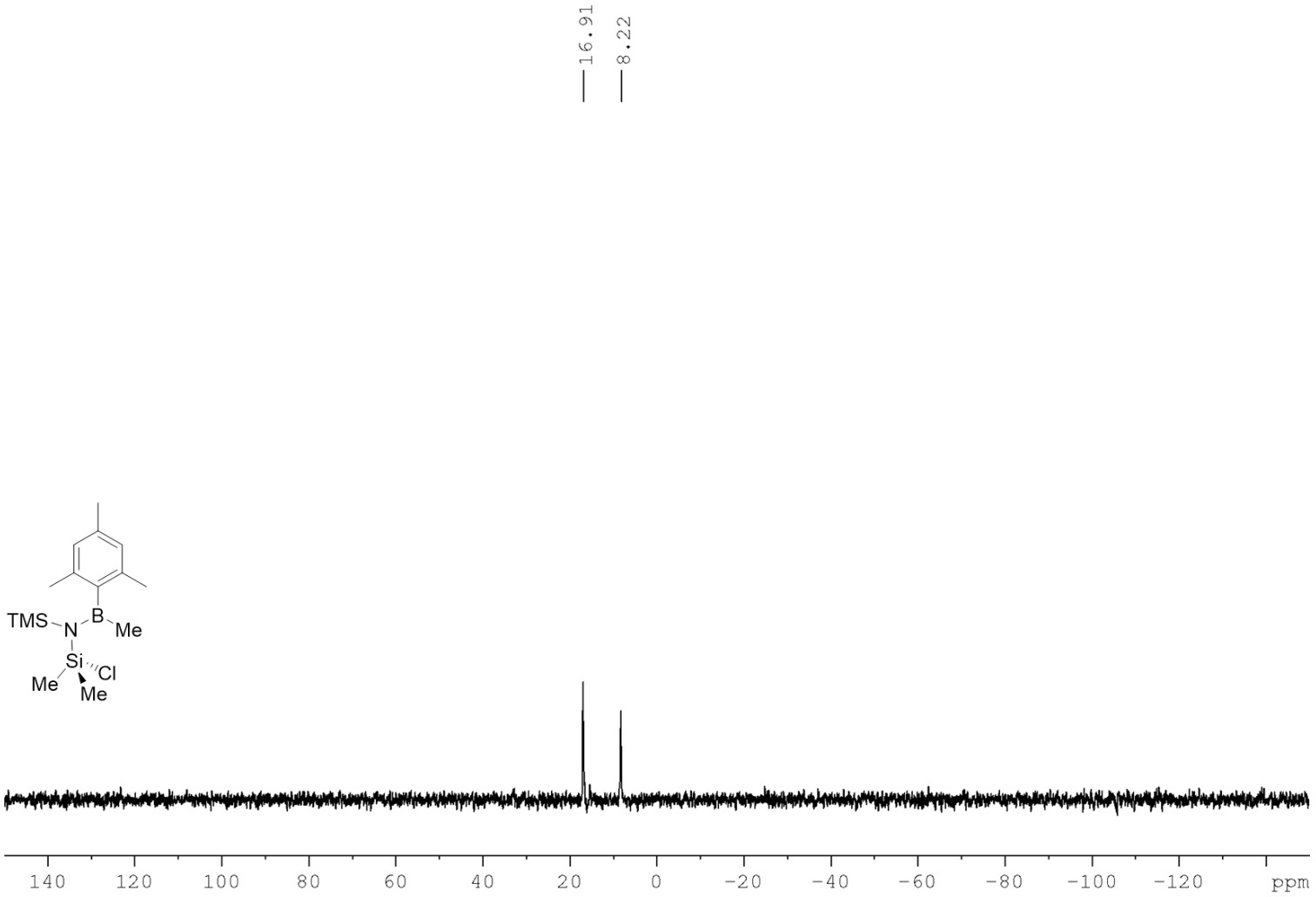

Figure S31. ^{29}Si NMR spectrum of **4** in C_6D_6.

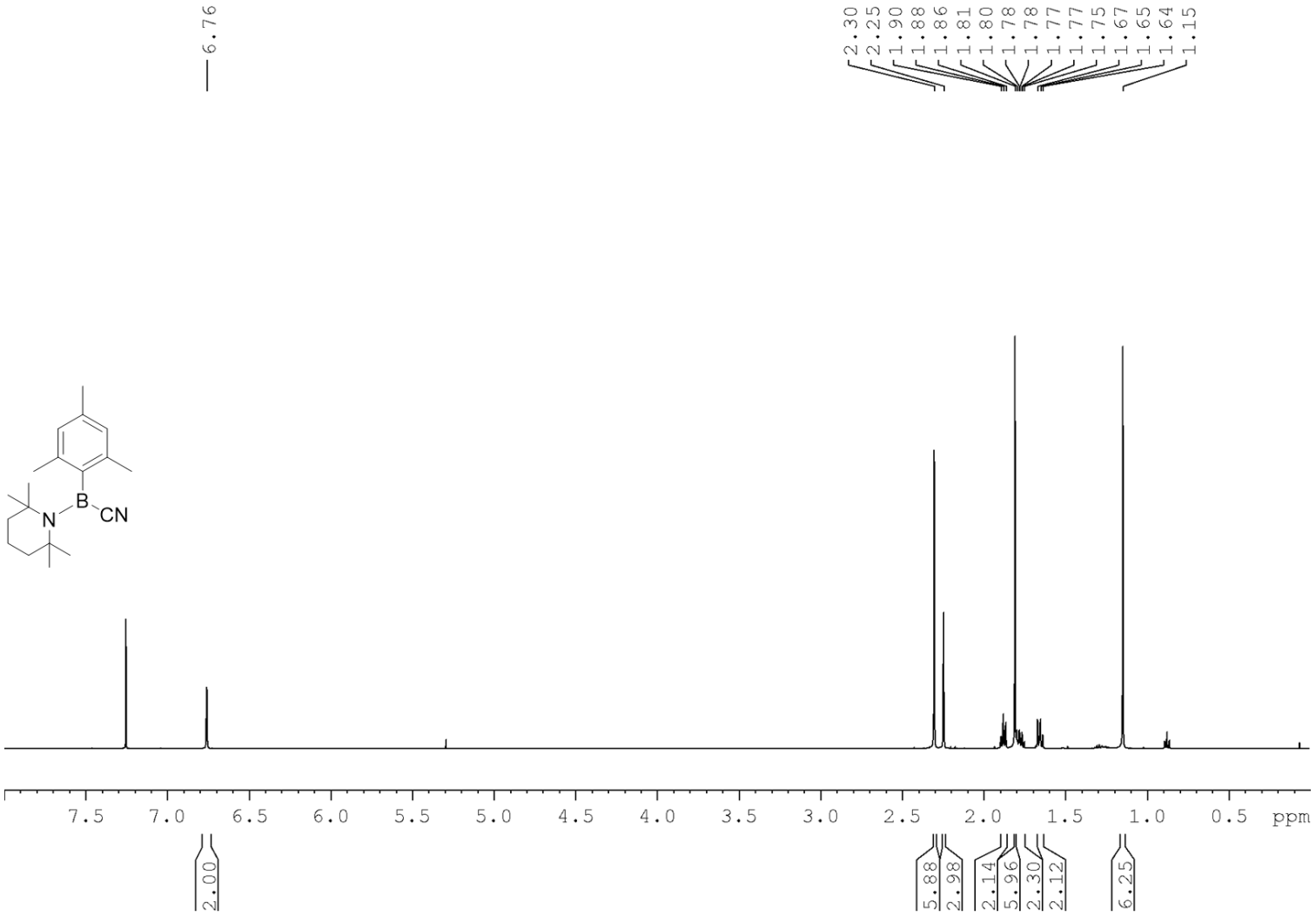

Figure S32. ^{1}H NMR spectrum of **MesB(CN)-TMP** in $CDCl_3$.

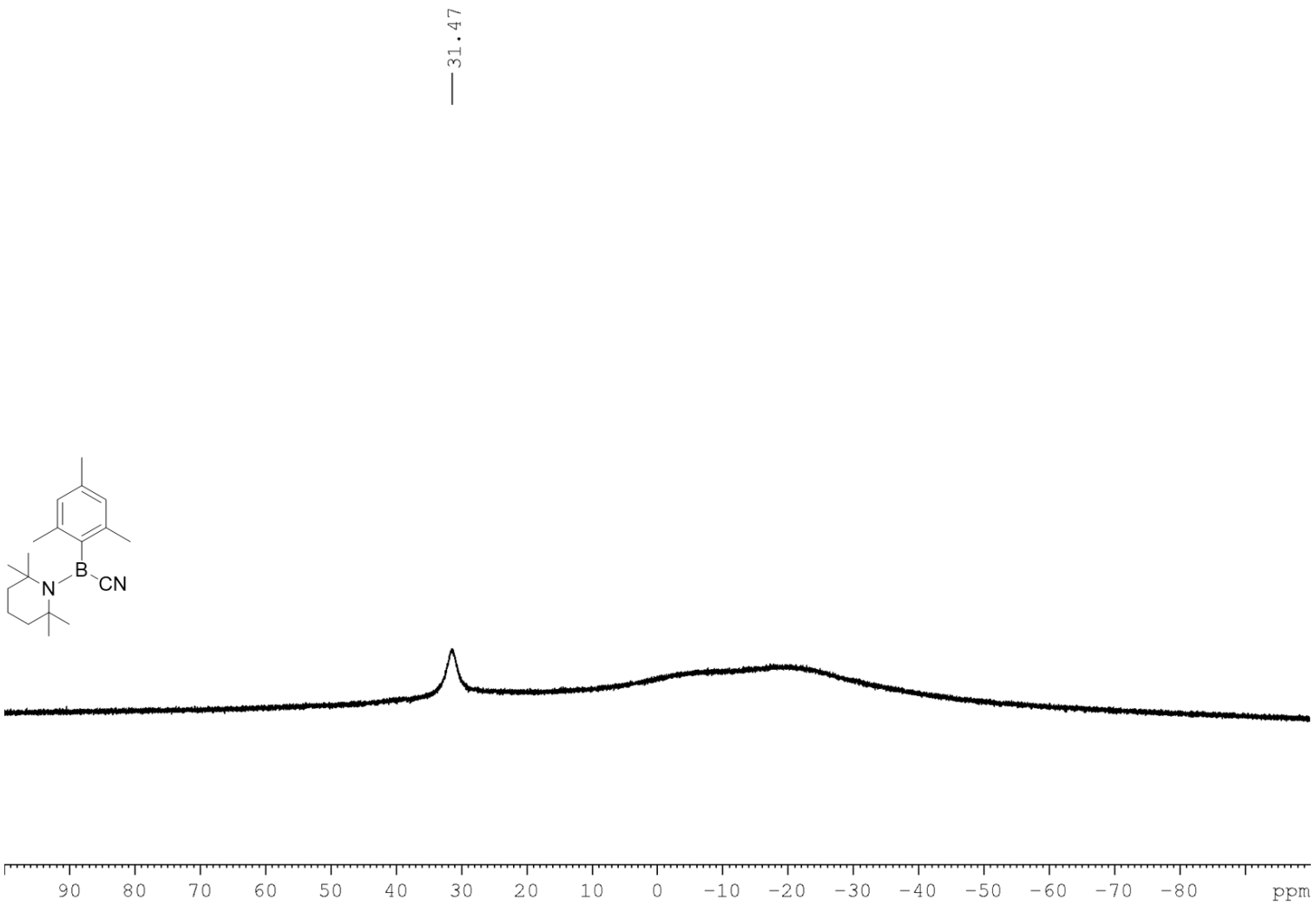

Figure S33. ^{11}B NMR spectrum of **MesB(CN)-TMP** in $CDCl_3$.

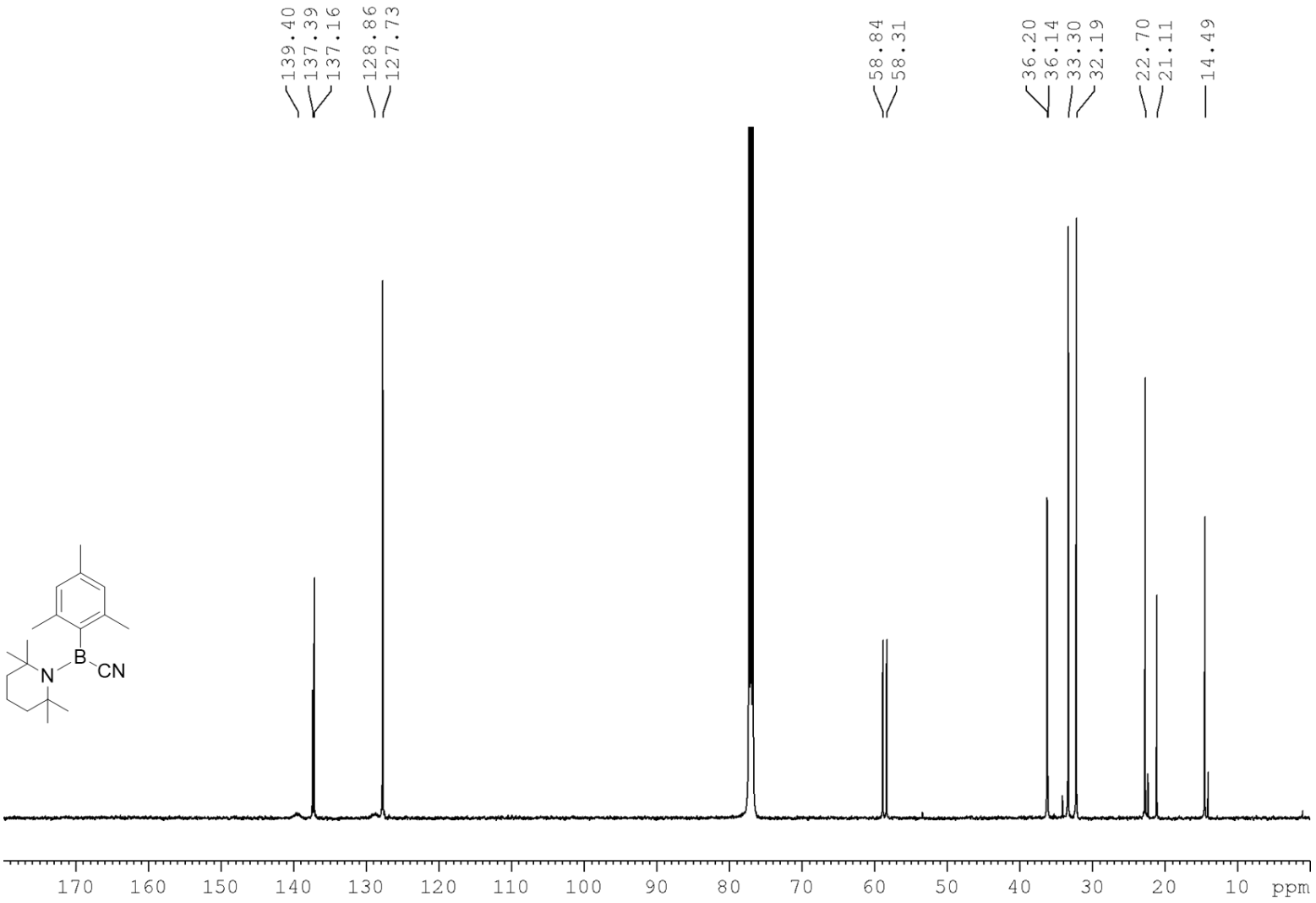

Figure S34. ^{13}C NMR spectrum of **MesB(CN)-TMP** in $CDCl_3$.

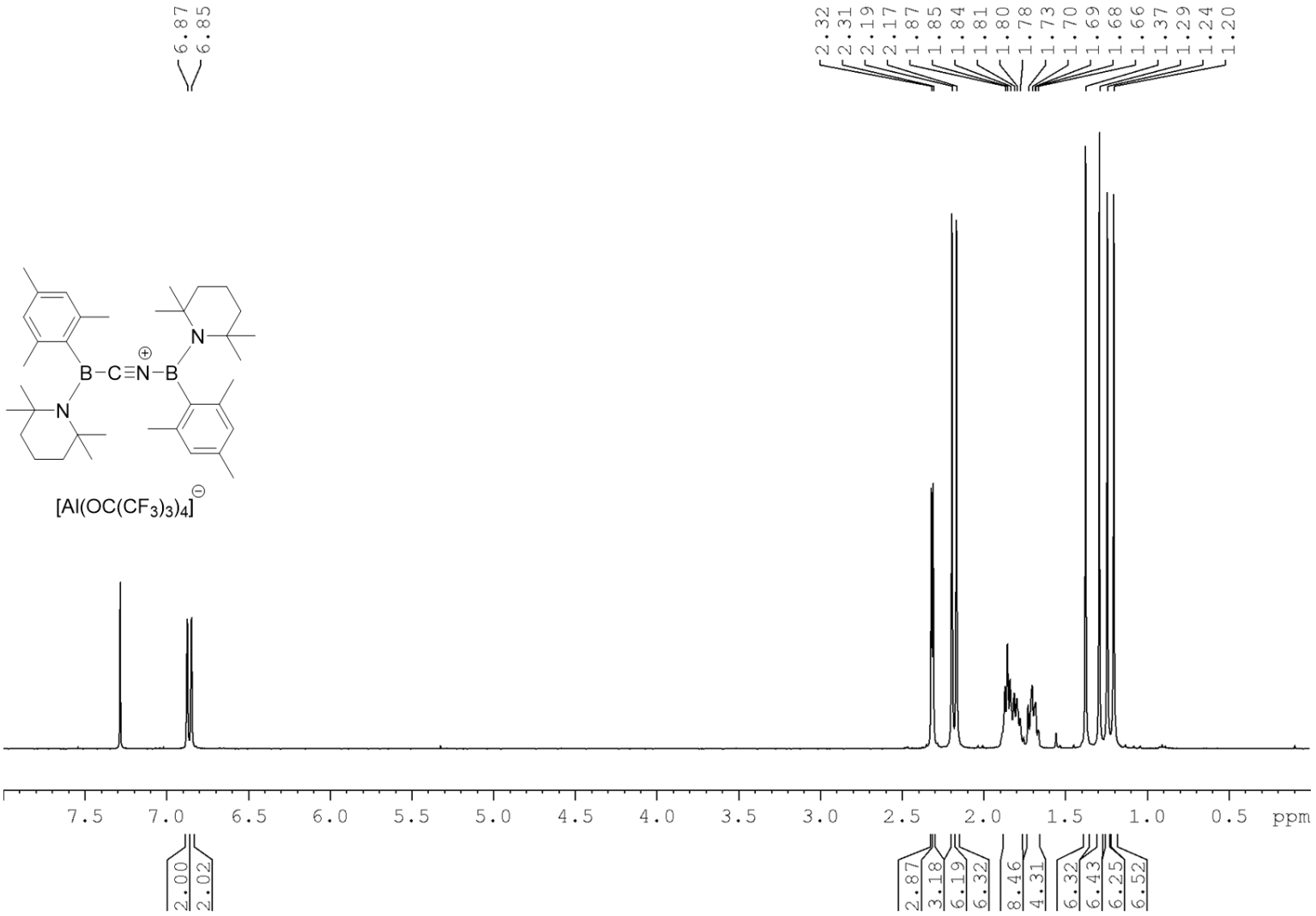

Figure S35. ^{1}H NMR spectrum of [**7**][Al(OC(CF$_3$)$_3$)$_4$] in $CDCl_3$.

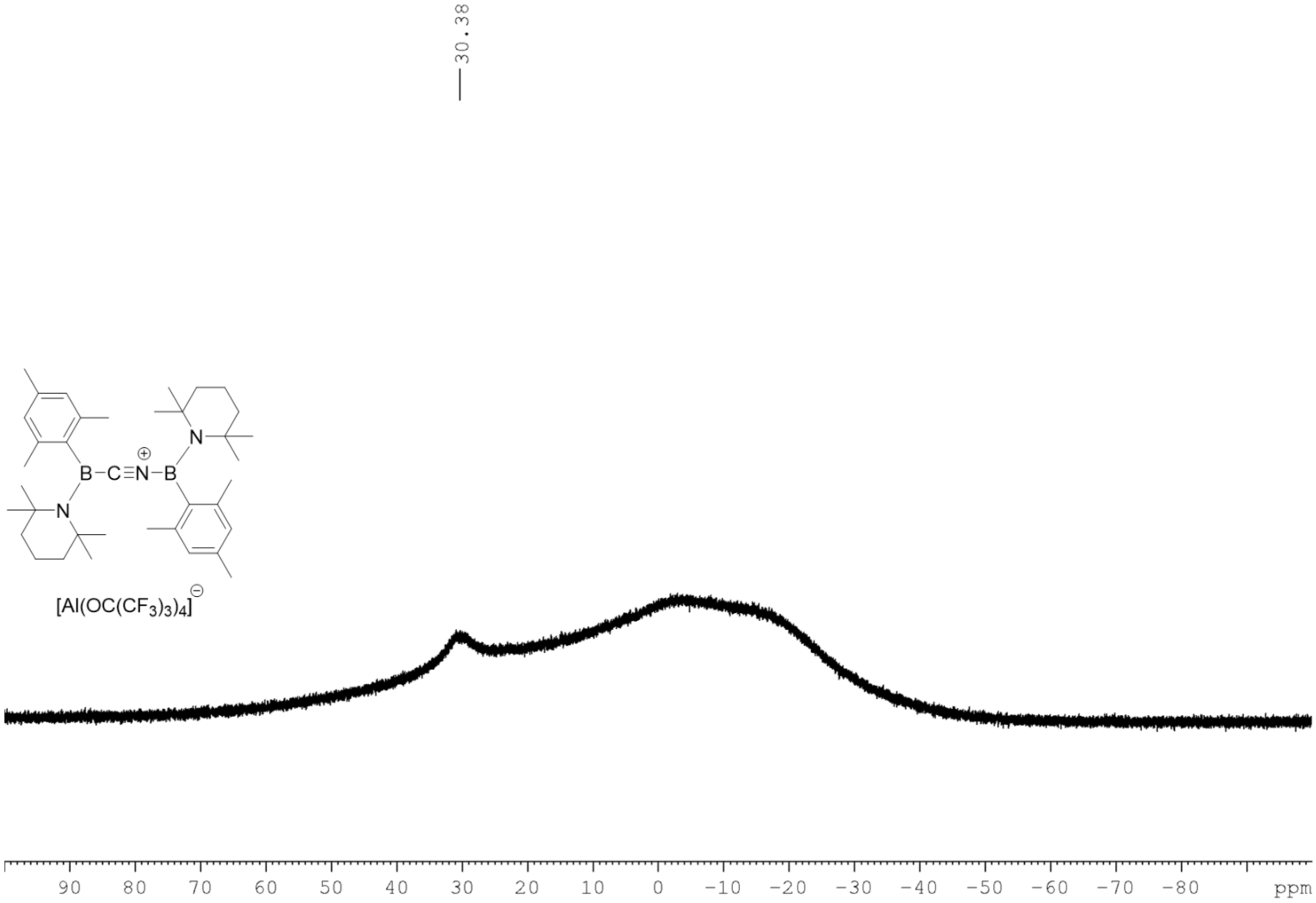

Figure S36. ^{11}B NMR spectrum of [**7**][Al(OC(CF$_3$)$_3$)$_4$] in CDCl$_3$.

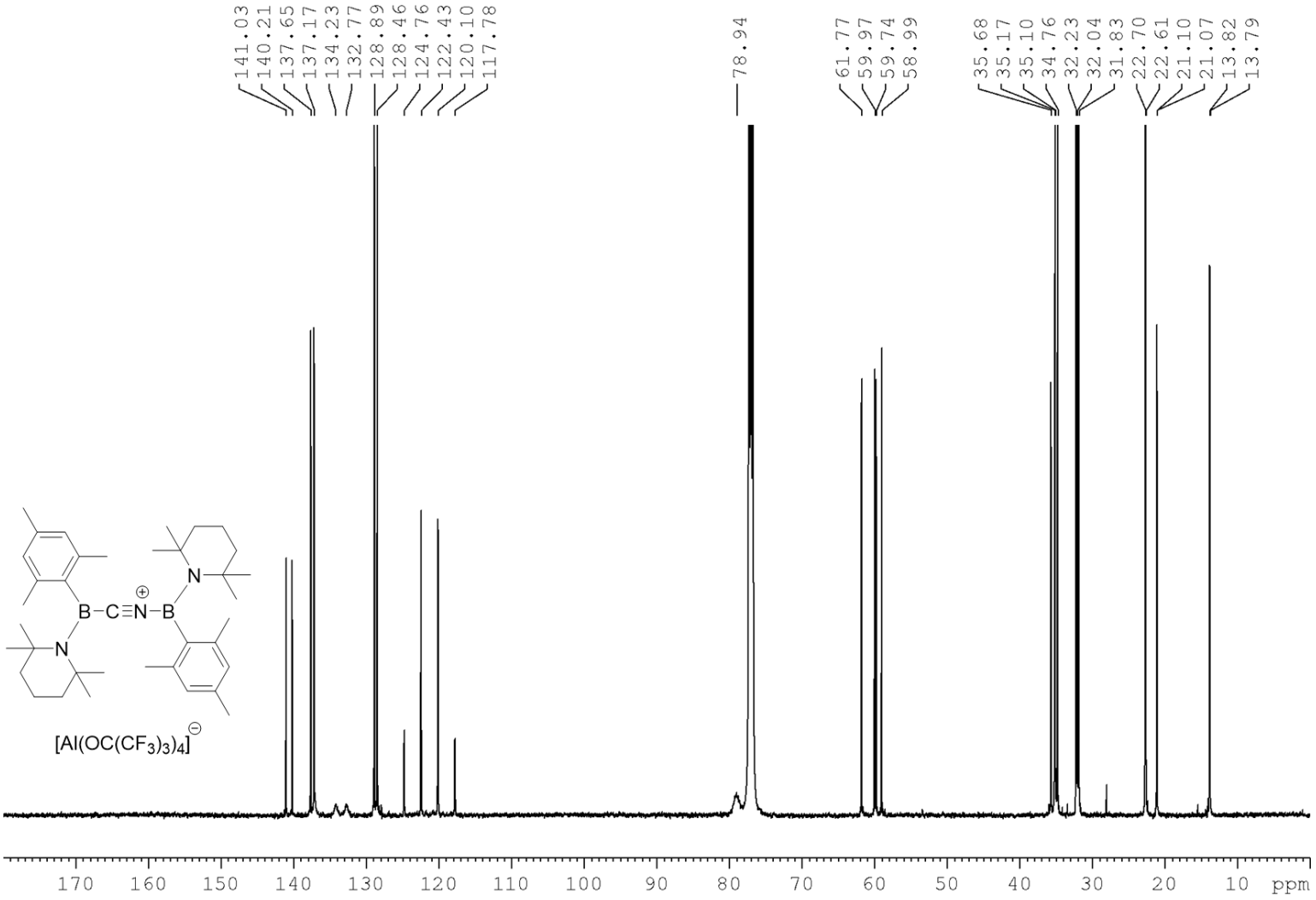

Figure S37. ^{13}C NMR spectrum of [**7**][$Al(OC(CF_3)_3)_4$] in $CDCl_3$.

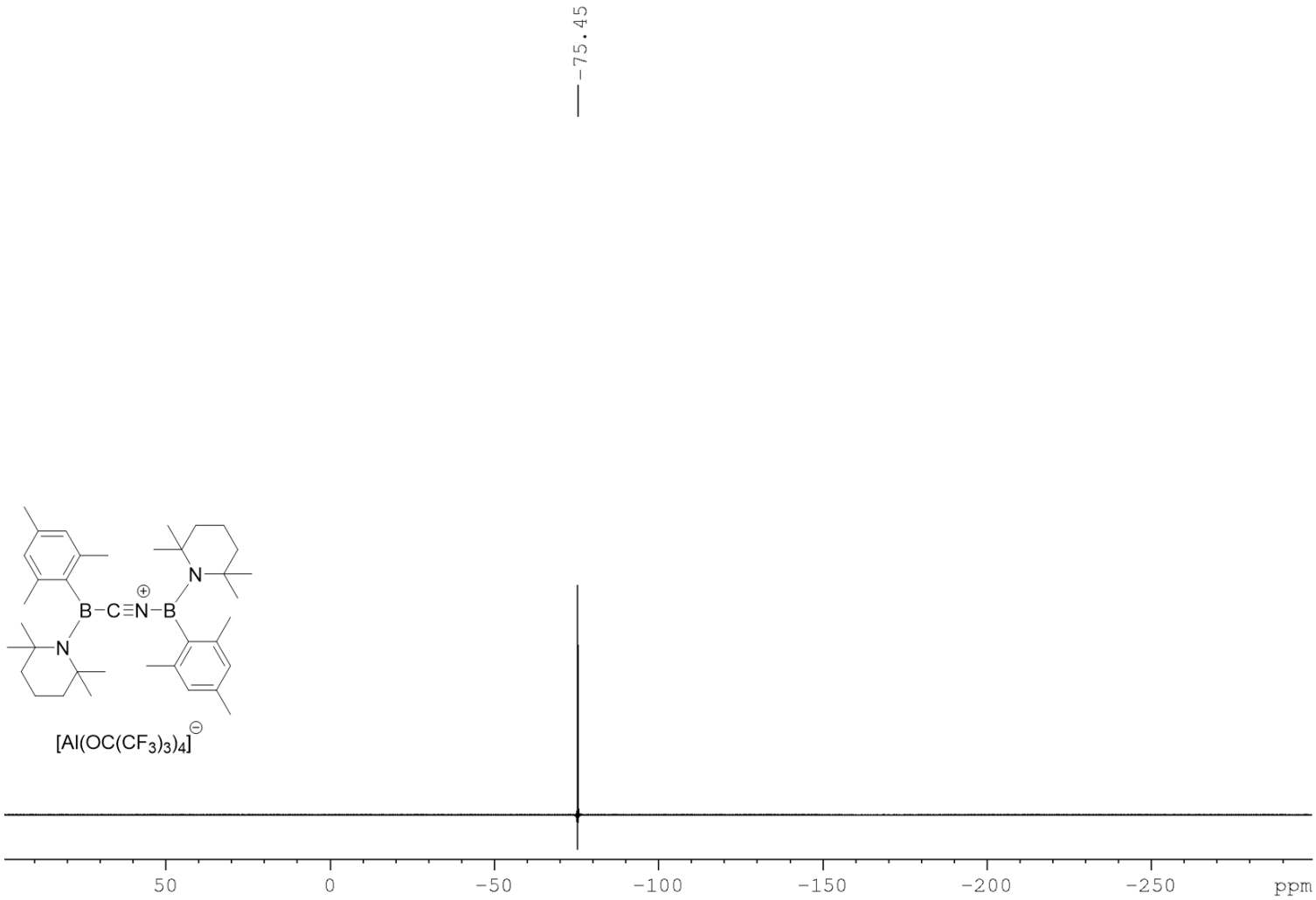

Figure S38. ^{19}F NMR spectrum of [**7**][$Al(OC(CF_3)_3)_4$] in $CDCl_3$.

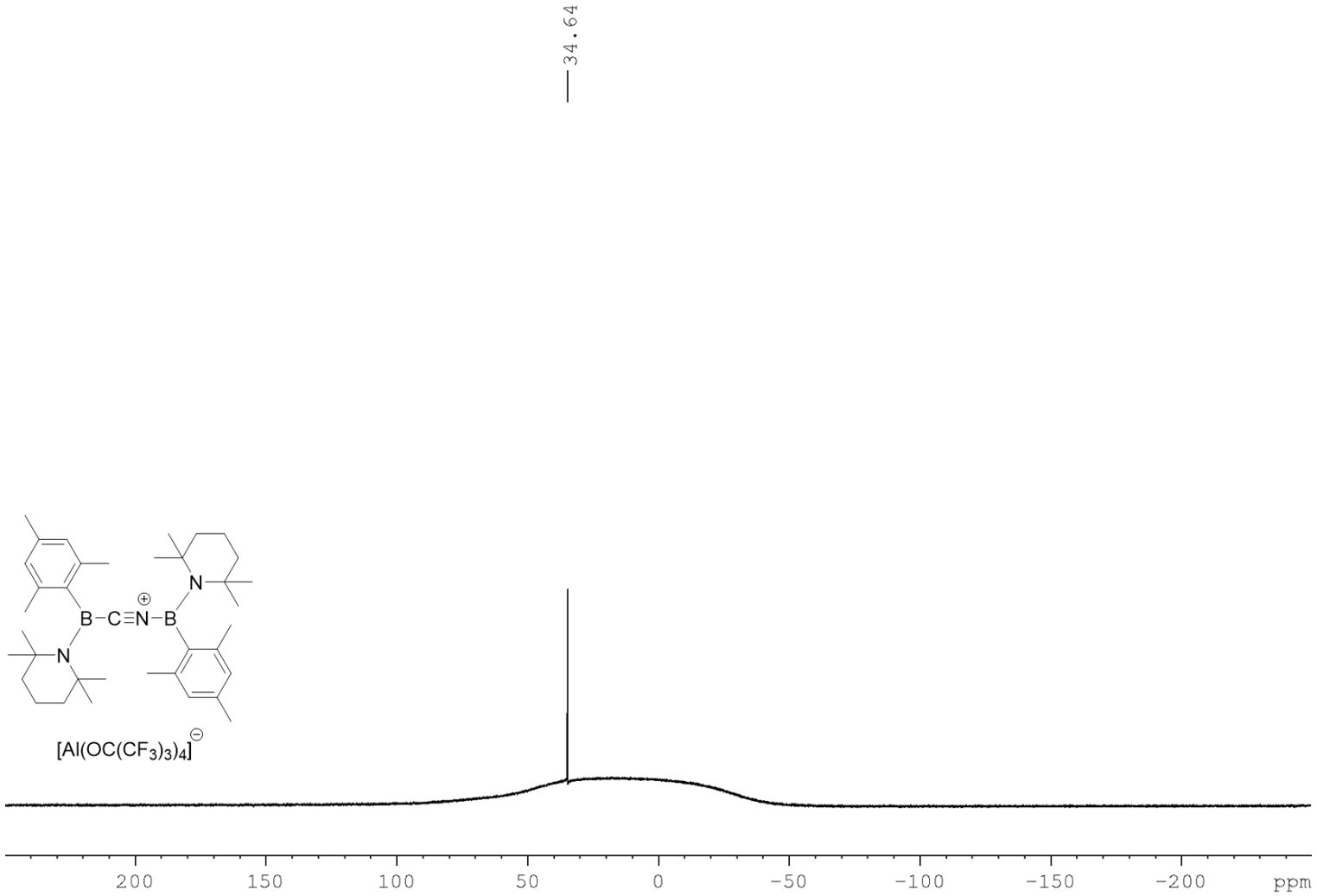

Figure S39. ^{27}Al NMR spectrum of [**7**][Al(OC(CF$_3$)$_3$)$_4$] in CDCl$_3$.

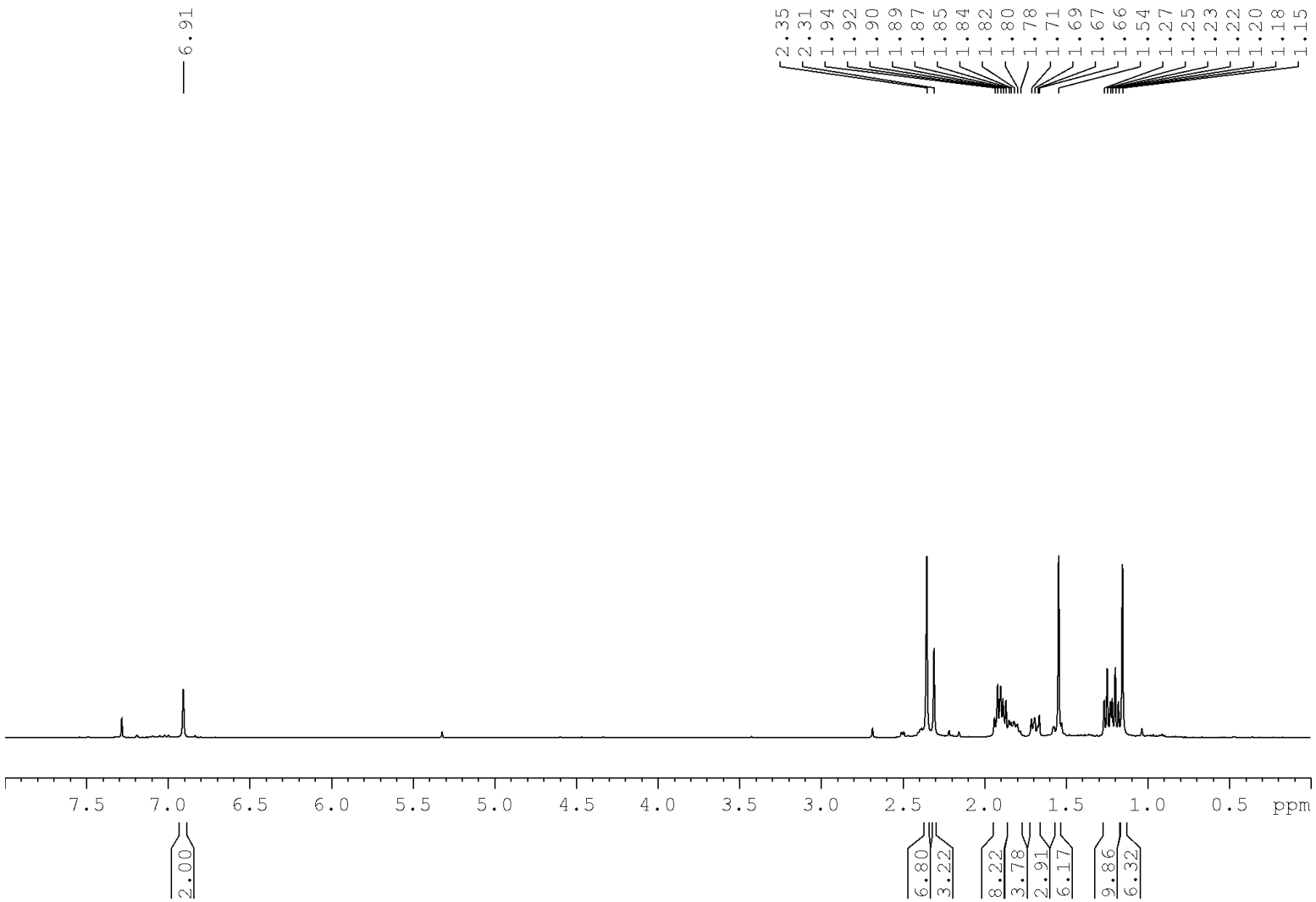

Figure S40. ^{1}H NMR spectrum of Et_3PO-[**2**][$Al(OC(CF_3)_3)_4$] adduct in $CDCl_3$.

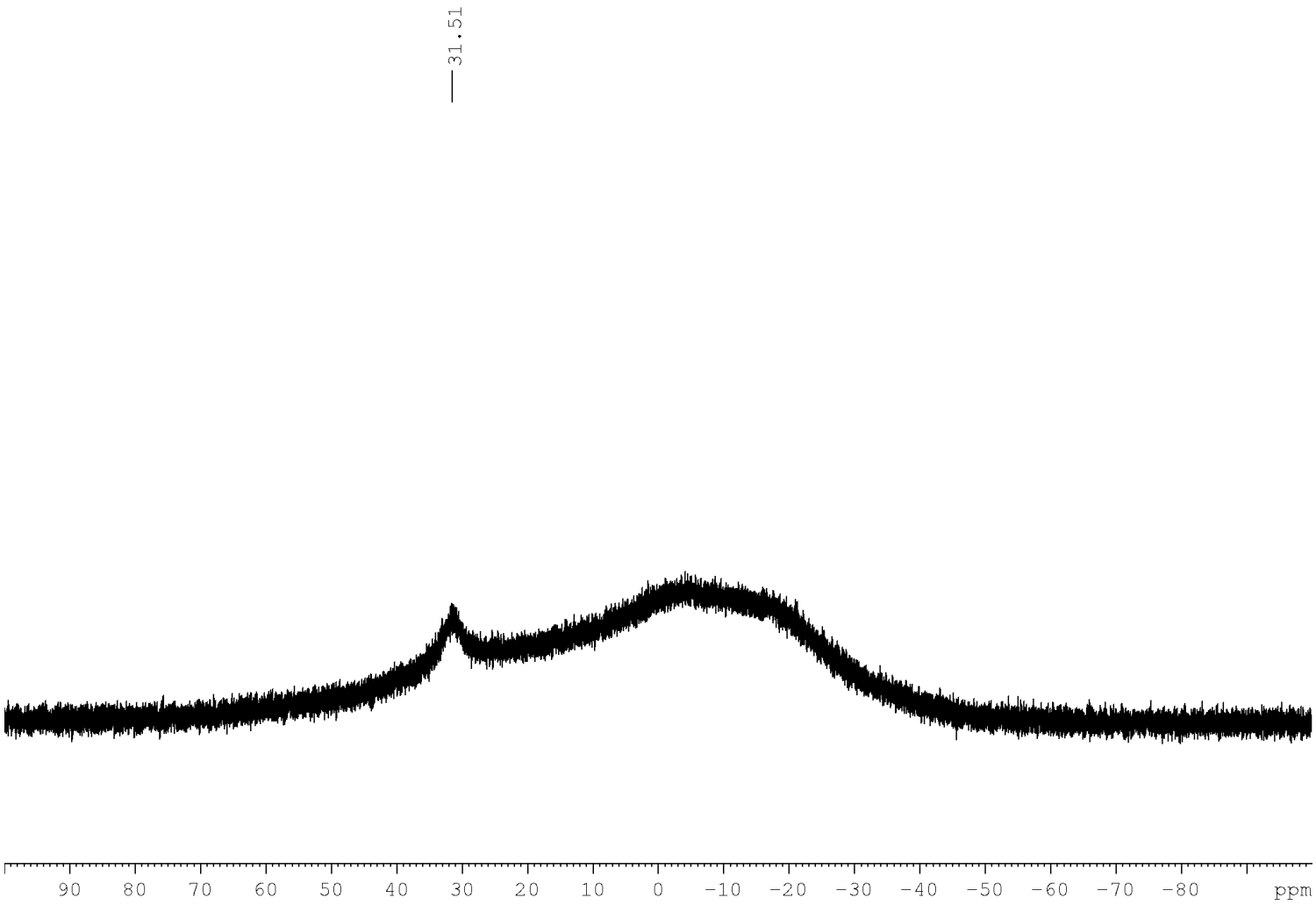

Figure S41. ^{11}B NMR spectrum of Et_3PO-[**2**][$Al(OC(CF_3)_3)_4$] adduct in $CDCl_3$

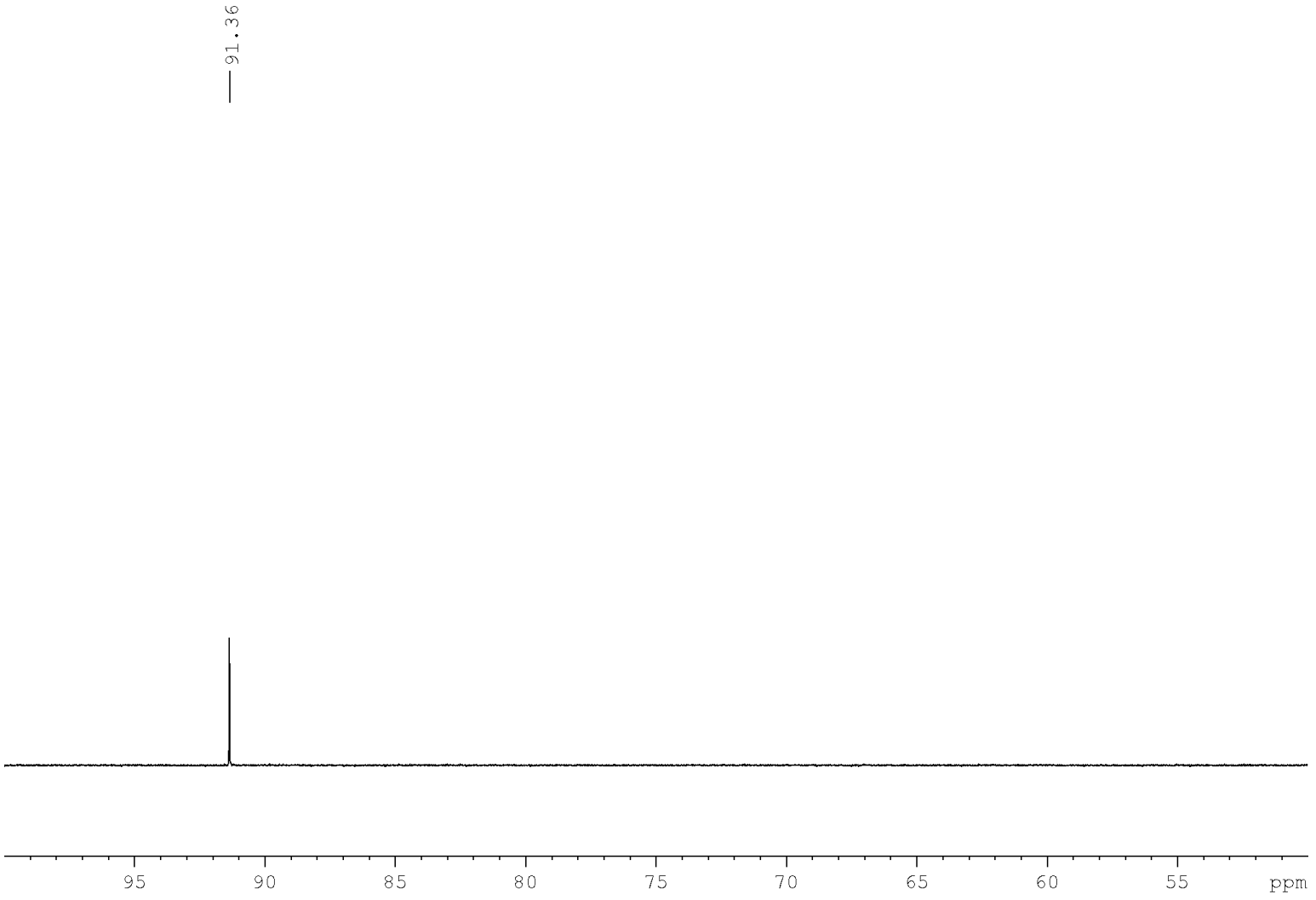

Figure S42. ^{31}P NMR spectrum of Et_3PO-[**2**][$Al(OC(CF_3)_3)_4$] adduct in $CDCl_3$

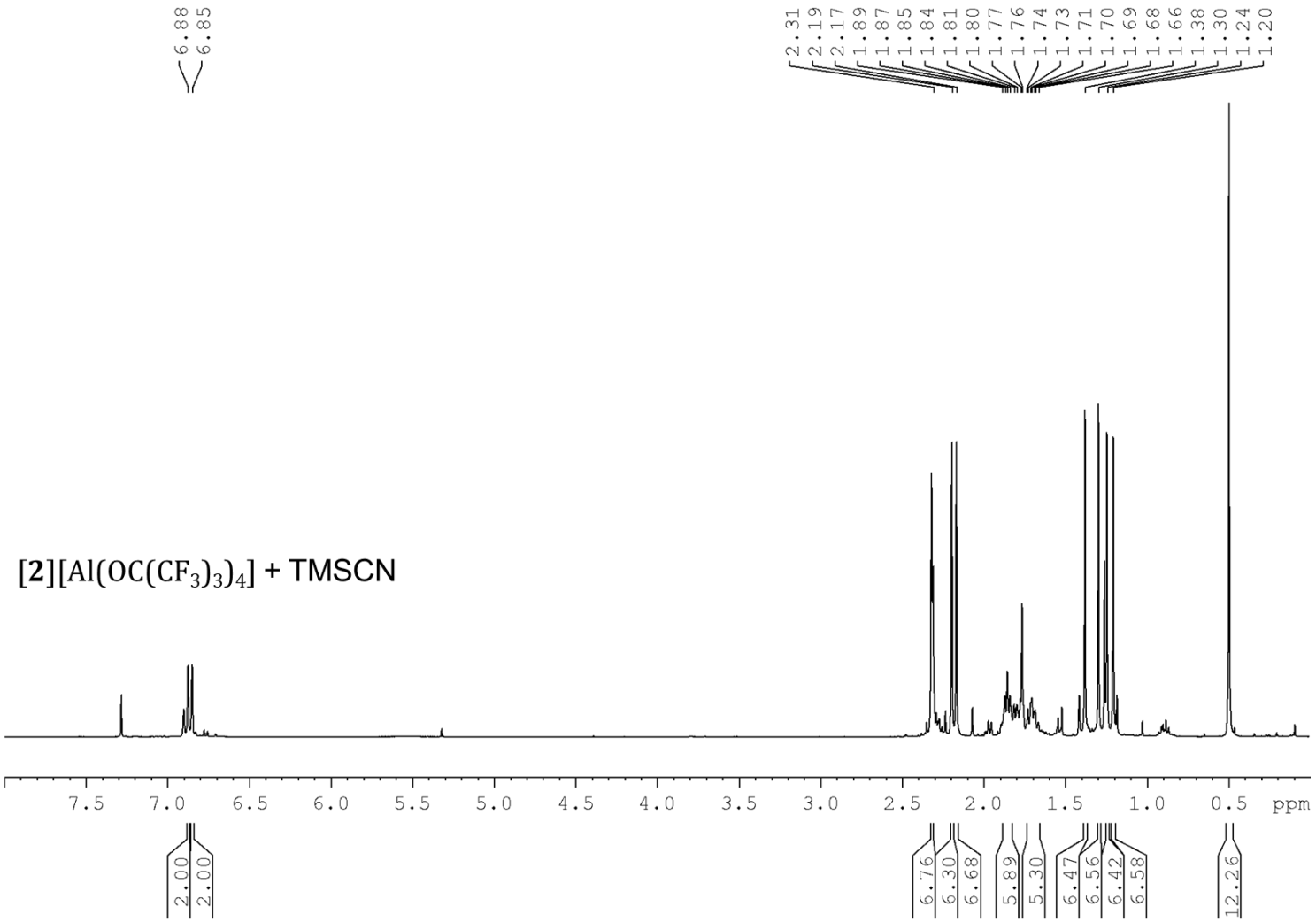

Figure S43. Reaction of TMSCN with [**2**][Al(OC(CF$_3$)$_3$)$_4$] by crude ^{1}H NMR spectroscopy.

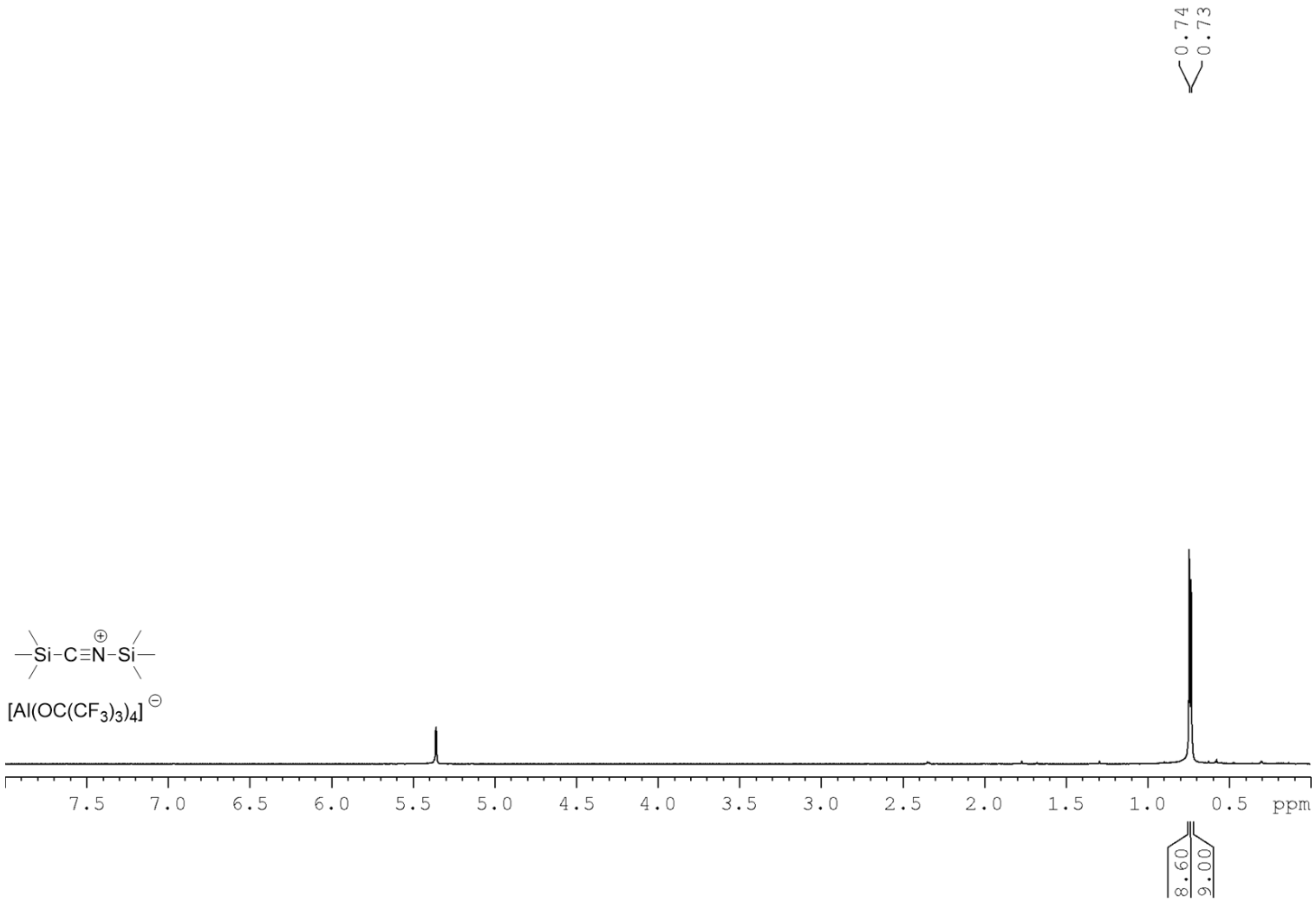

Figure S44. ^{1}H NMR spectrum of [TMS-CN-TMS][Al(OC(CF$_3$)$_3$)$_4$] in DCM-*d*$_2$.

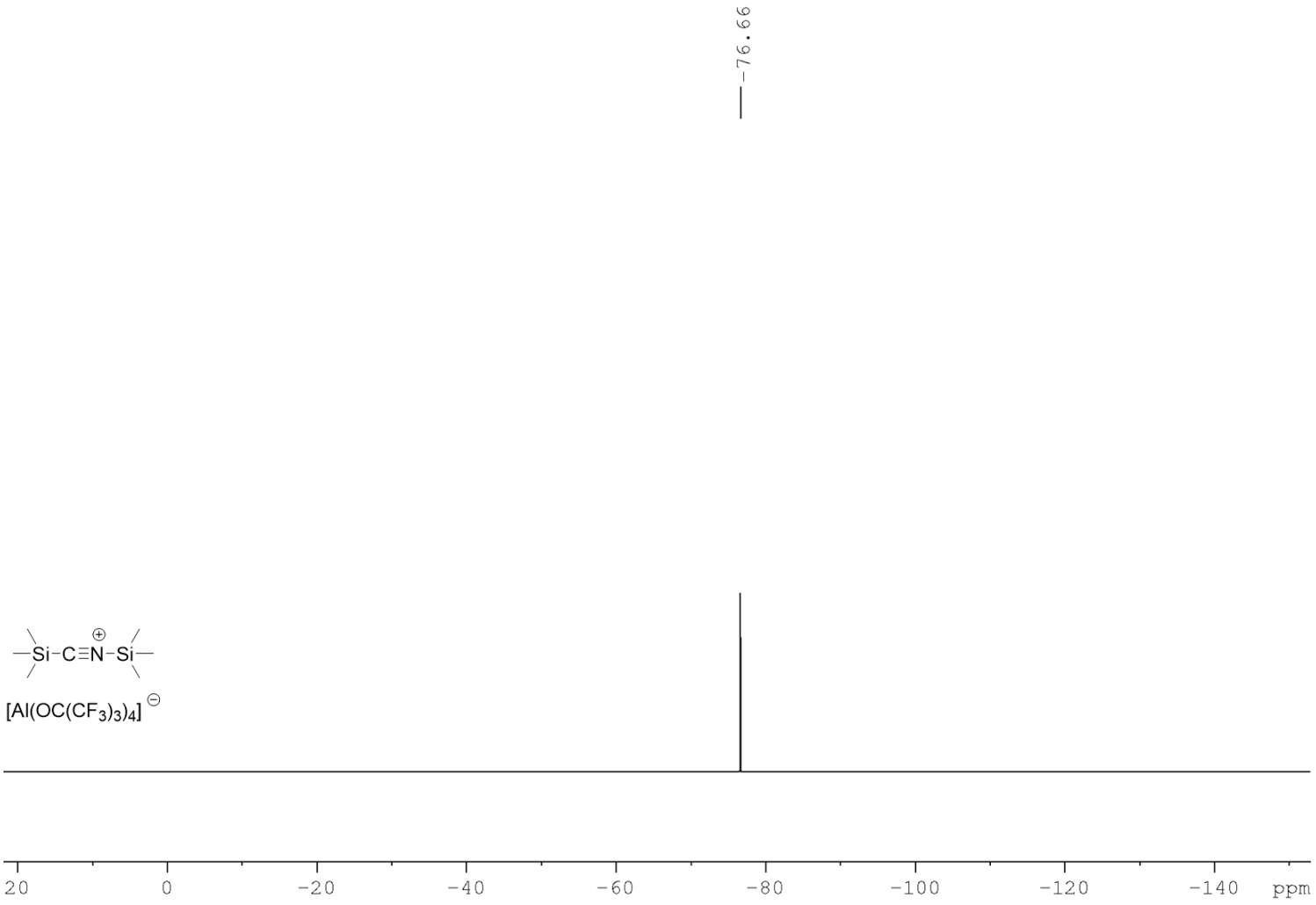

Figure S45. ^{19}F NMR spectrum of [TMS-CN-TMS][Al(OC(CF$_3$)$_3$)$_4$] in DCM-d_2.

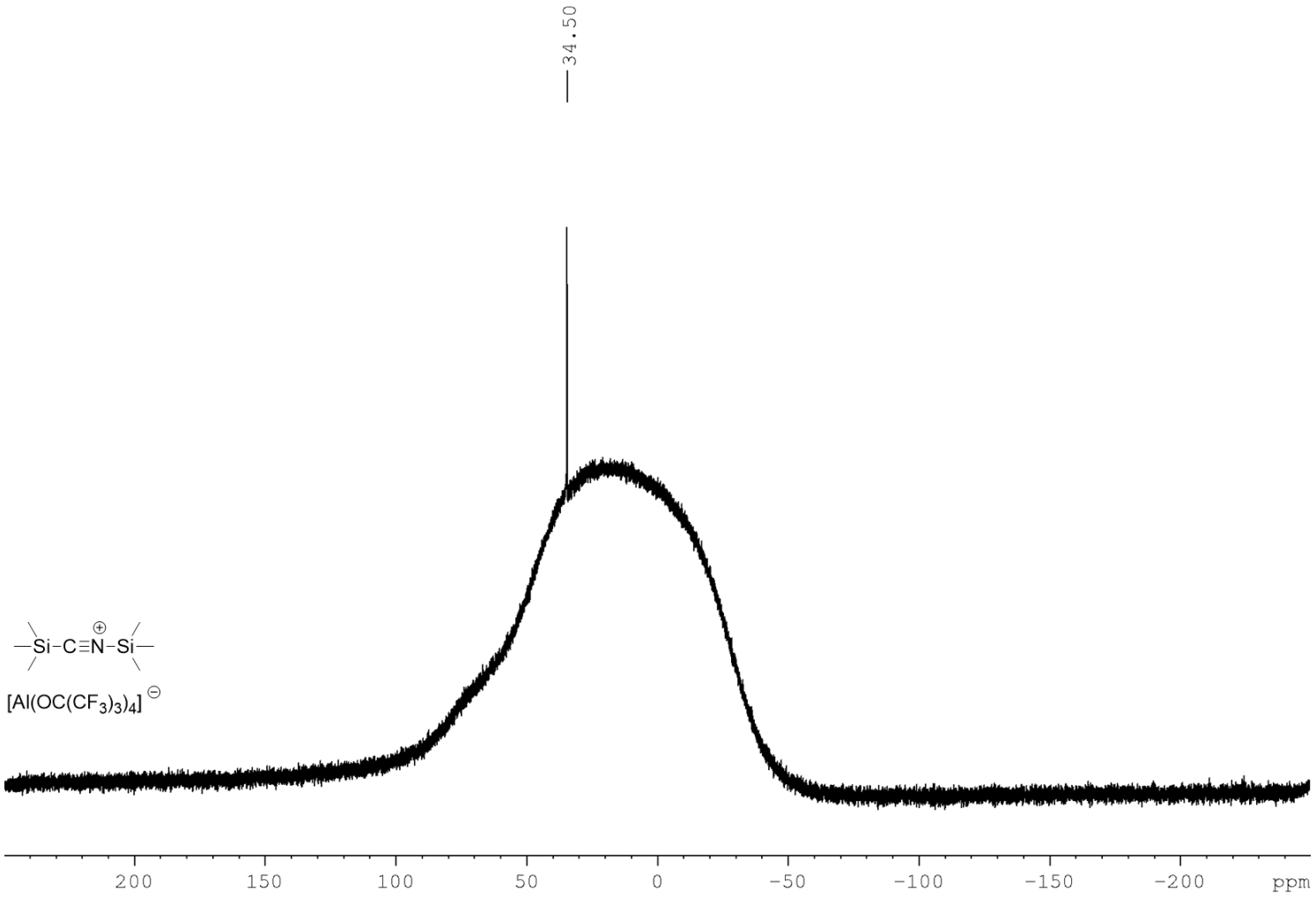

Figure S46. ^{27}Al NMR spectrum of [TMS-CN-TMS][Al(OC(CF$_3$)$_3$)$_4$] in DCM-d_2.

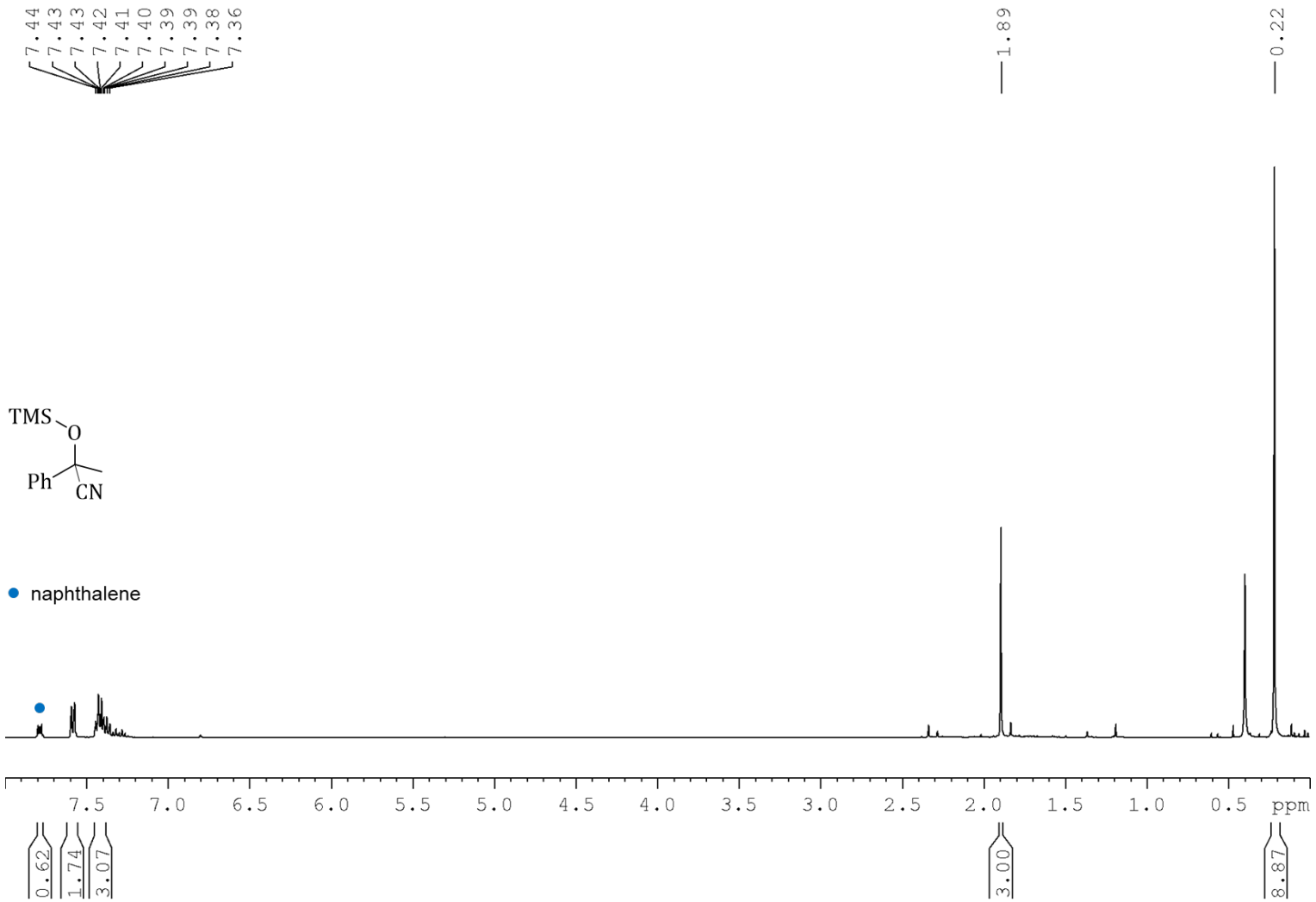

Figure S47. Crude ^{1}H NMR spectrum consisting of **6a** in $CDCl_3$.

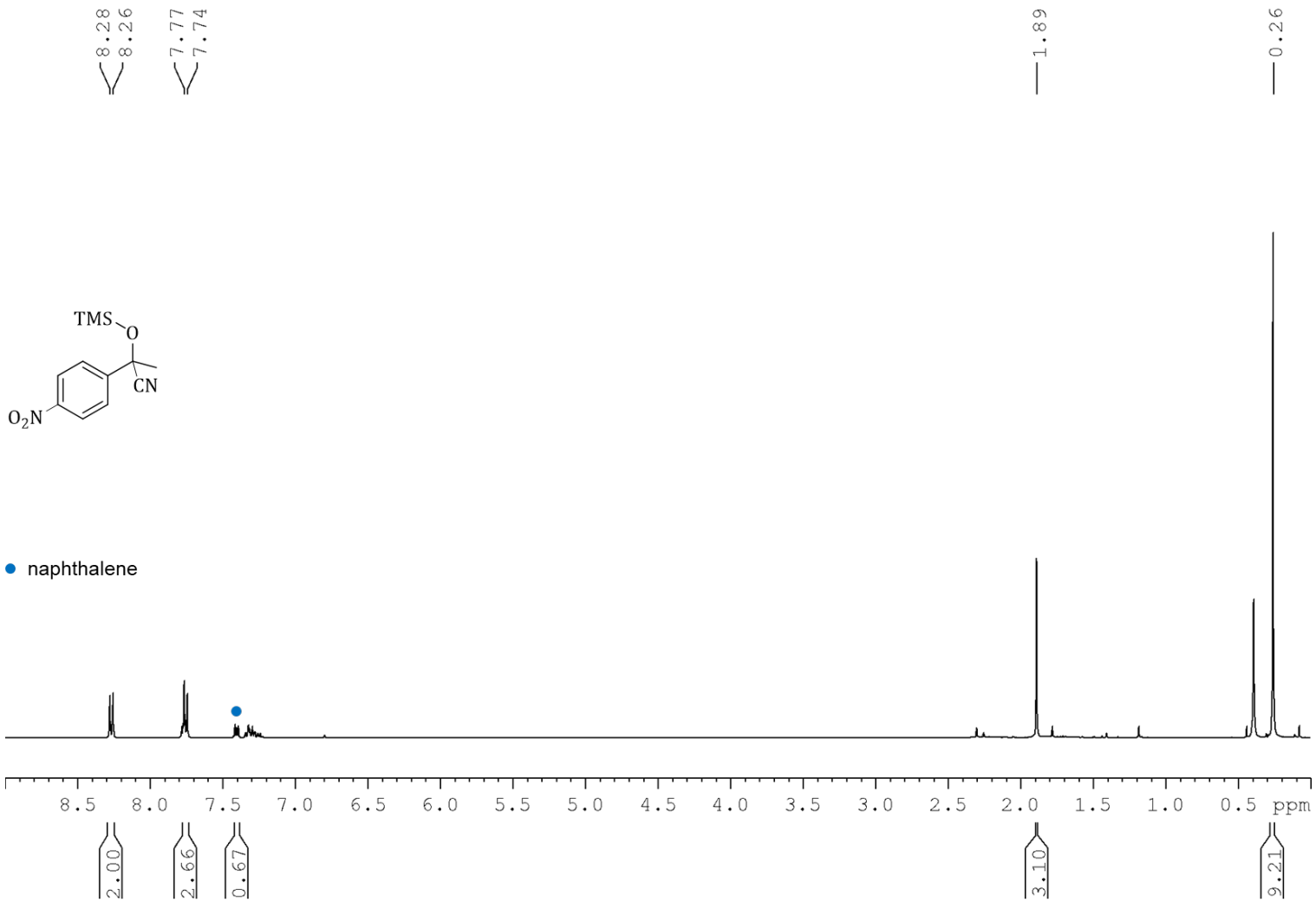

Figure S48. Crude ^{1}H NMR spectrum consisting of **6b** in $CDCl_3$.

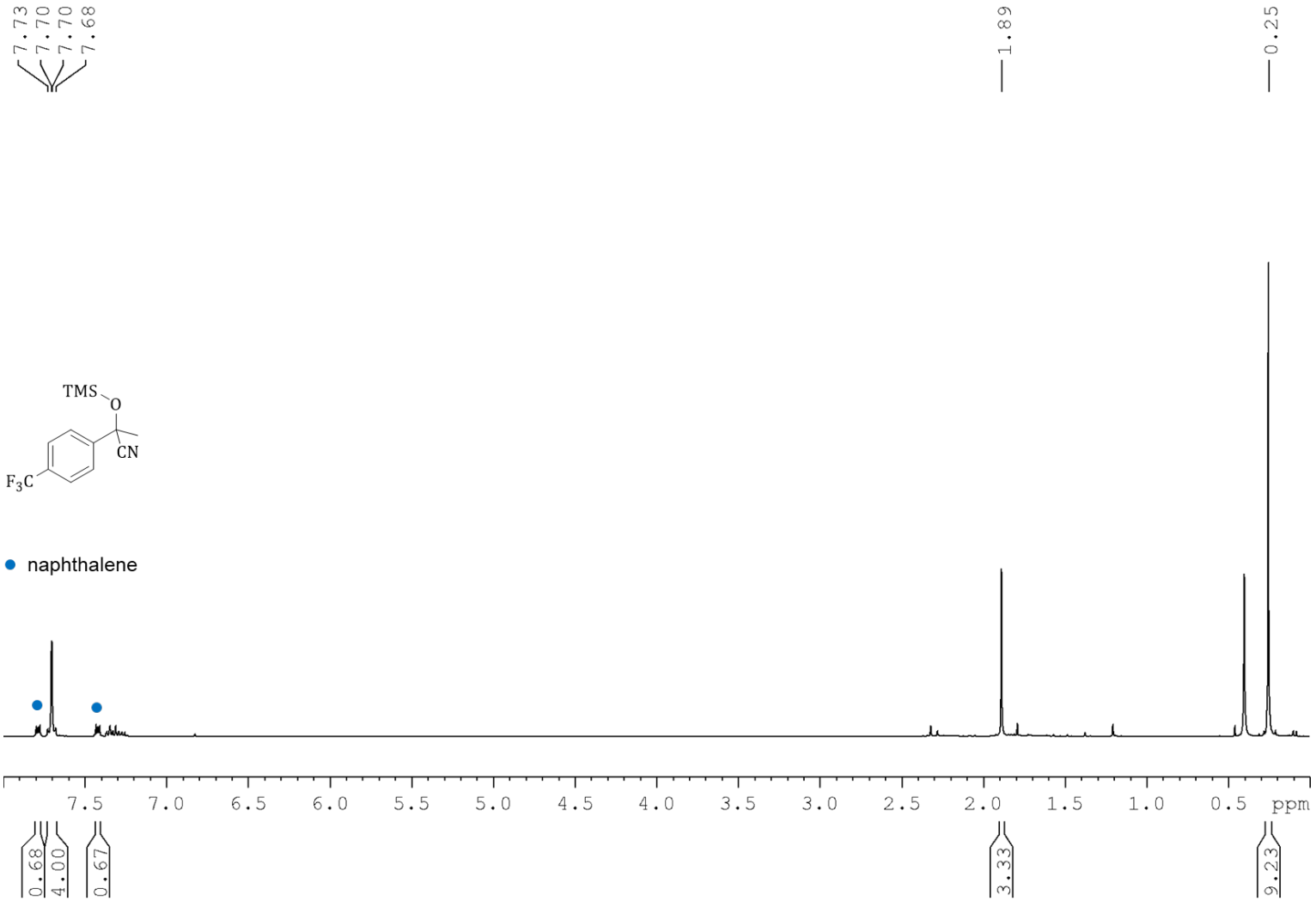

Figure S49. Crude ^{1}H NMR spectrum consisting of **6c** in $CDCl_3$.

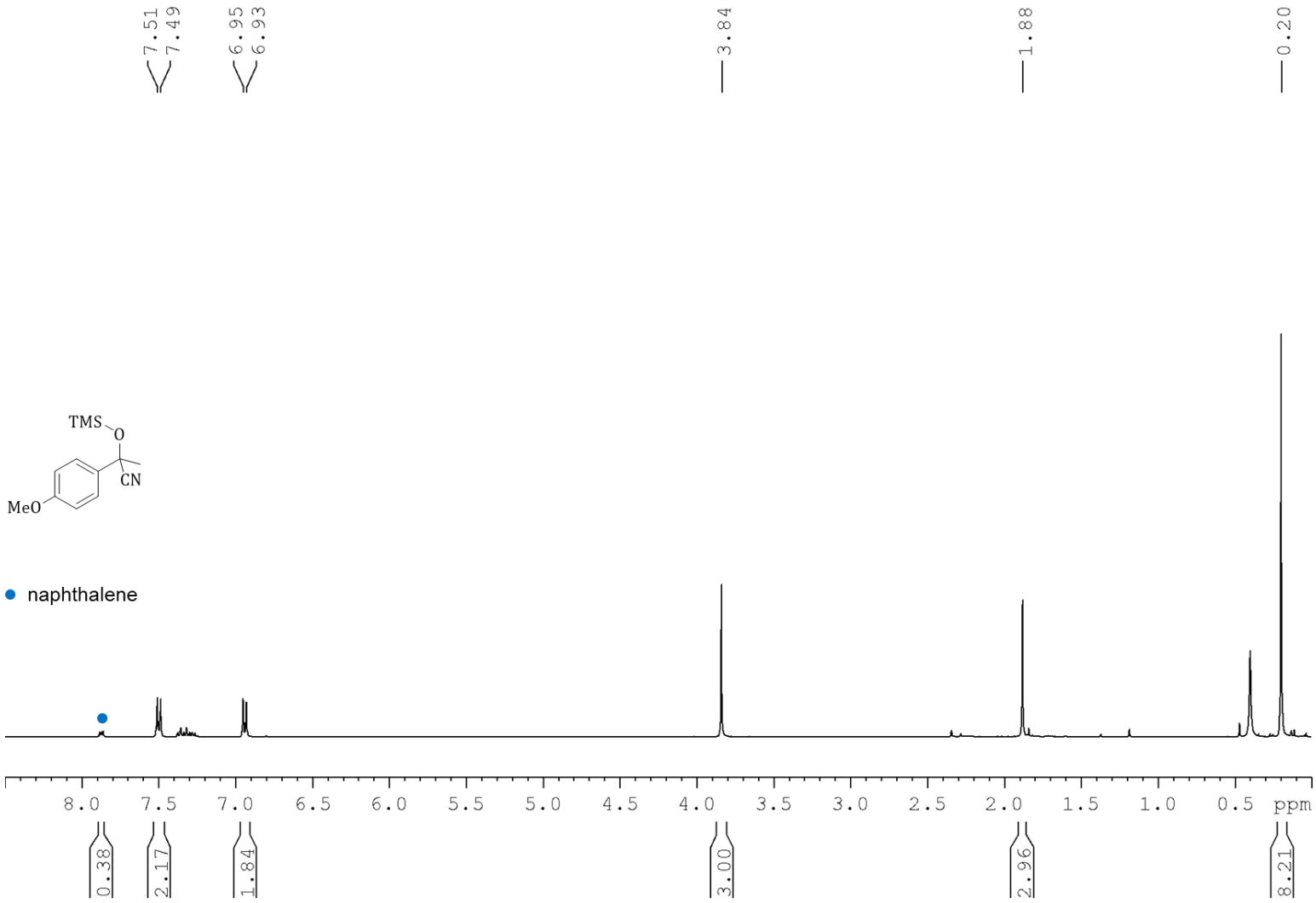

Figure S50. Crude ^{1}H NMR spectrum consisting of **6d** in $CDCl_3$.

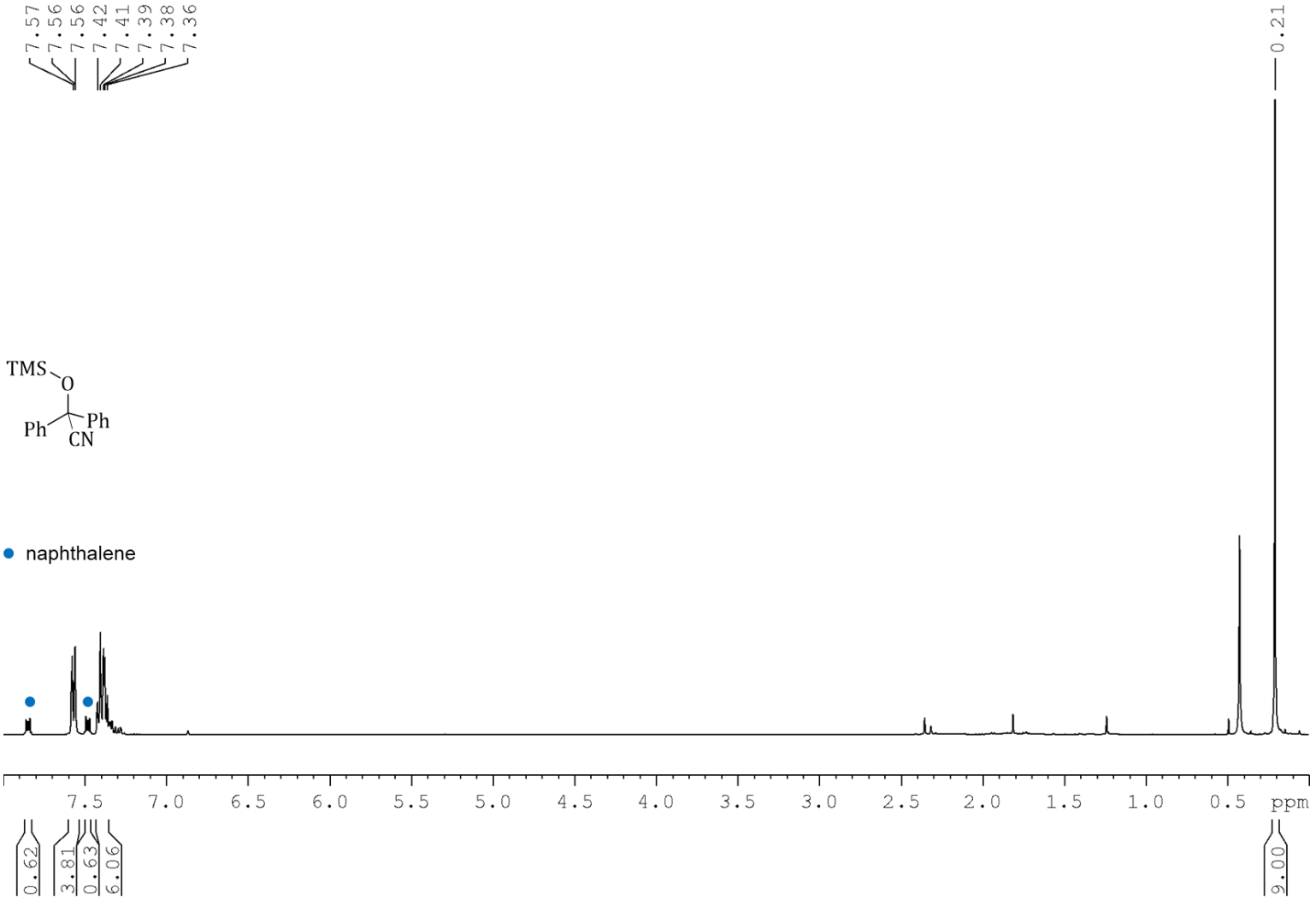

Figure S51. Crude ^{1}H NMR spectrum consisting of **6e** in $CDCl_3$.

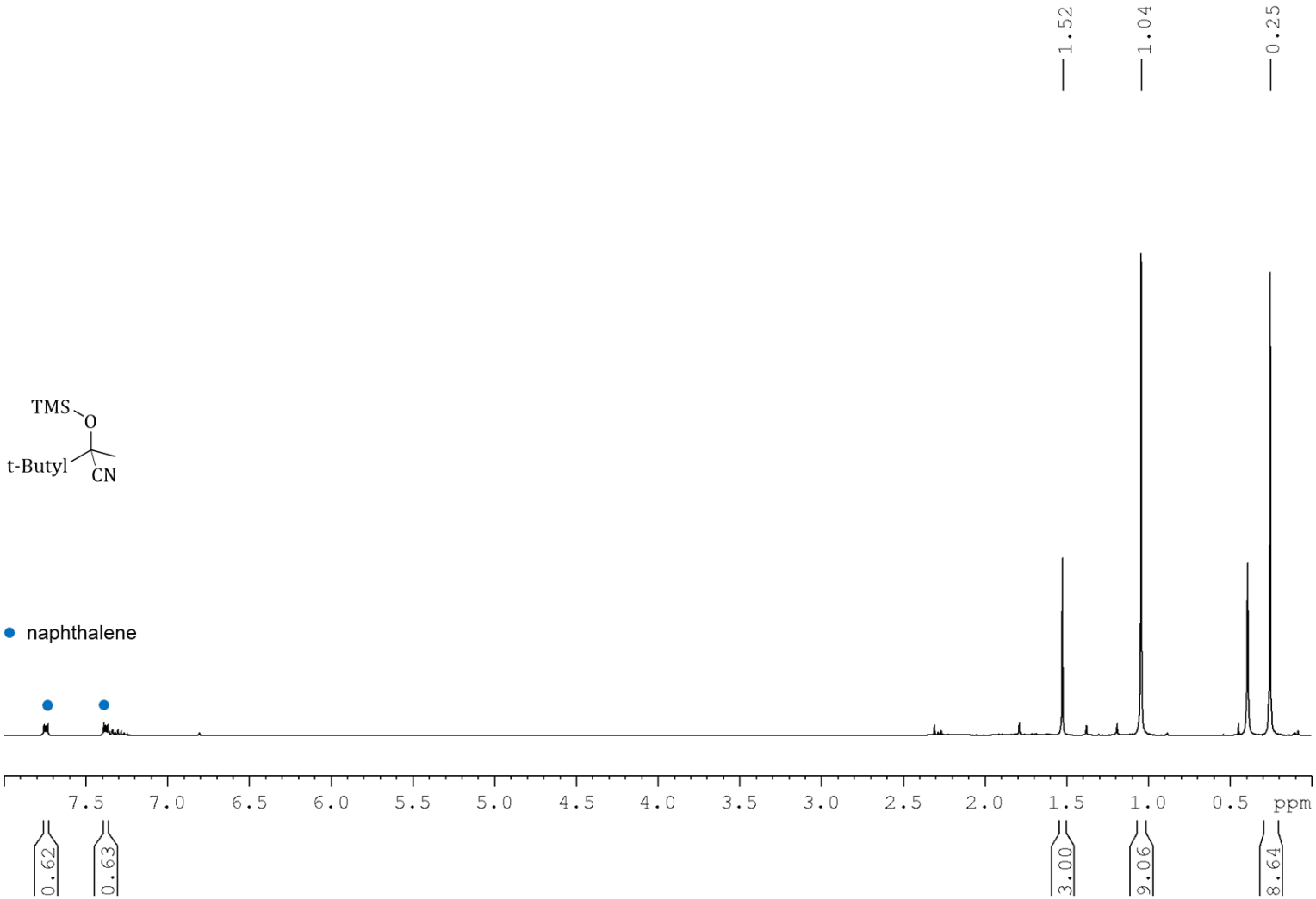

Figure S52. Crude ^{1}H NMR spectrum consisting of **6f** in $CDCl_3$.

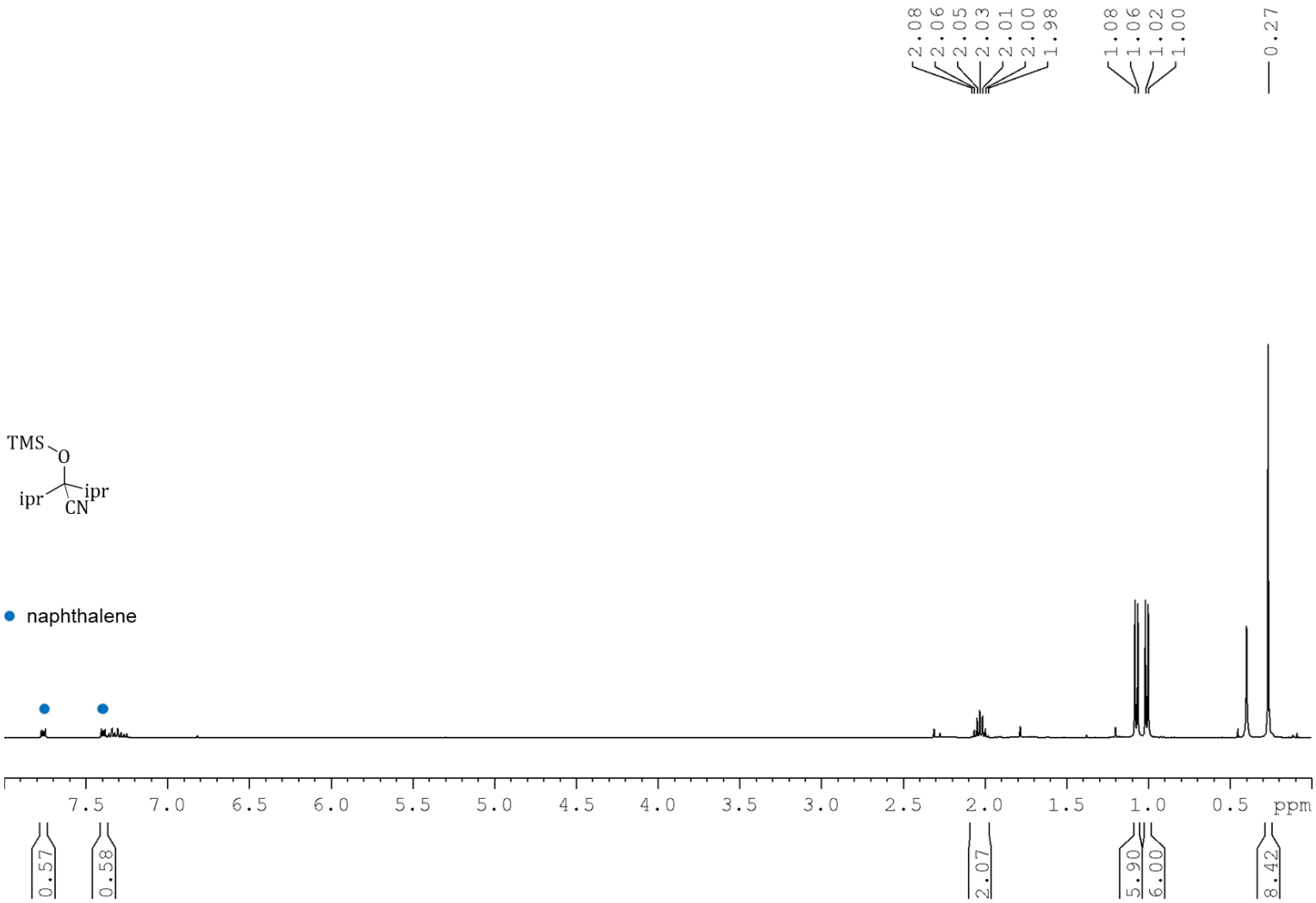

Figure S53. Crude ^{1}H NMR spectrum consisting of **6g** in $CDCl_3$.

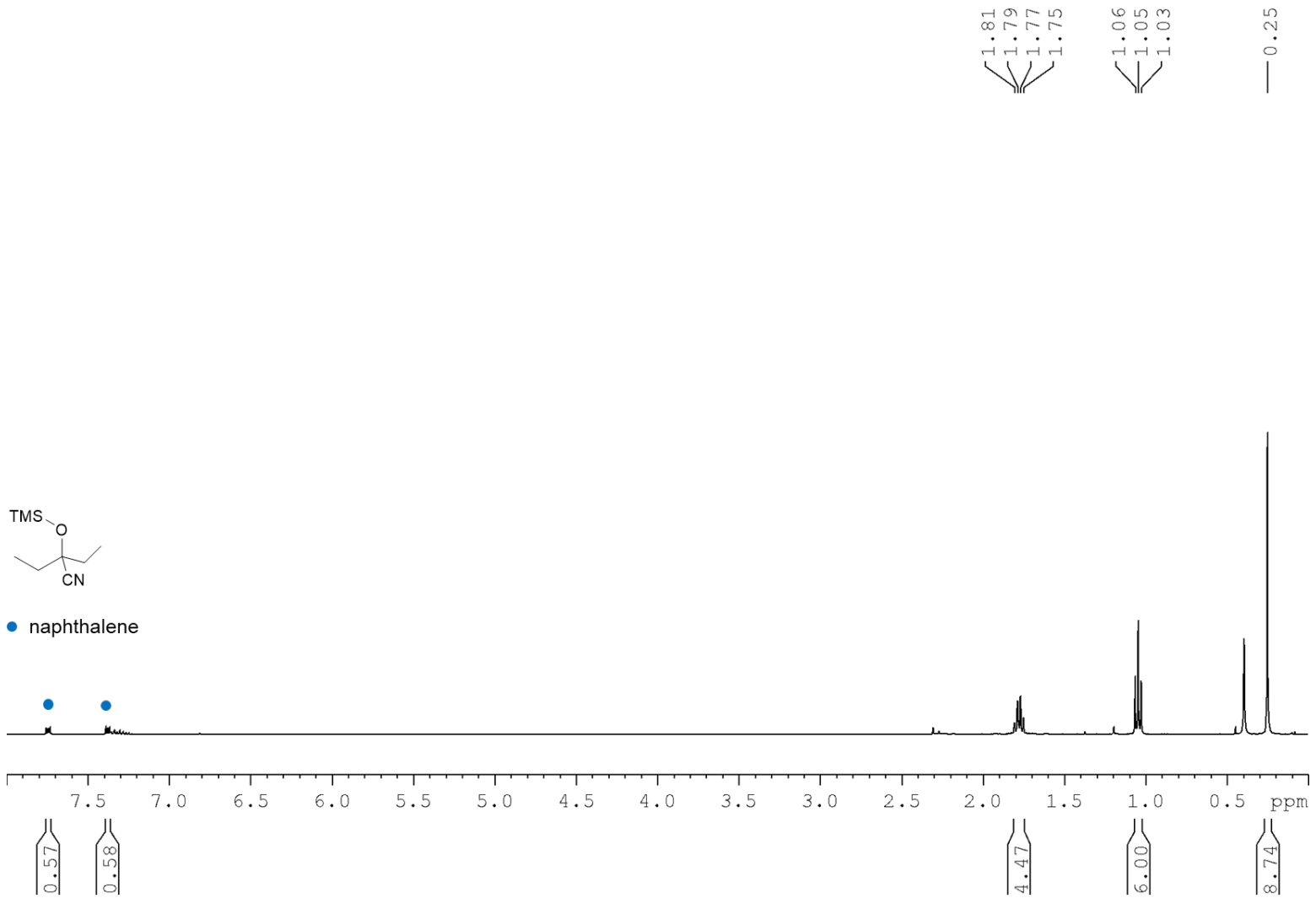

Figure S54. Crude ^{1}H NMR spectrum consisting of **6h** in $CDCl_3$.

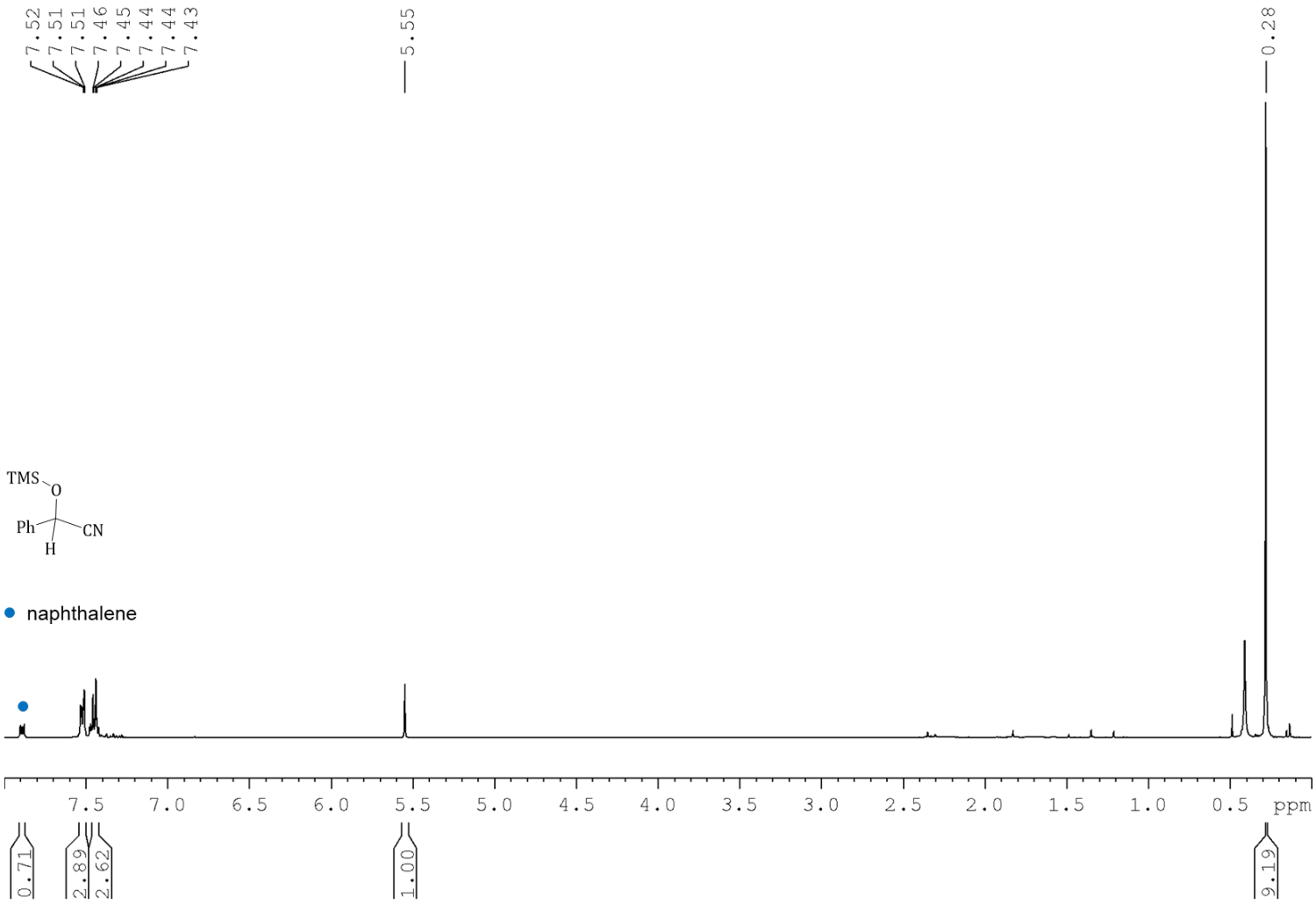

Figure S55. Crude ^{1}H NMR spectrum consisting of **6i** in $CDCl_3$.

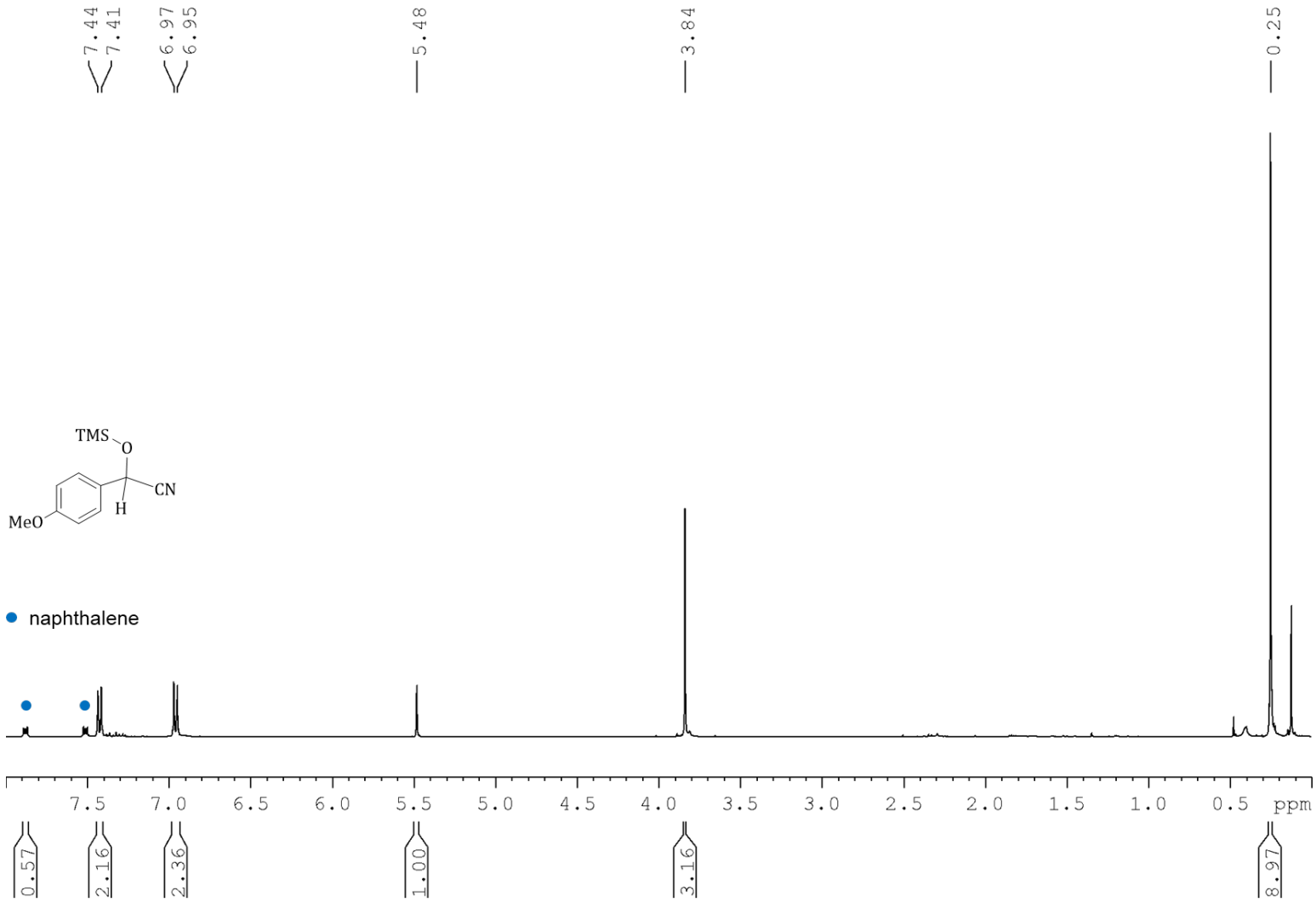

Figure S56. Crude ^{1}H NMR spectrum consisting of **6j** in $CDCl_3$.

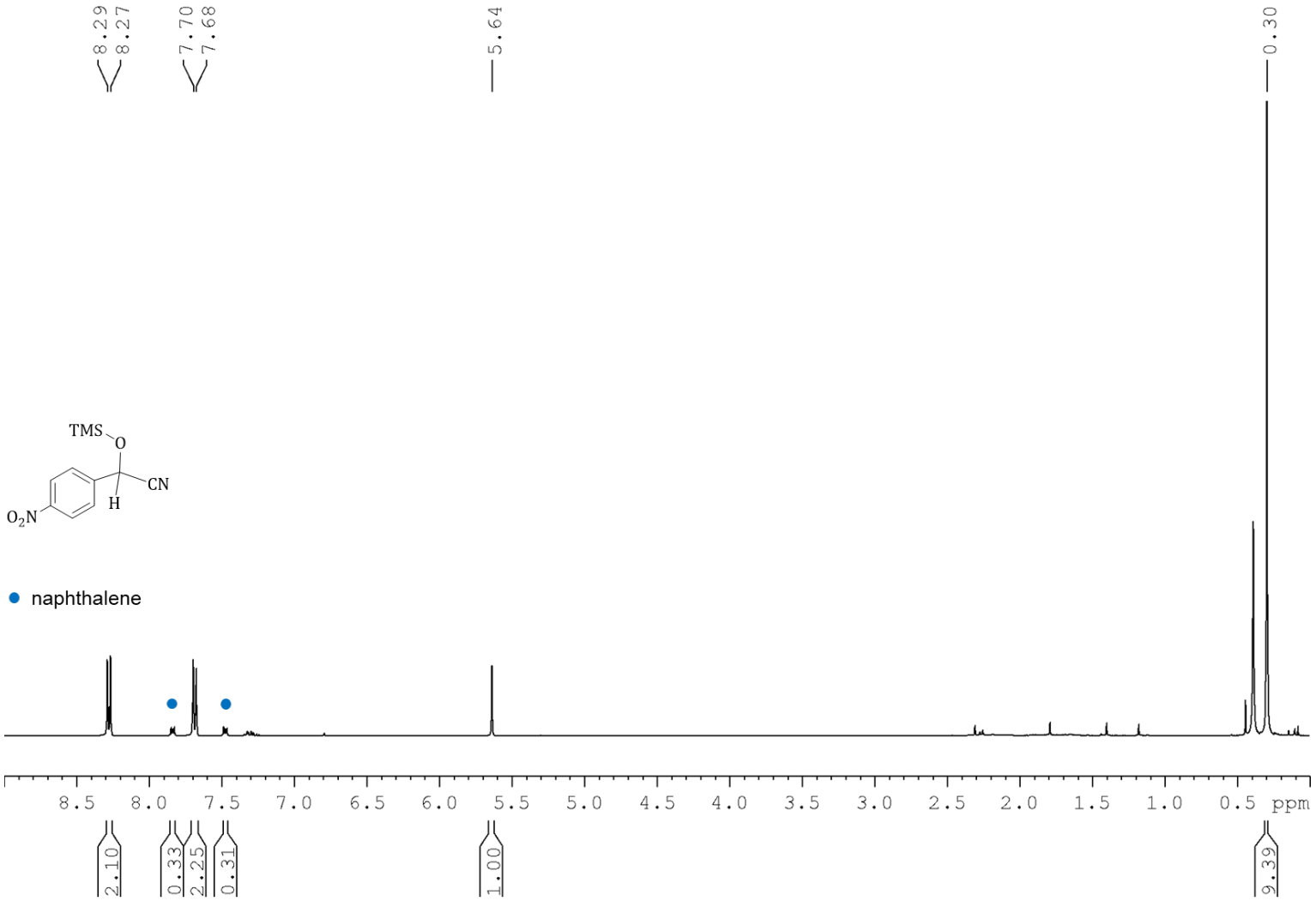

Figure S57. Crude ^{1}H NMR spectrum consisting of **6k** in $CDCl_3$.

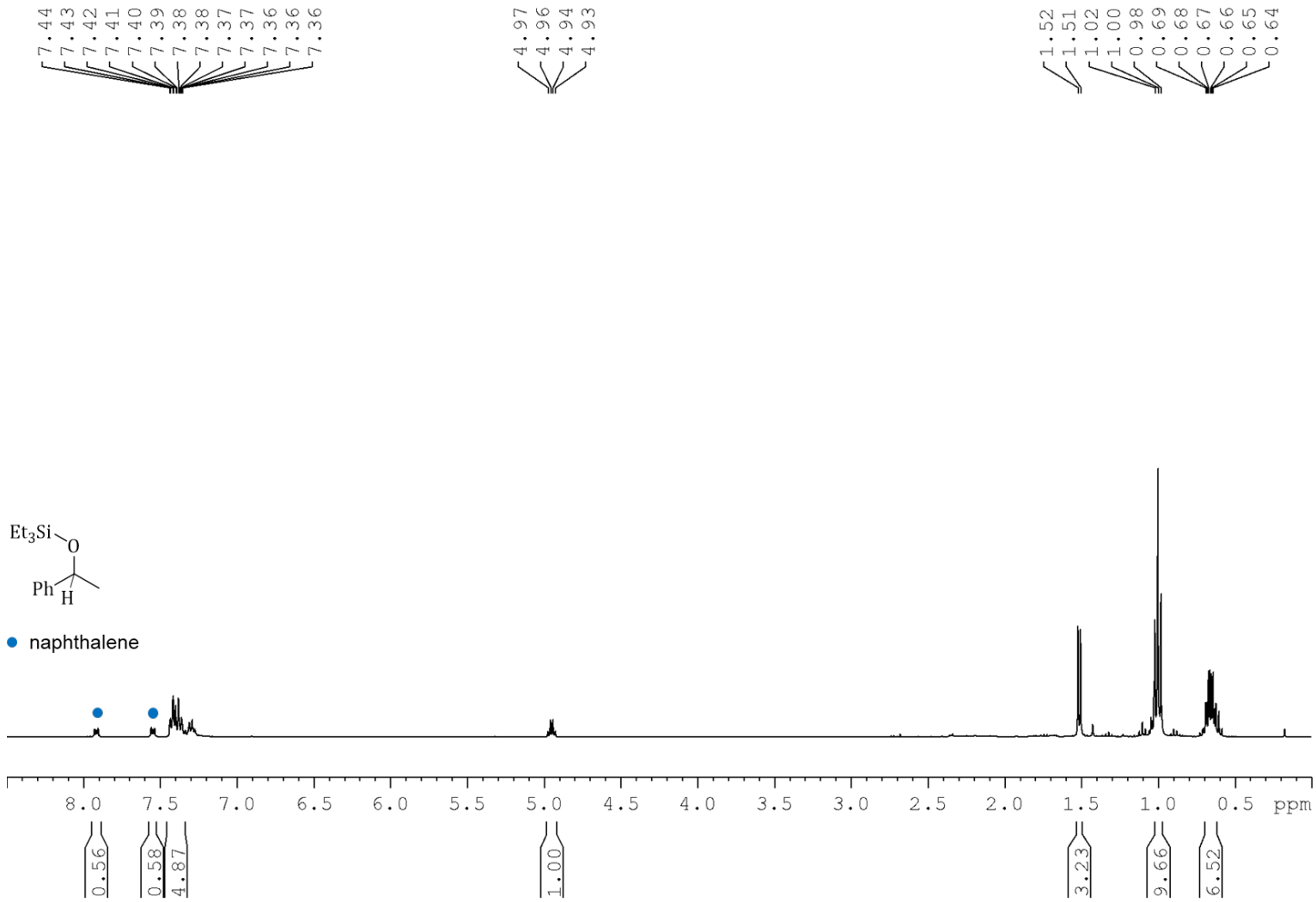

Figure S58. Crude ^{1}H NMR spectrum consisting of **8a** in $CDCl_3$.

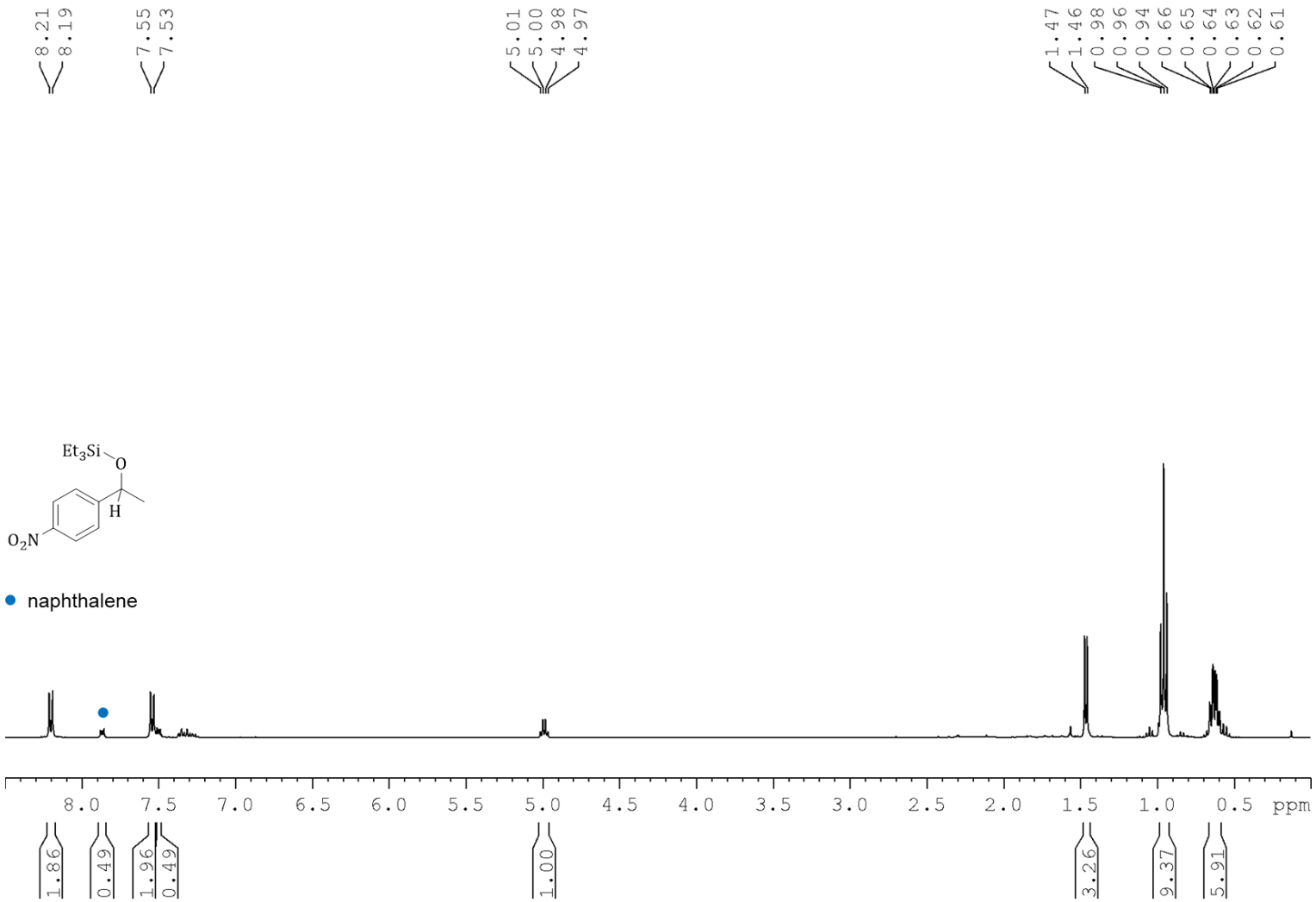

Figure S59. Crude ^{1}H NMR spectrum consisting of **8b** in $CDCl_3$.

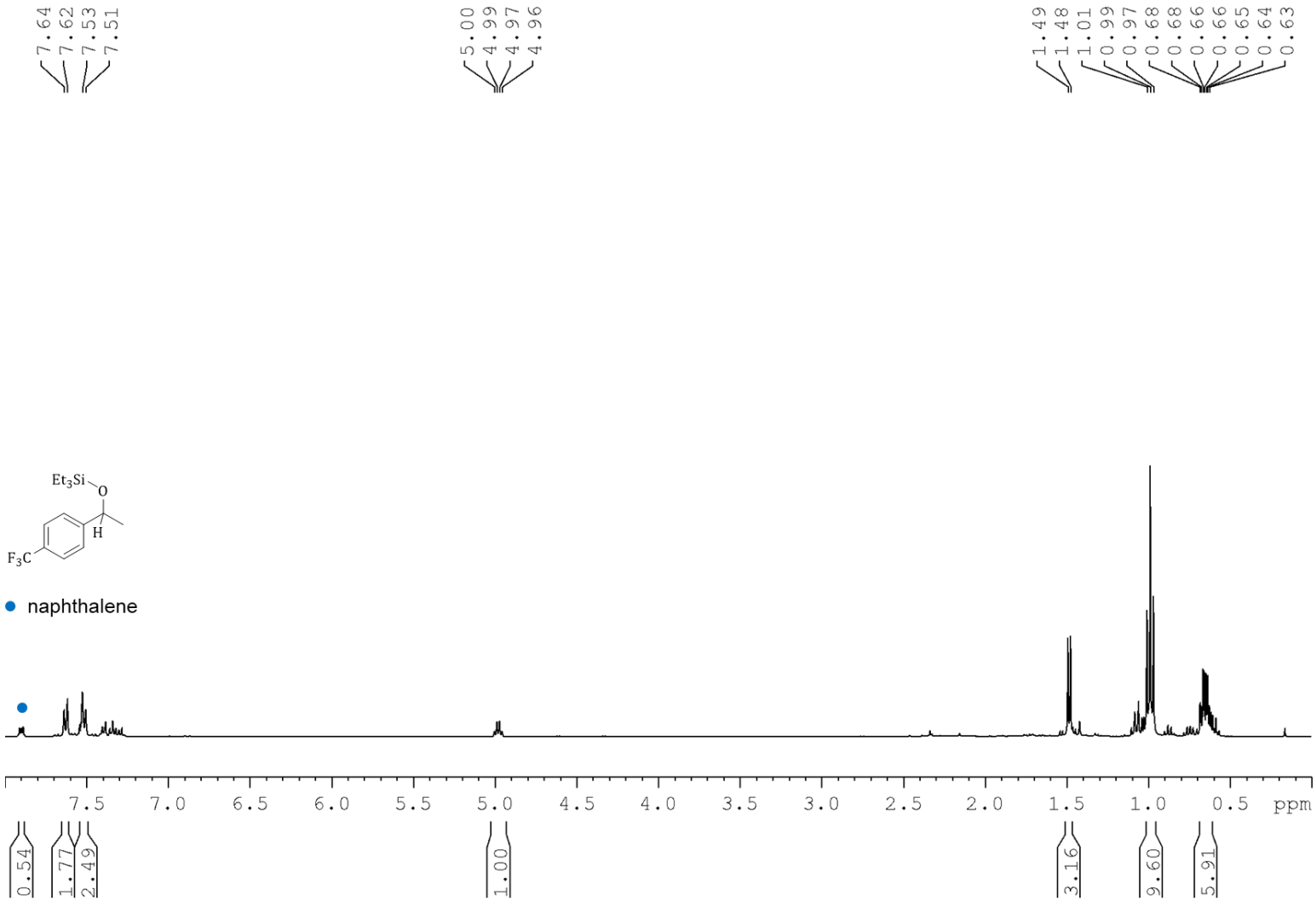

Figure S60. Crude ^{1}H NMR spectrum consisting of **8c** in $CDCl_3$.

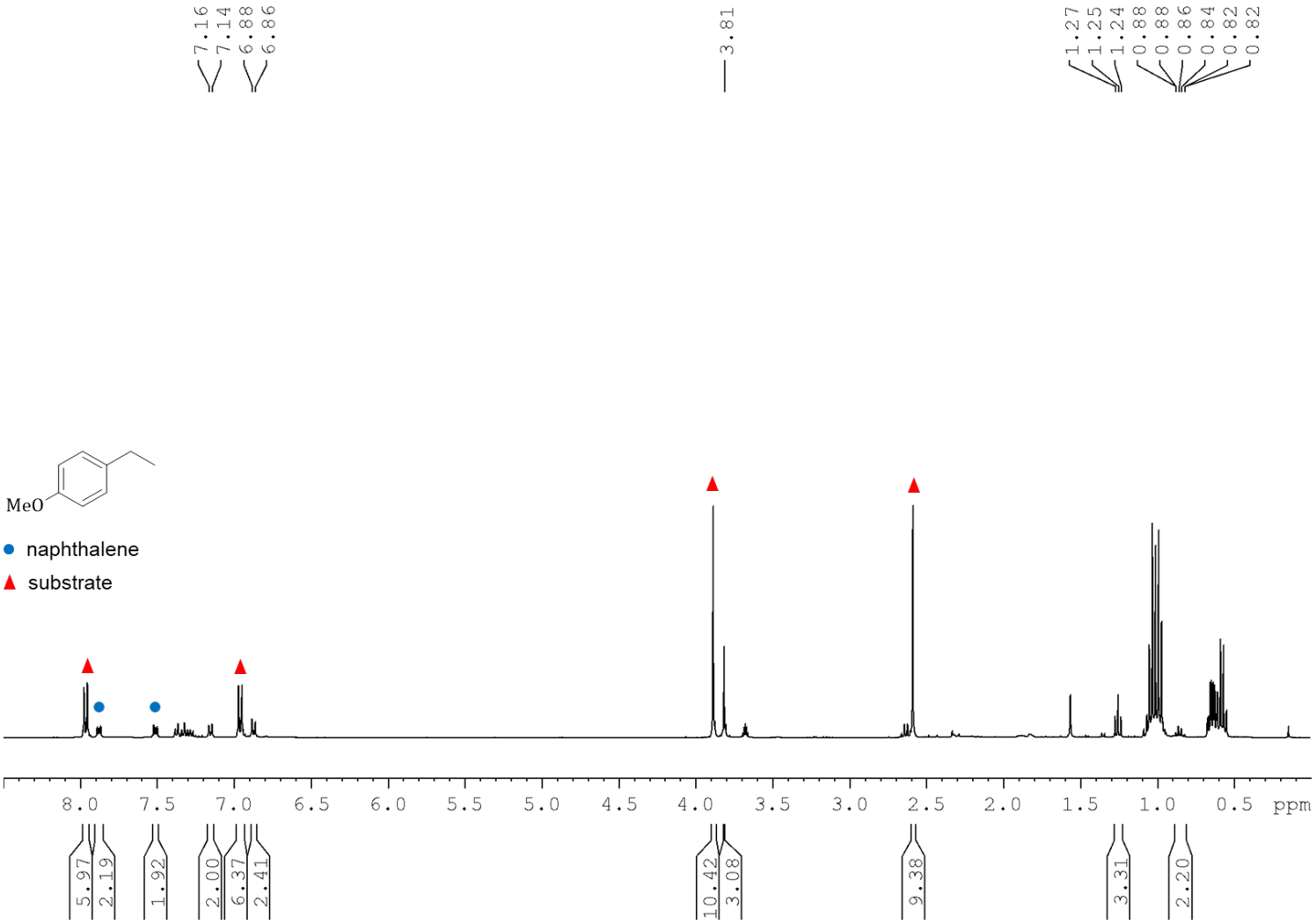

Figure S61. Crude ^{1}H NMR spectrum consisting of **9d** in $CDCl_3$.

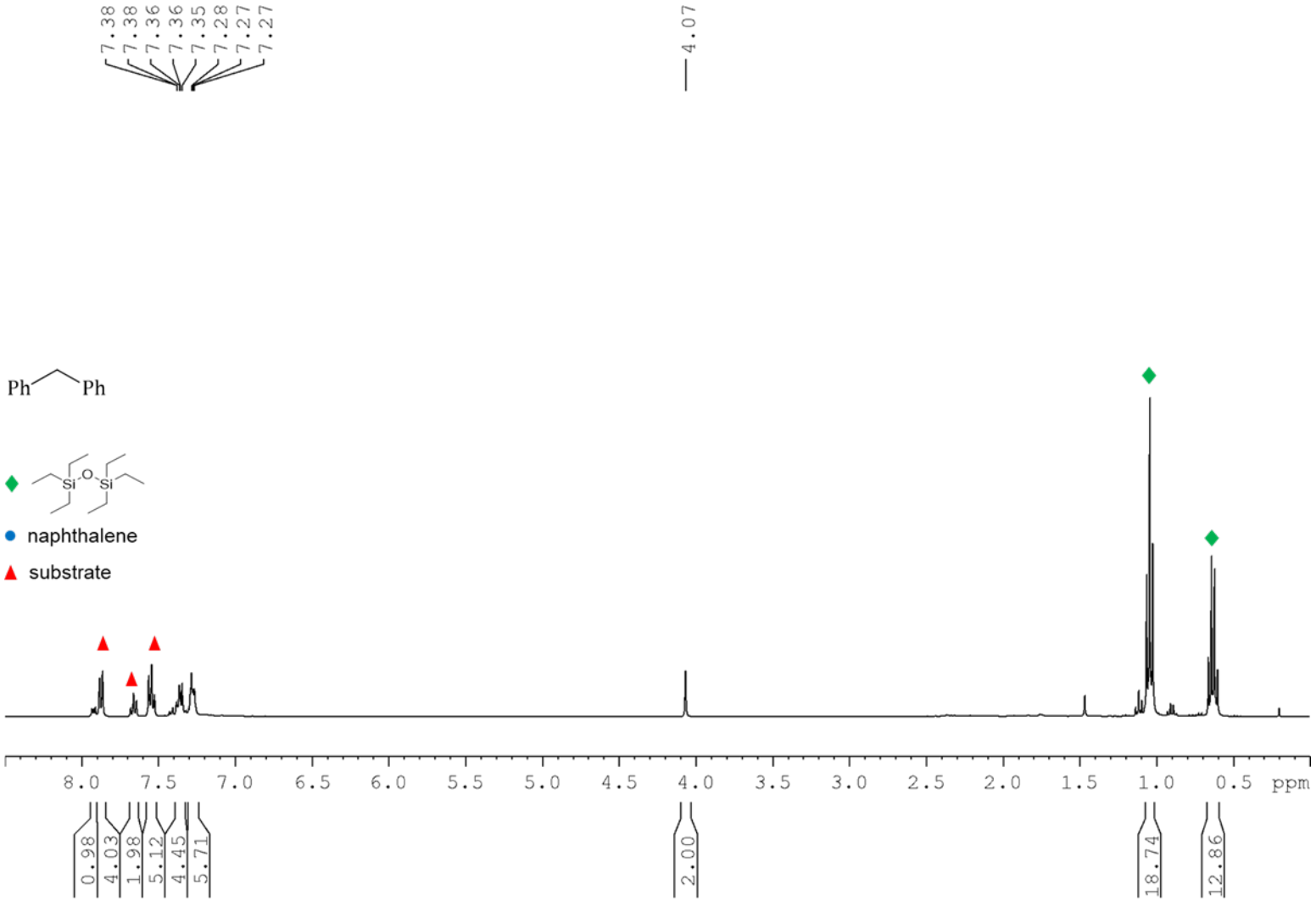

Figure S62. Crude ^{1}H NMR spectrum consisting of **9e** in $CDCl_3$.

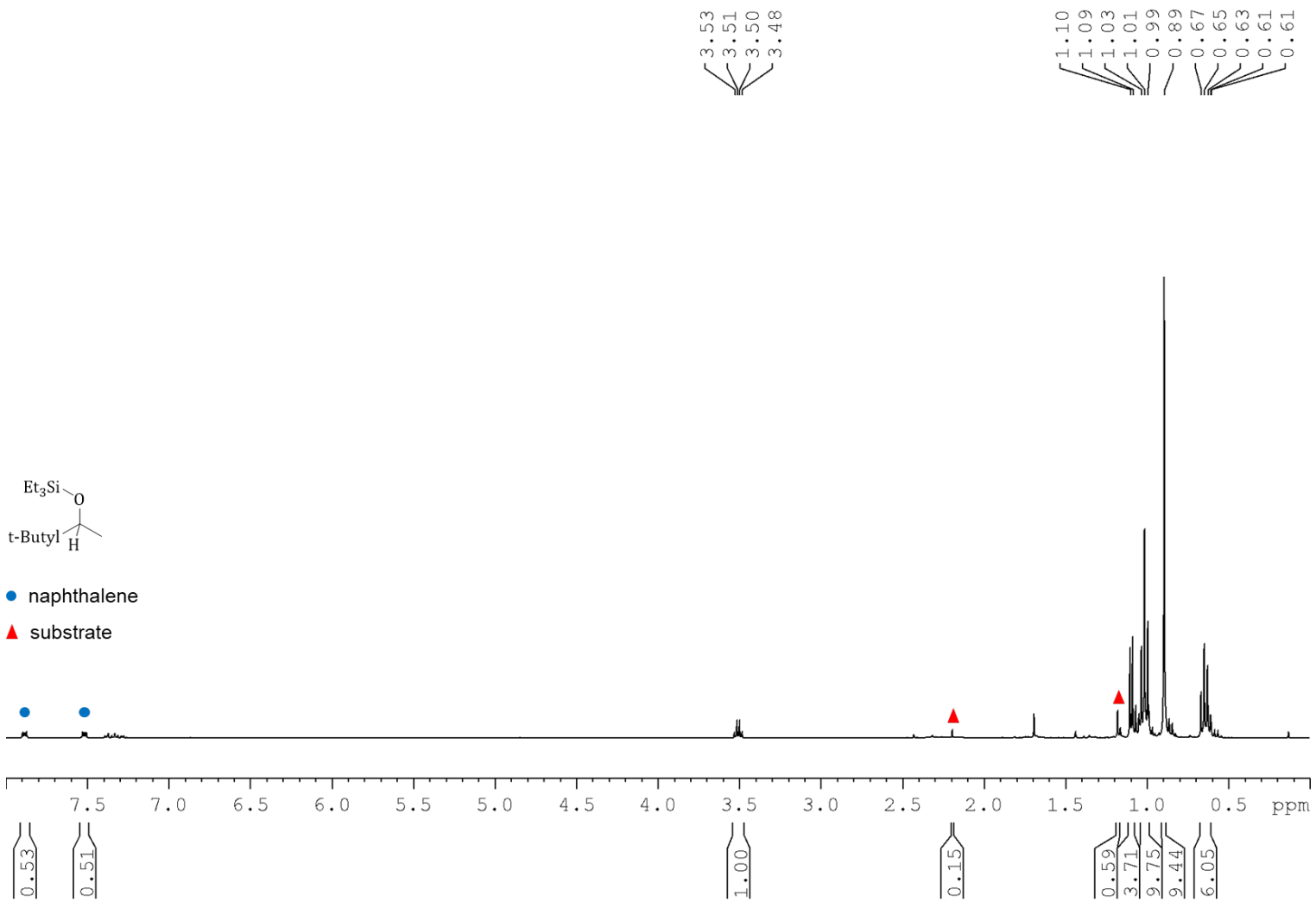

Figure S63. Crude ^{1}H NMR spectrum consisting of **8f** in $CDCl_3$.

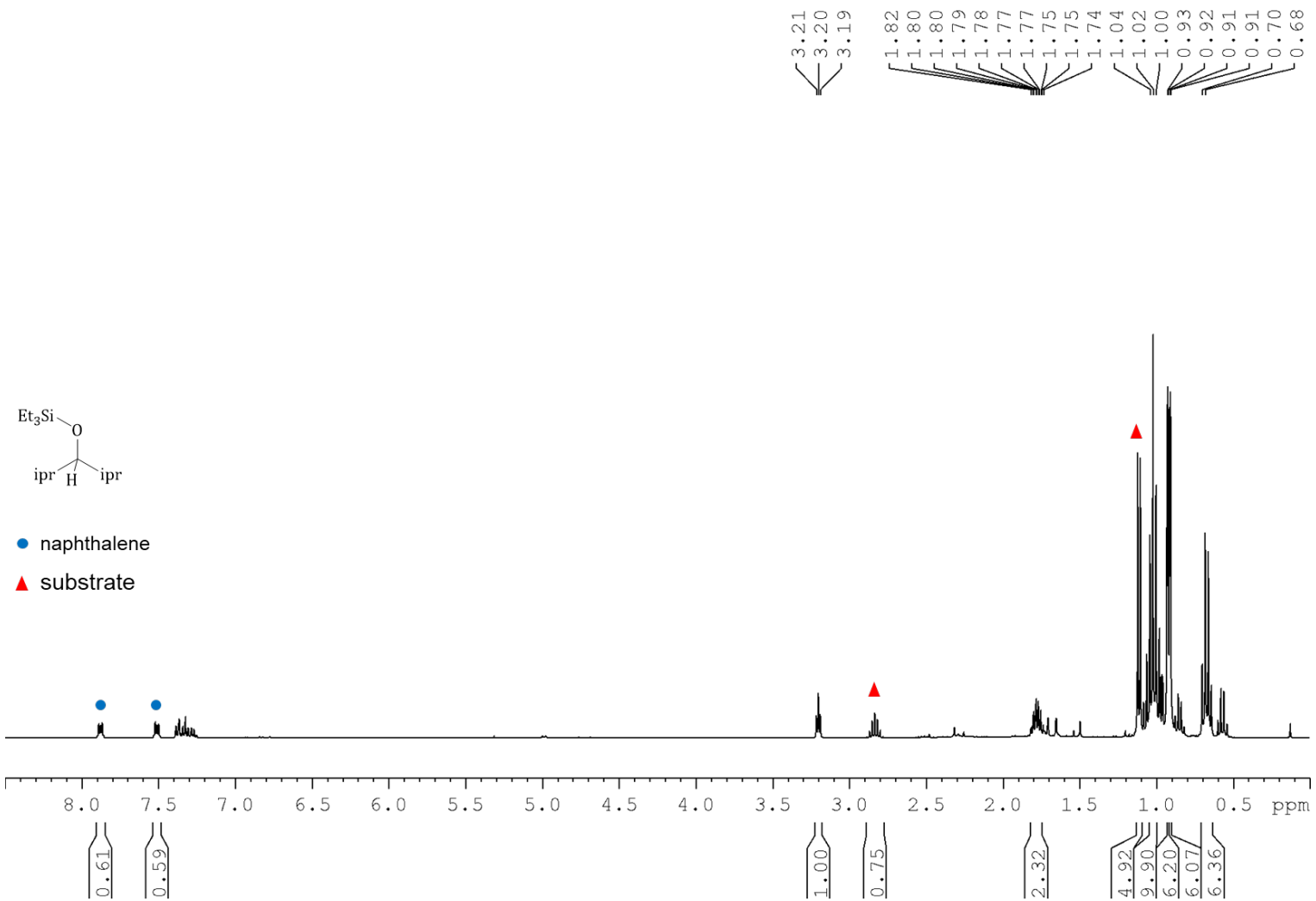

Figure S64. Crude ^{1}H NMR spectrum consisting of **8g** in $CDCl_3$.

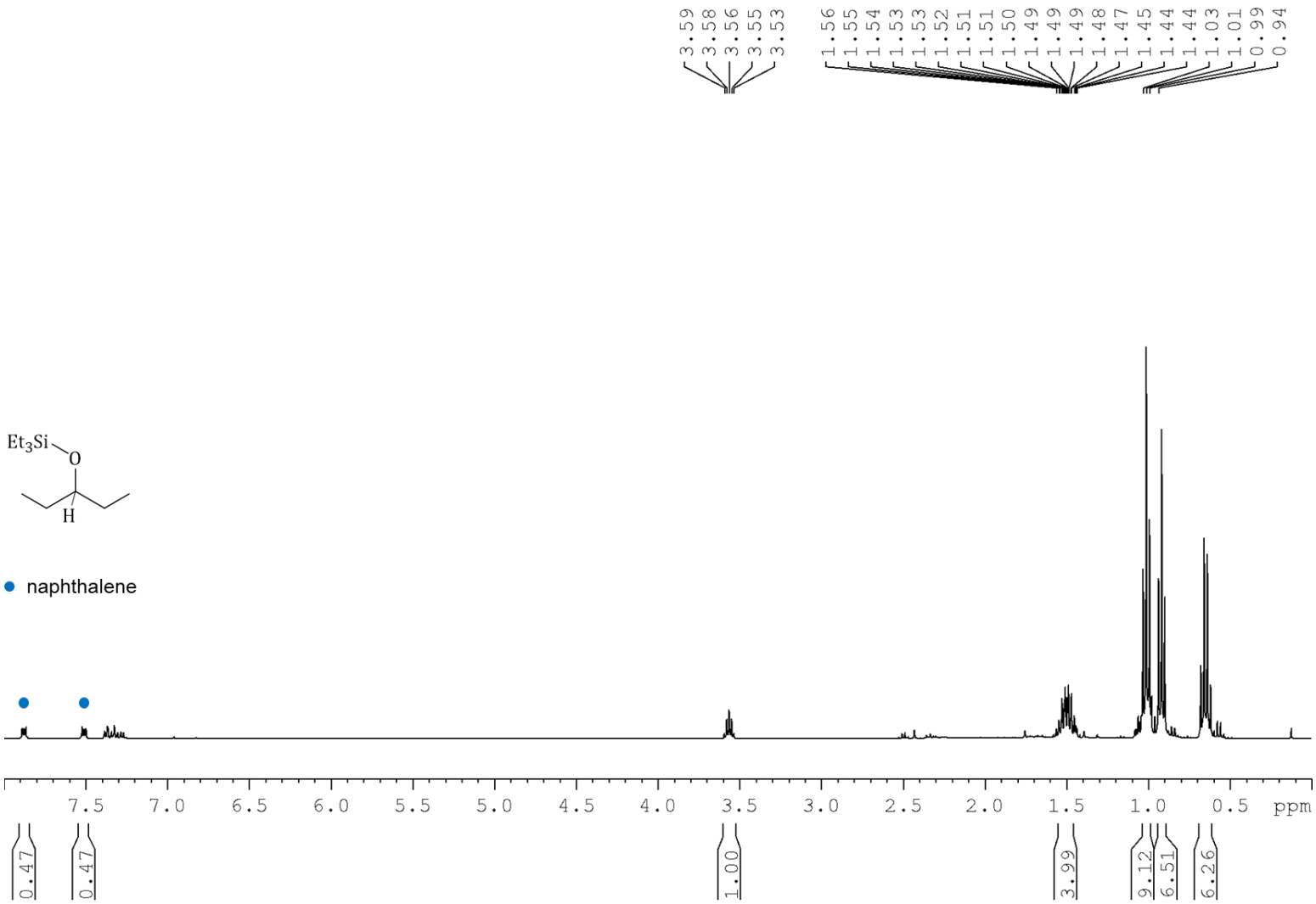

Figure S65. Crude ^{1}H NMR spectrum consisting of **8h** in $CDCl_3$.

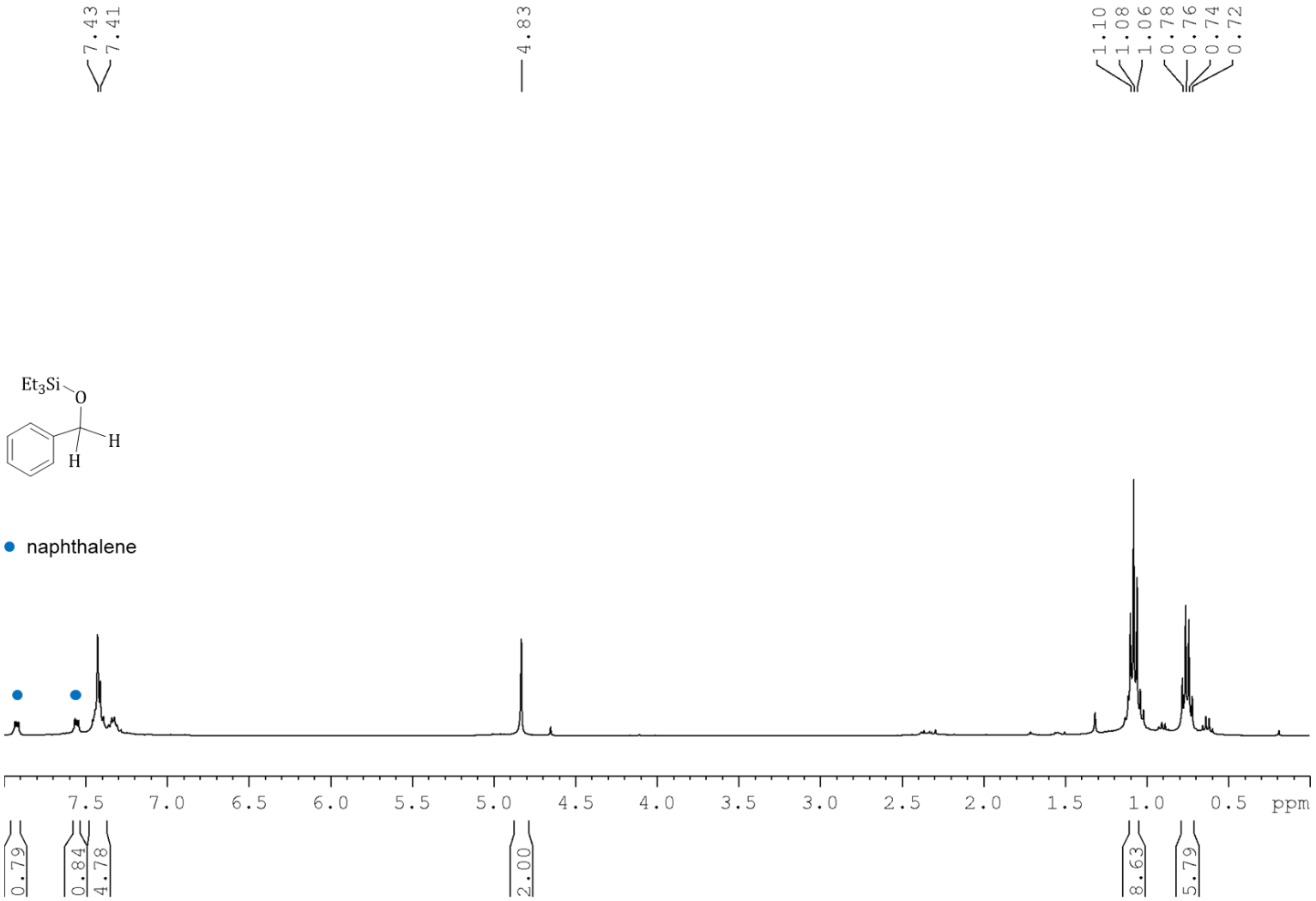

Figure S66. Crude ^{1}H NMR spectrum consisting of **8i** in $CDCl_3$.

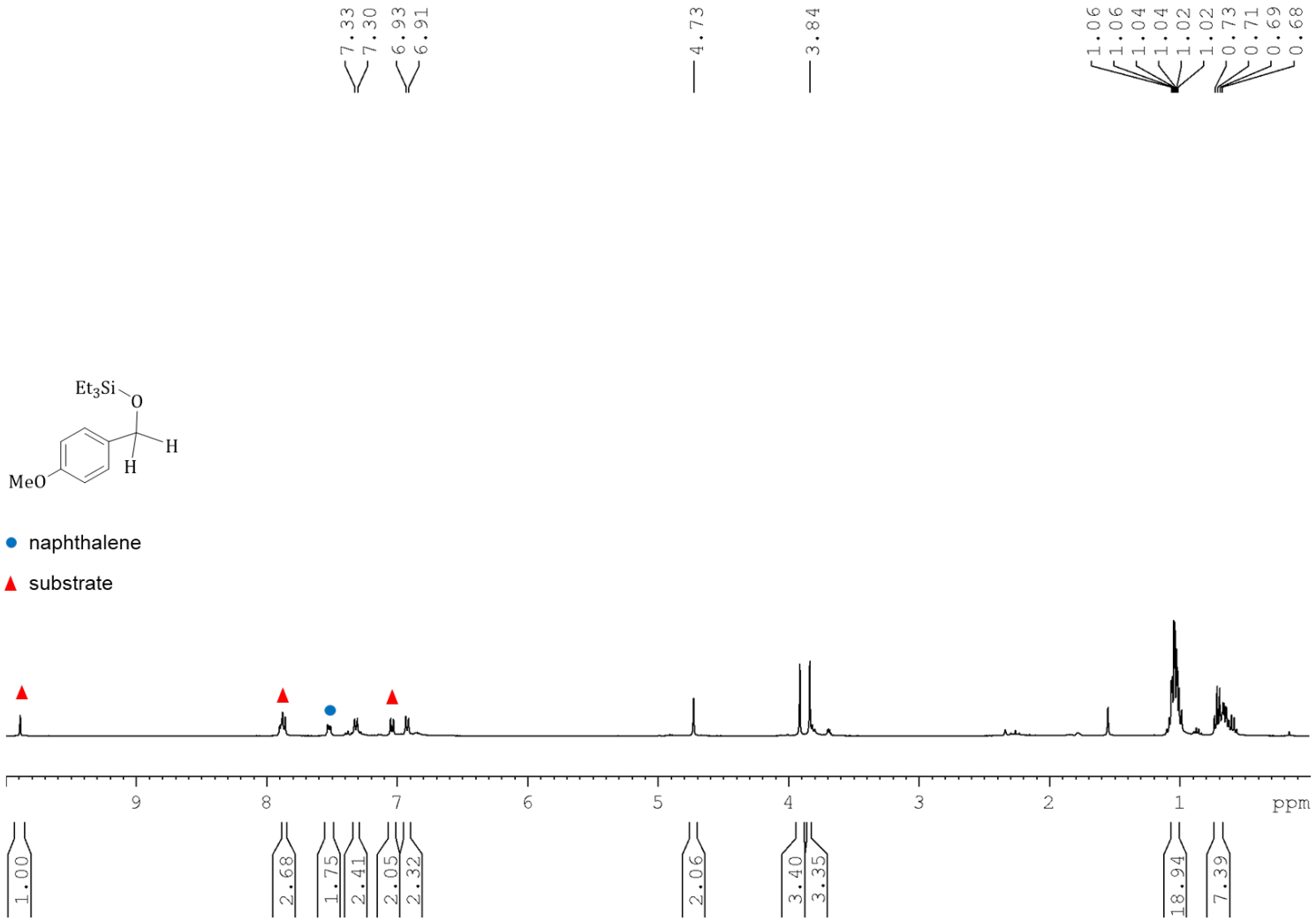

Figure S67. Crude ^{1}H NMR spectrum consisting of **8j** in $CDCl_3$.

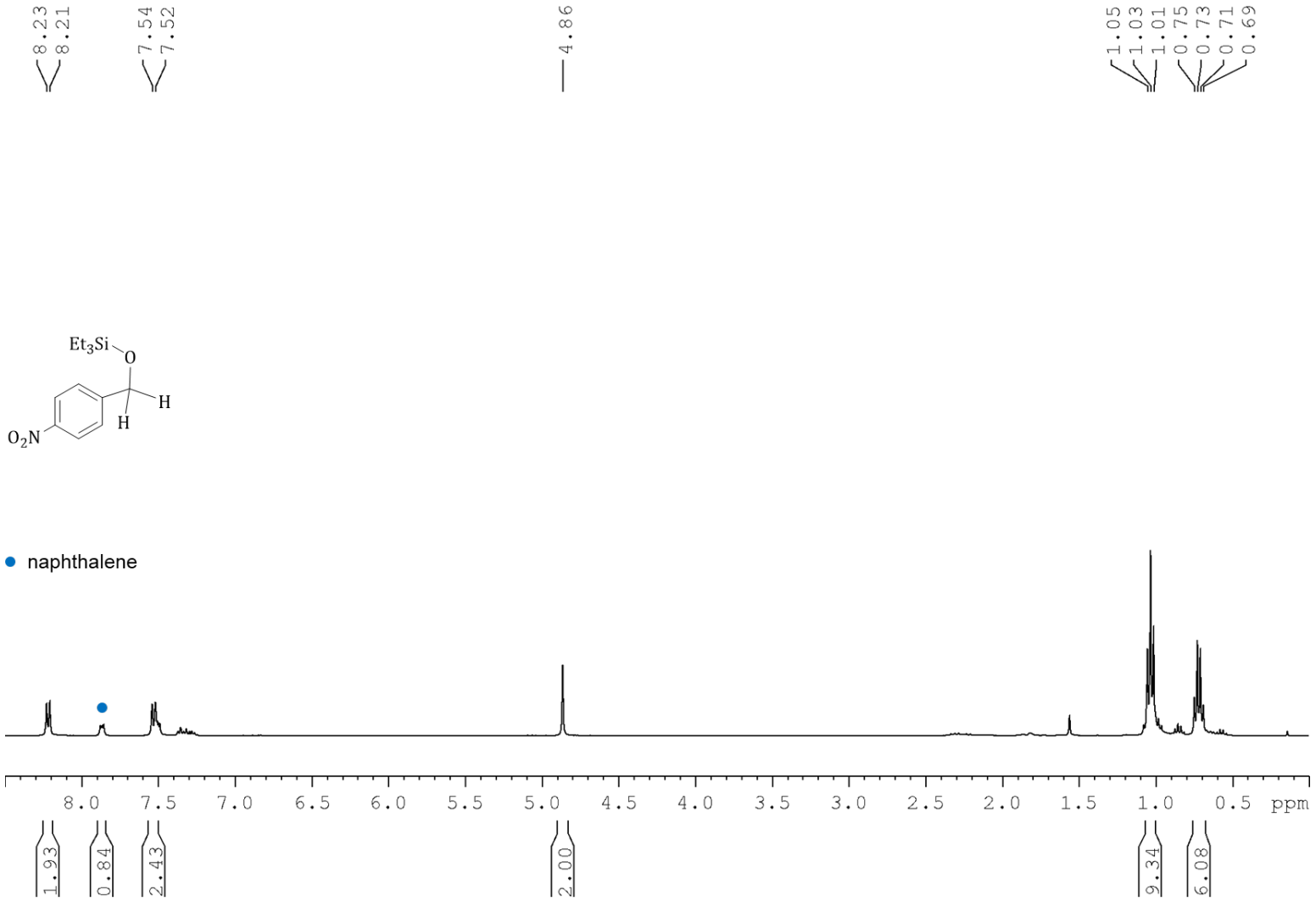

Figure S68. Crude ^{1}H NMR spectrum consisting of **8k** in $CDCl_3$.